UNIVERSITÀ
DEGLI STUDI
DI PADOVA

Sede amministrativa: Università degli Studi di Padova

Dipartimento di Farmacia

Dipartimento di Biologia

SCUOLA DI DOTTORATO DI RICERCA IN

BIOLOGIA E MEDICINA DELLA RIGENERAZIONE

INDIRIZZO: INGEGNERIA DEI TESSUTI E DEI TRAPIANTI

CICLO XXIV

IN VITRO AND *IN VIVO* STUDIES OF BIORESORBABLE ELECTROSPUN SCAFFOLDS FOR VASCULAR TISSUE ENGINEERING: ON THE EFFECTIVENESS OF BLENDING POLY(ε-CAPROLACTONE) WITH POLY(3-HYDROXYBUTYRATE-CO-3-HYDROXYVALERATE)

Direttore della Scuola: Ch.mo Prof. Maria Teresa Conconi

Coordinatore d'indirizzo: Ch.mo Prof. Maria Teresa Conconi

Supervisore: Ch.mo Prof. Marcella Folin

Correlatore: Ch.mo Prof. Alessandra Bianco

Dottoranda: Fabiana Marchi

Obstacles are those frightful things you see when you take your eyes off your goal.

Henry Ford

INDEX

SOMMARIO

La struttura di un vaso sanguigno è relativamente semplice essendo principalmente composto da uno strato di cellule muscolari lisce (SMCs) incorporato in una matrice di collagene. Il lume interno è rivestito da cellule endoteliali (ECs) che costituiscono l'interfaccia tra il flusso sanguigno e la parete del vaso. Lo strato esterno è ricoperto da fibroblasti (FBs) e da tessuto connettivo (*Seunarine et al., 2008*). Sebbene impianti autologhi di arteria e di vena rappresentino la migliore opzione clinica per il *bypass* o la sostituzione di vasi sanguigni stenotici a causa di processi patologici o traumi, diversi limiti influenzano questa pratica, in particolare malattie vascolari preesistenti e la limitata lunghezza o la scarsa qualità dei sostituti (*Pektok et al., 2008; Nottelet et al., 2009*). Protesi vascolari in politetrafluoroetilene espanso (ePTFE) o *Dacron* sono attualmente utilizzate con successo per superare i limiti sopra riportati e per il *bypass* di condotti vascolari di medio e grande calibro, superiore a 6 mm. L'ingegneria tissutale dei sostituti vascolari (TEVGs) è un approccio alternativo per la costruzione di vasi di piccolo diametro (<6 mm) con la possibilità di controllare fenomeni di trombosi, iperplasia cellulare ed eccessiva produzione di matrice. Inoltre, *in vivo* devono essere assicurati il mantenimento della pervietà del *graft* e di adeguate proprietà meccaniche e la formazione di un endotelio funzionale (*Zhang et al., 2009*). Questo argomento rappresenta una questione cruciale da affrontare per superare gli inconvenienti dei sostituti di piccolo diametro e per poter usufruire di questi anche nel settore della chirurgia pediatrica. Tale approccio si basa sull'utilizzo di uno scaffold polimerico poroso a cui le cellule endoteliali (ECs) possano aderire così da formare un monostrato antitrombogenico con proprietà vasoattive (*Williamson et al., 2006*). Obbiettivo finale è la realizzazione di un costrutto trapiantabile in grado di adattarsi alle modifiche dell'ospite. Lo scaffold ideale dovrebbe essere dotato di buona biocompatibilità e biodegradabilità. Esso dovrebbe inoltre disporre di adeguate proprietà biomeccaniche e di ampia disponibilità di svariate dimensioni per una vasta gamma di applicazioni cliniche (*Tillman et al., 2009*). Con la tecnica dell'elettrospinning si ottengono supporti polimerici per sostituti vascolari con particolari caratteristiche: degradazione controllata durante il rimodellamento *in vivo*, riproduzione di un ambiente adatto alla crescita cellulare e in grado di mimare le proprietà fisiche e strutturali della matrice extracellulare (ECM) nativa (*Baiguera et al., 2009*). Le matrici polimeriche biodegradabili prodotte con la tecnica

dell'electrospinning, sono tra i materiali più promettenti, grazie alla loro somiglianza alla matrice extracellulare (ECM) (*He et al., 2009*).

Il poli(ε-caprolattone) (PCL) è un poliestere alifatico, ampiamente studiato come biomateriale; i suoi vantaggi sono la facilità di fabbricazione, la duttilità e l'elevata resistenza meccanica. Può essere prodotto come scaffold tubulare con le dimensioni richieste e con porosità e viscoelasticità ottimali (*Pankajakshan et Agrawal, 2010*). Tuttavia, la sua generalmente scarsa affinità cellulare, dovuta all' idrofobicità, la mancanza di molecole segnale e la sua lenta degradazione *in vivo* (*Nottelet et al., 2009*) sono aspetti che precludono la sua considerazione come materiale ideale per l'ingegneria tissutale (*Xiang et al. 2011*). Di conseguenza, la realizzazione di un *blend* di PCL con polimeri naturali potrebbe essere un approccio promettente nel campo dell'ingegneria tissutale vascolare (*Pankajakshan et Agrawal, 2010*). Inoltre miscele di polimeri sintetici e naturali hanno già mostrato buona citocompatibilità con cellule staminali mesenchimali (*Tang et Wu, 2005*). Il poli (3-idrossibutirrato-co-3-idrossivalerato) (PHBV) è un materiale naturale prodotto da numerosi batteri. La sua degradazione *in vivo* comporta il rilascio di idrossiacidi, meno acidi e meno infiammatori rispetto ad altri polimeri bioriassorbibili (*Williams et Martin, 2002*). Le sue varie proprietà quali l'origine biologica, la biodegradabilità, la biocompatibilità, la non tossicità (*Ke et al., 2010*) ne fanno un buon candidato per la realizzazione di *blend* con PCL.

Partendo da tali presupposti, in questo progetto sono stati valutati i seguenti materiali: *soft* poli(ε-caprolattone) (PCL), di origine sintetica e già approvato dalla *Food and Drug Administration*, *hard* poli(3-idrossibutirrato-co-3-idrossivalerato) (PHBV), di origine microbica, e il loro *blend* PCL/PHBV (50% PCL/50% PHBV). Le matrici polimeriche e gli scaffold tubulari elettrofilati sono stati progettati, prodotti e caratterizzati presso l'Università di Roma "Tor Vergata", Dipartimento di Scienze e Tecnologie Chimiche, dalla Prof. Alessandra Bianco e dall'Ing. Costantino Del Gaudio.

Nella prima fase del lavoro, è stata testata la citocompatibilità su matrici e su scaffold ricavati da strutture tubulari di piccolo calibro (diametro interno<6mm) tramite saggi *in vitro* utilizzando cellule endoteliali di ratti Sprague-Dawley da due diversi distretti: microcircolo cerebrale (RCEC) ed aorta (RAEC). Sono stati effettuati saggi di adesione, di vitalità e di proliferazione che hanno dimostrato che le matrici a base di PCL permettono la sopravvivenza e la migliore crescita delle RCEC. Nel caso di scaffold ricavati da strutture tubulari di PCL e PCL/PHBV, le RCEC hanno ricoperto la superficie

dei polimeri organizzandosi in un monostrato come nei vasi sanguigni nativi. Diversamente dalle RCEC, le RAEC sono cresciute costantemente e hanno colonizzato anche le matrici e gli scaffold ricavati da strutture tubulari di PHBV.

Nella seconda fase del lavoro è stata valutata la biocompatibilità delle matrici polimeriche di PCL, PHBV e PCL/PHBV mediante l'impianto *in vivo* nel tessuto sottocutaneo dorsale di ratti Sprague-Dawley per 7, 14 e 28 giorni. Tutti i ratti sono sopravvissuti e tutti i polimeri espiantati sono apparsi conservati nel loro aspetto e forma. La colorazione con ematossilina ed eosina ha dimostrato il completo riassorbimento della capsula fibrosa a 28 giorni, sui polimeri di PHBV e di PCL/PHBV. L'infiltrato cellulare infiammatorio è diminuito nel tempo mentre è aumentato il numero di cellule migranti che hanno colonizzato la zona di confine tra tessuto e matrice e in parte l'interno di quest'ultima. I risultati ottenuti *in vitro* ed *in vivo* sembrano indicare il *blend* PCL/PHBV come possibile materiale alternativo al PCL nel campo dell'ingegneria tissutale vascolare sia per le caratteristiche intermedie tra PCL, di origine sintetica, e PHBV, di origine naturale rispettivamente, sia per la degradazione e il rimodellamento più rapidi *in vivo* rispetto al PCL.

SUMMARY

The structure of a blood vessel is relatively simple; its main structural component is a layer of smooth muscle cells (SMCs) embedded in a collagen matrix. The interior lumen of the vessel is lined with endothelial cells (ECs), who form the interface between the flowing blood and the vessel wall. The outer layer of the tube is covered with fibroblasts (FBs) and connective tissue (*Seunarine et al.,2008*). Although autologous arterial and venous grafts represent the best clinical option to bypass or replace blood vessels that became stenosed by disease processes or trauma, several limitations affect this practice, being related to pre-existing vascular disease, prior surgery, limited length or poor quality (*Pektok et al., 2008; Nottelet et al., 2009*). Conventional vascular prostheses made of expanded polytetrafluoroethylene (ePTFE) or polyethyleneterephtalate (Dacron) are currently used to overcome the above reported limitations, being shelf-ready and available only for large blood vessel replacement. Tissue engineering (TE) is an alternative approach for the preparation of small-diameter vascular grafts (<6 mm) due to the potential to control thrombosis, cellular hyperplasia and matrix production. This control also requires the maintenance of graft patency *in vivo*, appropriate mechanical properties and the formation of a functional endothelium (*Zhang et al., 2009*). This topic represents a crucial issue to be addressed in order to overcome the drawbacks of small-diameter grafts and offer potentially growing devices for pediatric surgery. TEVGs needs a compliant polymer scaffold to which endothelial cells (ECs) can adhere, form an anti-thrombogenic monolayer and exhibit vasoactive properties (*Williamson et al., 2006*). For a new tissue to be generated or regenerated it requires a porous scaffold which acts as substratum for cell attachment in order to obtain a construct able to adapt to the host modifications to improve the clinical outcome after graft implantation. An ideal scaffold should have good biocompatibility and biodegradation characteristics. It should also have appropriate biomechanical properties, good saturability to ensure secure implantation, and availability in a variety of size for a wide range of grafting applications (*Tillman et al., 2009*). The electrospinning technology is efficient and cost-effective to produce polymeric mats and vascular grafts with definite characteristics to control their degradation during remodeling and to reproduce a suitable cell environment able to mimic the physical and structural properties of native extracellular matrix (ECM) (*Baiguera et al., 2009*). Bioresorbable polymeric

scaffolds produced by electrospinning are among the most promising materials due to their similarity to the native extra cellular matrix (ECM) (*He et al., 2009*).

The poly(ε-caprolactone) (PCL) is a synthetic aliphatic polyester, intensively investigated biomaterial; its advantages are ease of fabrication, pliability, and tunable mechanical strength. It can be produced to conduits with the required dimensions, optimum porosity and viscoelasticity (*Pankajakshan et Agrawal, 2010*). However, its generally poor cell affinity due to hydrophobicity, lack of cell-binding signals and its slow degradation rate *in vivo* (*Nottelet et al., 2009*) have become the major obstacle to be an ideal tissue engineering material (*Xiang et al., 2011*). Consequently PCL blended with natural polymers could be a promising approach in vascular tissue engineering (*Pankajakshan et Agrawal, 2010*). Moreover, blend of synthetic and natural polymers have shown good cytocompatibility with mesenchymal stem cells (*Tang et Wu, 2005*). The poly(3-hydroxybutyrate-co-3-hydroxyvalerate) (PHBV) is a natural material produced by numerous bacteria. Its *in vivo* degradation involves the release of hydroxy acids, less acid and less inflammatory than other bioresorbable polymers (*Williams et Martin, 2002*). Its various properties such as natural origin, biodegradability, biocompatibility, non-toxicity (*Ke at al., 2010*) make it a good candidate for blending with PCL.

Starting from these assumptions, in this project *soft* PCL, already approved by the Food and Drug Administration, *hard* PHBV and their intimate blend PCL/PHBV (50% PCL/50% PHBV) were considered. The electrospun bioresorbable polymeric mats and tubular scaffolds were designed, produced and characterized at the University of Rome "Tor Vergata", Department of Science and Chemical Technology, by Prof. Alessandra Bianco and Eng. Costantino Del Gaudio.

In the first step of the work, cytocompatibility studies were addressed. Sprague-Dawley rat endothelial cells from two different compartments, cerebral endothelial cells (RCECs) and aortic endothelial cells (RAECs) were seeded on polymeric mats and samples cut out from tubular scaffolds of small caliber (inner diameter <6 mm) in *in vitro* static culture to assay adhesion, viability and proliferation. The biological results have shown that the mats based on PCL allowed the survival and better growth of RCECs. In case of samples cut out from the tubular structures of PCL and PCL/PHBV, the RCECs have covered the surface of scaffolds by organizing themselves into a monolayer as in the native blood vessel. On the contrary, the

RAECs have grown steadily and have also colonized mats and samples cut out from the tubular scaffolds of PHBV.

In the second step the PCL, PHBV and PCL/PHBV mat biocompatibility has been evaluated by implanting them *in vivo* in the Sprague-Dawley rat dorsal subcutaneous tissue for 7, 14 and 28 days. All rats survived and all explanted mats were integrated into the host tissue, were partially vascularized and preserved their appearance and shape. The PHBV mat explants folded during the time lapse but their form was conserved. Explanted polymeric mat sections, stained with hematoxylin and eosin, showed a complete PHBV and PCL/PHBV fibrous capsule resorption at 28 days. The inflammatory cell infiltrate decreased over time whereas migratory cells increased. They colonized the border area and the polymeric mat inner part. The results obtained *in vitro* and *in vivo* experiments suggest the blend PCL/PHBV as a possible alternative material to the PCL in the field of vascular tissue engineering, thanks to its intermediate characteristics between synthetic (PCL) and natural (PHBV) material and thanks to a more rapid *in vivo* degradation and remodeling compared to PCL.

ABBREVIATIONS

A	Absorbance
BSA	Bovine Serum Albumin
DAPI	DiAmidino-2-Phenyl-Indole
DMTA	Dynamic Mechanical Test Analysis
E	Tensile Modulus
EC	Endothelial Cell
ECM	ExtraCellular Matrix
EPCs	Circulating Endothelial Progenitor Cells
FB	Fibroblast
FDA	Food and Drug Administration
GAG	GlycosAminoGlycans
MIT	Massachusetts Institute of Technology
MPa	MegaPascal
MTS	3-(4,5-dimethylthiazol-2-yl)-5-(3-carboxymethoxyphenyl)-2-(4-sulfophenyl)-2H-tetrazolium, inner salt
MV2	Endothelial Cell Growth Medium
PBS	Phosphate Buffer Solution
PBS	Phosphate Buffer Solution
PCL	Poly(ε-CaproLactone)
PGA	Poly(Glycolic Acid)
PHA	PolyHydroxyAlcanoates
PHBV	Poly(3-HydroxyButyrate-*co*-3-hydroxyValerate)
PLA	Poly(Lactic Acid)
PLGA	Poly(Lactic-Glycolic Acid)
PTFE	PolyTetraFluoroEthylene
RAEC	Rat Aortic Endothelial Cell
RCEC	Rat Cerebral Endothelial Cell
SC	Stem Cell
SEM	Scanning Electronic Microscopy
SMC	Smooth Muscle Cell
SRS	Suture Retention Strength
TE	Tissue Engineering
TEVG	Tissue Engineering Vascular Graft
TS	Tensile Strength
vWF	von Willebrand Factor

1 INTRODUCTION

Cardiovascular diseases, such as myocardial infarction, peripheral circulatory disorders, coronary occlusion and atherosclerosis are the leading cause of death in Western countries (*Rainer et al., 2010*). The treatment of these diseases involves tissue transplantation and organ replacement surgery by means of natural or synthetic materials and drug therapy.

The simple structure of a blood vessel includes smooth muscle cells (SMCs) embedded in a collagen matrix, endothelial cells (ECs) lining the vessel inner surface, fibroblasts (FBs) and connective tissue in the vessel outer side (*Seunarine et al., 2008*). Although arterial and venous autologous substitutes represent the best clinical choice to bypass or replace blood vessels clogged due to diseases or traumas, their use is limited in the clinical practice due to concomitant diseases, the lack of immunologically compatible cells, the non-availability of biomaterials owning appropriate mechanical, chemical and biological properties, and finally the difficulty to easily regenerate and integrate vascular tissue into the host circulatory system (*Pektok et al., 2008; Nottelet et al., 2009*).

Until now the biomaterials used in the clinical field have been various and dependent to a specific application, as shown in Figure 1 (*Chlupác et al., 2009*).

	Vascular regions				
Vascular substitute choice	**Large-caliber arteries (≥ 8 mm)**	**Medium-caliber arteries (6-8 mm)**	**Small-caliber arteries (≤ 6 mm)**	**Venous reconstructions**	**Hemodialysis arterio-venous access**
	Aorta, arch vessels, iliac and common femoral arteries	Carotid, subclavian, common femoral, visceral and above-the-knee arteries	Coronary, below-the-knee, tibial and peroneal arteries	Superior and inferior vena cava, ilico-femoral veins, portal vein, visceral veins	Upper > lower extremity
1st choice	Prosthesis (Dacron, ePTFE)	Prosthesis or autograft (equal)	Arterial or venous autograft	Saphenous spiral vein graft, deep venous autograft	Native material
2nd choice	Allograft, deep venous autograft	Prosthesis or autograft	Composite graft, vein interposition, prosthesis (ePTFE, Dacron), allograft, biosynthetic	Allografts, ePTFE, Dacron, biografts	ePTFE, PU, xenografts, biografts, TEBV (clinical trial)

ePTFE (expanded polytetrafluoroethylene), PU (polyurethane), TEBV (totally-engineered blood vessels).

Fig. 1: Vascular substitutes in clinical use (*Chlupác et al., 2009*).

In particular, the use of biomaterials, such as Dacron ™ (PET) or Teflon ™ (PTFE) demonstrated to be a successful strategy to prepare vascular substitutes greater than 6 mm in diameter. In contrast, vascular smaller diameter grafts demonstrated to fail within 5 years (*Leon et Greisler, 2003*), due to intimal hyperplasia, plaque formation, stenosis, sclerosis and occlusion of vessel. The use of blood vessels prepared with these materials is therefore limited to cases where there are high flows and low resistance conditions. In particular, the failure of these biomaterials for a wider use is due to their low elasticity and pliability to the blood flow (compliance), to their thrombogenicity surface and finally to their inability to accommodate the growth of new cells (*Pankajakshan et Agrawal, 2010*).

In the last decade, the request of a suitable small-diameter vascular graft has led the world scientific community to explore different strategies (*Nuti, 2010*).

In this context, tissue engineering of blood vessels revealed to be functional to overcome the above mentioned limits of small vascular grafts (thrombosis, intimal hyperplasia) providing engineered vessels transplantable *in vivo* and prepared with autologous vascular cells seeded on natural or synthetic scaffolds. A successful tissue engineered blood vessel substitute is prepared using a porous and biodegradable polymeric scaffold to allow the cell adhesion/growth and the deposition of neo-extracellular matrix (ECM). The construct must adapt to the host changes through the remodelling process in order to improve long-term results of transplantation.

1.1. Tissue Engineering

Tissue engineering (TE) is an interdisciplinary field that applies the principles of engineering and biology to the development of biological substitutes to restore, maintain or improve the function of damaged tissues and organs (*Langer et Vacanti, 1993*). In TE expertise in cell biology, engineering, materials science and surgery coexist in order to construct new functional tissues, by combining cells and materials. Therefore, it’s important to understand the cell-substrate interactions, the transport of biomolecules into the matrix, cell differentiation and to study technologies to control the chemical and physical-mechanical processes to regulate blood flow into matrix. The aim of TE is the realization of a "living tissue" that better represents the unique characteristics of each patient. In fact, the cells can be isolated from an healthy patient, expanded and/or modified by means of gene therapy *in vitro* and *in vivo*, and then transplanted into a

damaged site. However, the success of the engineered tissue *in vivo*, despite the progress made in isolation and *in vitro* culture of large numbers of cells and the design of biomaterials, depends on the survival of cells seeded for as long as possible. The scaffold, consisting of biological matrices, synthetic biomaterials (polymers, ceramics, metals or composites), or derived from biological sources (for example: chitosan, collagen, alginate, glycosaminoglycans) (*Cortesini, 2005*), must have appropriate biomechanical properties and microstructure to preserve the integrity of the tissue in long term.

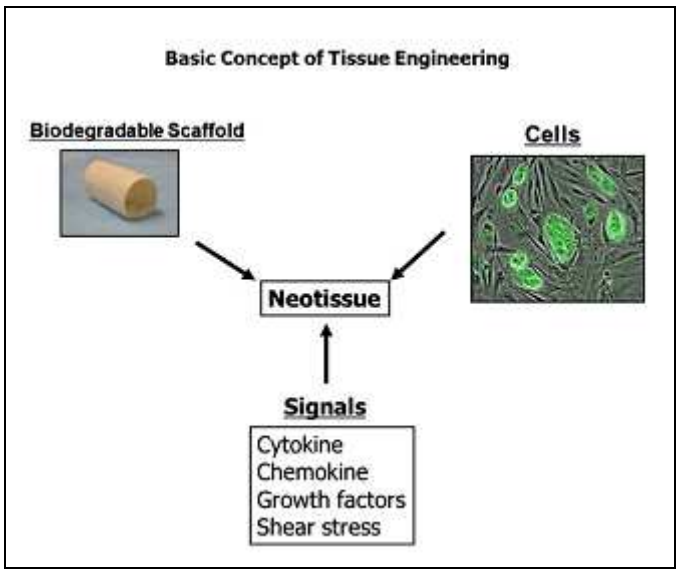

Fig. 2: Basic concepts of TE (*Naito et al., 2011*).

Until now, the main techniques for *in vitro* tissue reconstruction are three:

1. cell injection, after appropriate *in vitro* expansion, directly in the organ as in the liver and in the pancreas (*Gould et al. 1977; Gupta et al., 1987*);
2. encapsulation (closed system) of cells in a semi-permeable membrane to protect them from the host immune response. This type of approach has been successful in treating diseases such as Parkinson's disease in animal models (*Aebischer et al., 1988*);
3. open system in which the cells are expanded *in vitro* and seeded onto biodegradable polymer matrix and then implanted *in vivo*.

The matrices are used as a support and guide for the reorganization of cells and the spread of nutrients. The blood supply comes from the host tissue and can be stimulated by binding angiogenic factors to the matrix. The materials can be natural or synthetic and must possess two important characteristics: to be biocompatible and to provide nutritional support to cells. In TE the cells used can be autologous, allogenetic or xenogenetic and

characterized by different differentiative potentials. Currently, the approach followed in the field of TE involves the combination of different cell types and biodegradable natural or synthetic matrices, and the use of dedicated bioreactors (*Shieh, 2005*).

In vitro and *in vivo* studies led to the production of vascular and cardiovascular components, bone, cartilage, nerves, skin, gastrointestinal and urinogenital tissues. Over the past twenty years at Harvard Medical School in collaboration with the Massachusetts Institute of Technology (MIT) over 30 different types of complex biological and functional tissue have been developed in animal models (*Shieh, 2005*). Autologous chondrocyte transplantation to repair the knee (*Mayhew et al., 1998*) are used daily. Nowadays skin, cartilage, bones, blood vessels, corneas, and urinary structures are in clinical trials in humans (*Vacanti, 2010; Lysaght, 2008*) while the Food and Drug Administration (FDA) approved at least 5 engineered tissues: dermal substitutes, epidermal and cartilage (*Shieh, 2005*). Moreover, some results about the first experiments on the *in vitro* growth of "organoids" and organs such as kidneys, liver and heart begin to be available (*Shieh, 2005*).

1.1.1. The tissue engineering triad

The triad of TE is based on the following factors, among them independent, but essential to produce a highly organized tissue (*Bell, 2000*):

- cells
- scaffolds
- signal molecules.

The success of the technique depends on the cell culture, the ability of the scaffold to provide mechanical support, to promote cell growth and ensure the direct and indirect control of intercellular contacts (*Molnar 2010*). The use of 3D scaffolds with high porosity and able to mimic the native ECM ensures the recognition which is necessary to promote cell colonization in order to obtain a biological functional tissue (*Harrington et al., 2008*).

Cells

Cells play a crucial role in the repair and regeneration processes of tissues due to their biological and functional characteristics including: proliferation, differentiation, intercellular interactions, production of biomolecules, formation of the ECM. The cellular sources may be autologous (cells are taken from the same individual and transplanted, eliminating rejection problems), syngenetic (taken from an individual genetically

identical), allogenetic (taken from a different individual of the same species) or xenogenetic (taken from a different individual of different species).

The ideal cells for TE should be:

- ✓ readily available;
- ✓ easily doubling without phenotypic or functional alteration;
- ✓ not able to transmit pathogens interspecies;
- ✓ able to differentiate into different cell types;
- ✓ lead to a minimal immunological response.

The strategies adopted so far are very different. The colonization of the biomaterial can be performed *in vitro* using differentiated adult cells to perform a particular function (as in the case of skin substitutes containing keratinocytes and/or FBs) and *in vivo* transplanting the scaffold in the organism or in a mixed way: first incubating in cell culture the 3D biomaterial and early transplanting it in the body. TE uses cells derived from primary cultures, that is derived from an organism, or cell lines from cell banks. Recently it has been proposed to use as the universal source of cells, stem cells (SCs) which have excellent characteristics in terms of differentiation.

Scaffolds

The other key component of TE is the scaffold that is not only material support but also a mean to deliver cells precise signals to activate specific cellular processes.

The main characteristics of these scaffolds are:

- ✓ high porosity and 3D structure with a network of interconnected pores to allow cell growth, nutrient transport and elimination of waste substances;
- ✓ high biocompatibility to avoid any form of rejection;
- ✓ controlled biodegradability, to allow cell growth *in vitro* and/or *in vivo*;
- ✓ surface chemically suitable for cell adhesion, proliferation and differentiation;
- ✓ mechanical properties similar to those of the tissues that will be replaced by the scaffold;
- ✓ easy reproducibility, in different shapes and sizes.

The materials studied for TE applications as scaffolds can be grouped into four categories:

1. natural or organic materials (collagen, fibrin gel, hyaluronic acid, chitosan, gelatine);
2. natural inorganic materials (coral hydroxyapatite);
3. synthetic organic materials (aliphatic polyester [*Dacron*], polyethylene glycol, polylactide, polyamide [*Nylon*], polytetrafluoroethylene [*Teflon and Gore-Tex* ®]);
4. synthetic inorganic materials (hydroxyapatite, plaster, calcium phosphate, ceramic glass).

Generally natural materials are preferred because they closely reproduce the native cellular environment. However the benefits in terms of control of the mechanical properties, offered by synthetic materials, make the choice very hard and linked to the type of application.

A fast evolution has been observed for the scaffold materials: between 1960 and 1970 materials biologically "inert" were used, which did not give rise to any type of response by the biological tissues, no inflammation, no adhesion and no cell growth (first-generation biomaterials). The second generation of biomaterials (for example ceramics, hydroxyapatite) stimulated a "bioactive" response by biological tissues. Today the third generation of biomaterials should have the ability to integrate the two features in order to stimulate a specific cellular response (*Hench et al., 2002*). With this latest generation, biomaterials become able to promote complex biological events such as cell adhesion and migration or the controlled release of growth factors. An appropriate characterization is useful to identify the main properties of the materials. The scaffold is therefore a determining factor, as it promotes the organization of the cells until the complete three-dimensional tissue formation, and then it is gradually replaced by regenerated tissue, very similar to the original, with a degradation rate comparable to the rate of cellular synthesis.

Signal molecules

A third component, useful but not essential in TE to obtain optimal implants, consists of signalling molecules such as adhesion, angiogenic and growth factors, that are placed in the support. These are able to differentially activate genes, whose products are responsible for the growth and differentiation of tissue. In fact, because the replaced engineered tissue must display the same function of damaged tissue, vascularization and innervation *in vivo* must be also promoted. Cells about 50 µm from the blood are

metabolically inactive or necrotic due to limited diffusion of oxygen and nutrients. Consequently, it is necessary to encourage the growth of blood vessels through the new tissue, incorporating angiogenic factors and promoting the regeneration of peripheral nerves with guide channels and nerve growth factors (*Barbarisi et al., 2010*).

Once assembled these three components *in vitro*, the processes that occur during the formation and maturation of tissue are:

- cell proliferation and differentiation;
- production and organization of the ECM;
- degradation of the scaffold;
- remodelling *in vivo* and tissue growth.

Three fundamental moments characterize TE technique:

- explant of natural tissue;
- tissue engineering application;
- realization of the biological engineered substitute.

In these three passages, the innovative and essential step is represented by its own engineering that determines the fundamental changes in the tissue of origin to obtain a final product that is implantable in humans and is able to facilitate or determine in different ways tissue repair. To date in reconstructive surgery, synthetic polymers are not able to provide the quality and functionality of the original tissue, since they may rupture and induce an immune response. Moreover, contrary to natural materials, most of them are not colonized by host cells and then transformed into a living tissue. TE is one of the most promising sectors able to solve these problems and to ensure greater availability of tissues, that leads to the realization of biological products with such characteristics to be used in clinical practice like skin tissue healing, bone reconstruction and, more generally, in the *in vitro* expansion of cells.

1.1.2 Vascular tissue engineering

The aim of vascular tissue engineering is to develop tissue-engineered, biocompatible, small-diameter vessels suitable to withstand *in vivo* systolic pressures as well as to be immunologically compatible with the patient, in order to minimize graft rejection.

Autologous veins or arteries are sometimes not considered ideal for a patient undergoing a coronary artery bypass grafting procedure due to complications such as artery disease, trauma, and/or previous surgery(*Khait et Birla, 2011*).

The idea of creating an *in vitro* blood vessel was first proposed in 1986 by Weinberg and Bell, who used tubular structures in collagen gel. They built the first Tissue Engineering Vascular Graft (TEVG) with ECs, SMCs and FBs from bovine aorta. Over time, different methods have led to the creation of blood vessels with adequate biological features using hydrogels, synthetic polymer scaffolds biodegradable, biological cell-free matrices or assembly of cell mono-layers (*Mironov, 2008*). To proceed to transplant surgery is necessary that the engineered replacement is not thrombogenic, but vasoactive and with biomechanical characteristics similar to those of native vessels (*Nerem, 2001*). Cytograft Tissue Engineering Inc. in the U.S. has produced vascular substitutes based on the assembly of cell monolayers in a bioreactor. The positive results are still strongly limited by issues related to the use of the bioreactor such as long timing, high costs, laborious process and not automated. In 1999, Niklason et al. have pioneered the use of a biodegradable synthetic scaffold of poly(glycolic acid) (PGA) seeded with ECs and SMCs from porcine aorta. More recently, applying the same technique remarkable results were obtained with engineered vascular substitutes in the pulmonary circulation of calves (*Shin'oka et al., 2001*). This success has allowed the transfer of clinical trial in transplanting engineered pulmonary artery in a child with a complex congenital heart disease and pulmonary atresia (*Shin'oka et Breuer, 2008*). As mentioned before TE requires viable cells, in this case ECs and SMCs. The most important *in vivo* function of ECs is the thrombus resistance. Indeed, the presence of a continuous monolayer on the scaffold inhibits the formation of thrombi and prevents the development of hyperplasia of the *intima* inhibiting the synthesis of bioactive substances responsible for the migration and proliferation of SMCs and ECM production. However, the literature shows that the functionality of the ECs is less than 10% compared to that of the native vessel cells and this can be explained by their limited capacity for regeneration: their growth stops at 1-2 cm anastomoses in vascular substitutes transplanted in humans (*Naito et al., 2011*).

Several mechanisms have been proposed to explain the endothelialization of vascular substitutes:

- the presence of seeded ECs;
- migration of the ECs through anastomoses from the native vessel;
- the deposition of circulating endothelial progenitor cells on the luminal surface of the substitute;
- the growth of ECs derived from the capillaries that pass through the pores of the substitute (transmural endothelialization).

As in the past ECs were suggested to be not able to produce a stable *intima* without SMCs and FBs, different cell types have been used by Noishiki et al. in 1998 to promote the formation of the endothelial monolayer with variable results depending on the choice. SMCs seeded onto biodegradable scaffolds and implanted in the aorta of rats showed a rapid development of an uniform neo tunica *media* (*Naito et al., 2011*).

1.2. Native blood vessels

1.2.1. Vasculogenesis and angiogenesis

The blood vessels penetrate every organ and tissue to supply cells with nutrients and oxygen, providing for the circulation of fluids and various signalling molecules. The formation of new vessels occurs by two different processes: vasculogenesis and angiogenesis.

Vasculogenesis is the *ex novo* formation of blood vessels. This process occurs in embryogenesis, in the growth and in the regeneration of tissue during wound healing, while in adult age, the vascularization is generally quiescent, and blood cell renewal takes years (*Persson et Buschmann, 2011*). The development of the blood vascular system, is one of the first events in embryogenesis. During early embryonic development, mesodermal cells differentiate into hemangioblasts, progenitors of both hematopoietic and ECs giving rise to blood vessels. During differentiation, hemangioblasts produce angioblasts and their aggregation results in the formation of blood islands. The fusion of blood islands results in the appearance of the primary blood vascular plexus consisting of fine capillaries formed by ECs. At this stage capillaries acquire an arterial or venous character. The stage of vasculogenesis is completed together with the formation of the primary vascular plexus and all further transformations of the vascular net proceed during angiogenesis (*Karamysheva, 2008*).

Angiogenesis is the outgrowth of new vessels from pre-existing capillaries. It is an essential process during embryogenesis, wound healing and the ovarian cycle but it also plays a major role in several pathologic processes such as tumor vascularisation, diabetic retinopathy, psoriasis and rheumatoid arthritis (*Bouïs et al., 2006*). In adults, formation and growth of new vessels are under strict control. These processes are activated only under strictly defined conditions like wound healing. Strict regulation of this system and balanced functioning is very important for the organism because both excessive formation of blood vessels and their insufficient development lead to serious diseases (*Karamysheva, 2008*). The process of capillary growth has been studied by scientists since 1939 when Clark and Clark (1953) observed the process in real time using intravital microscopy of the microvascular network within rabbit ear chamber. In the early 1970s Gimbrone and colleagues (1973) first achieved the establishment of long-term EC cultures. Subsequently the development of *in vitro* models of capillary network formation contributed to the understanding the angiogenic process (*Folkman et Haudenschild, 1980*).

The most common stimuli for the angiogenesis are the lack of oxygen (hypoxia), a reduced blood supply (ischemia), mechanical factors and inflammatory processes. In response to these specific signals ECs, which play a key role in angiogenic phenomenon, degrade the basement membrane with appropriate enzymes (protease) and migrate toward the source of stimuli, where they proliferate, get mature, release growth factors, and form new capillaries recalling SMCs and also periendothelial cells (*Kurz, 2000*).

Almost all cells of vertebrates are probably located not more than 50 µm from a capillary. Similarly, after injury, an explosion of capillary growth is stimulated all around the damaged tissue (*Kovacs et Di Pietro, 1994*). Local irritant agents and infections cause the proliferation of new capillaries, but the process regress and disappear when the inflammation disappears (*James et Anderson, 1993*).

The formation of new blood vessels is also an important process of cancer progression: it promotes the transition from hyperplasia to neoplasia, the transition from a state of cell growth to a state of uncontrolled proliferation, characteristic of cancer cells (*Pontini, 2010*). The development of cancer is closely bound to the supply of oxygen and nutrients; a cancer with not sprayed blood vessels, has a limited size growth as it depends on adjacent cells for survival.

1.2.2. Blood vessel anatomy

Blood vessels are the channels or conduits through which blood is distributed to body tissues. Based on their structure and function, blood vessels are classified as either arteries, capillaries, or veins. Arteries carry blood away from the heart and branch repeatedly into smaller and smaller arteries until into microscopic arterioles. The arterioles play a key role in regulating blood flow into the tissue capillaries. Capillaries, the smallest and most numerous of the blood vessels, form the connection between the vessels that carry blood away from the heart (arteries) and the vessels that return blood to the heart (veins). The primary function of capillaries is the exchange of materials between the blood and tissue cells. Veins carry blood toward the heart. After blood passes through the capillaries, it enters the smallest veins, called venules. From the venules, it flows into progressively larger and larger veins until it reaches the heart.

Arteries are muscular-membranous canals, lined inside with ECs, originate from the heart ventricles and lead towards the peripheral areas of the body, branching into channels more and more slender, up to lead to capillaries (*Pasqualino et Nesci, 1980*).

The artery wall consists of three tunics, which are called from outside to inside: *adventitia*, *media* and *intima*. The *adventitia* consists of connective tissue composed by fibrillary collagen and elastic fibers, the *media* is made of elastic *laminae* between which there are collagen fibers and SMCs circularly oriented, and the *intima* consists of a layer of ECs that delimits the vascular cavity. The endothelium, by means of a thin basal membrane, rests on a layer consisting of connective tissue mainly composed by fibrillary collagen, between it and the *media* there is the internal elastic *lamina* (*Pasqualino et Nesci, 1980*).

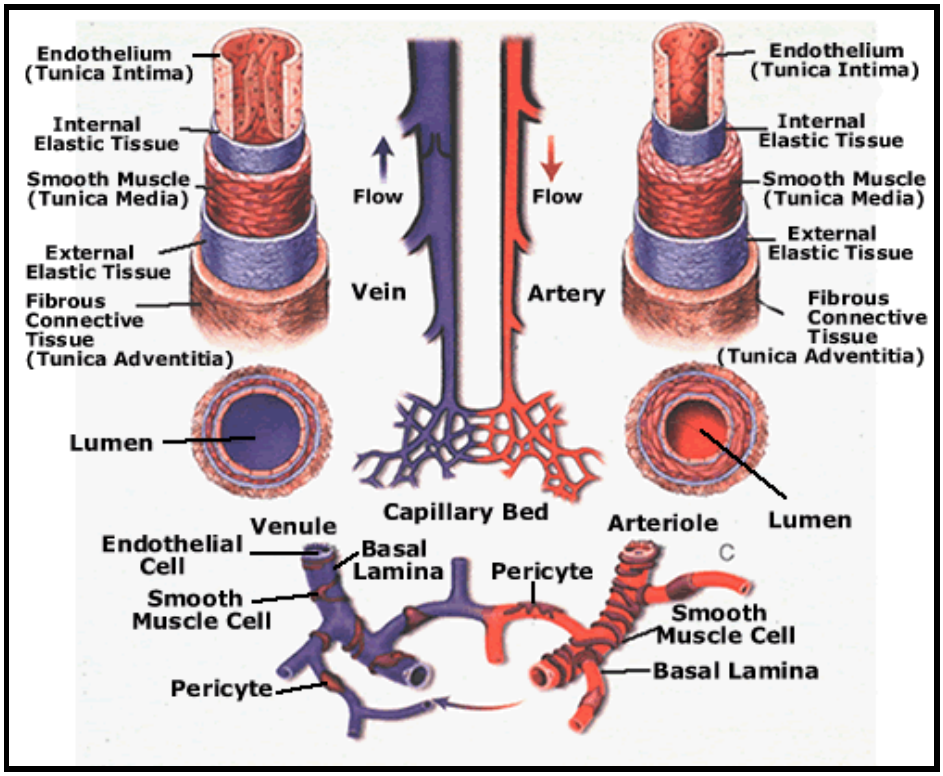

Fig. 3: The blood vessels anatomy (*Marieb et al., 2007*).

Arteries have thick walls and are capable of resisting high blood pressures. The capillaries have the thinnest walls and are highly permeable to water and small solutes (*Pasqualino et Nesci, 1980*). They derived from the most fine branches of arterioles and they are arranged into a network. Their main function is to allow the exchange of molecules and gas between blood and tissues. The capillary wall is composed of endothelium set on a thin basal *lamina*.

The veins are large vessels with thin walls (*Pasqualino et Nesci, 1980*). Most of them have valves that allow blood to reach the heart but not to flow to the periphery. The vein structure is very similar to that of the arteries even if the distinction between the three tunics is not always clear, the vein walls are thinner and less elastic than artery and when the vein is empty they are usually collapsed. The structural distinction among the veins of small, medium and large diameter, is difficult, but in all cases, the *tunica media* is poorly developed. All the layers that make up a native blood vessel contribute to its natural function (*Pasqualino et Nesci, 1980*). The continuous and smooth monolayer over the inner surface of vessels is formed by ECs that are on inactive state and aligned in the direction of the flow to increase cell retention. In the middle layer, SMCs, are arranged in a circular direction and are in non-proliferative state. The outer layer, the *adventitia*,

consists of collagen and FBs producing connective tissue. The combination of collagen and elastin in vessels produces an anisotropic viscous-elastic structure that allows to vessel greater elasticity at low pressure and higher stiffness at high pressures (*Baguneid et al., 2006; Isenberg et al., 2006*).

The endothelial tissue is a special type of epithelial tissue, derived from mesenchyme and morphologically similar to simple epithelial tissue. It is the cellular layer lining the inner surface of blood and lymph vessels. It lies on the basement membrane, including two layers named *basal lamina* in contact with the endothelium, and *reticular lamina* in the outer side. The basal lamina layer can further be divided into *lamina lucida*, the clear layer closer to the epithelium, and *lamina densa*, the dense part in contact with to the connective tissue (*Calò et Semplicini, 1998*). The basement membrane contains laminin, a structural glycoprotein that allows ECs to anchor the type IV collagen of the membrane, fibronectin, type IV collagen and heparan sulfate that play an essential role in the overall organization of the endothelial basement membrane. At the capillary level, there are pericytes with contractile activity in support to vessels (*Hirschi et D'Amore, 1996*).

1.2.3. Morpho-functional aspects of vascular endothelium

The vascular endothelium is a veritable "endocrine breeding ground", producing a range of factors involved in the general vascular homeostasis. It has been recognized the crucial role of this structure in the regulation of vascular tone of the underlying SMCs, through a balance between vasoconstrictor and vasodilatory substances. Moreover, the endothelium has demonstrated to affect thrombolytic and fibrinolytic processes by the release of coagulants or anticoagulants and also the growth and vascular remodelling by the production of factors with proliferative and anti-proliferative activities. Finally, it contributes to the regulation of vascular permeability by substances involved in the inflammatory process (*Calò et Semplicini, 1998*).

ECs are mechanically stimulated by the blood flow (*Gimbrone et al., 1997*) by friction stress (*shear stress*) and *tensive stress*. The *shear stress* is produced by the friction of the laminar flow on the endothelium and affects only ECs, while *tensive stress* is produced by hydrostatic pressure inside the vessel and it interests the entire vessel wall (endothelium, FBs, SMCs). The *shear stress* activates ECs and promotes the release of vasodilator mediators, while *tensive stress* stimulates SMCs directly, inducing their contraction, and produces the EC stretching. The net effect on vascular tone results from the interaction between muscle contraction induced by pressure and endothelium-dependent flow-

induced dilation (*Calò et Semplicini, 1998*). The endothelium role in modulating the response to the flow changes was evidenced by Holtz (1983), that observed for the first time that the flow-induced dilation is *in vitro* and *in vivo* dependent on the endothelium integrity.

1.2.4. The endothelial cell (EC)

The EC is a mononuclear, polygonal, flat cell, about 30x10 μm in its largest and smallest diameters, respectively. It is connected with surrounding cells by juxtaposition of their membranes and/or through particular areas of the plasma membrane. Under normal conditions the arterial ECs appear elongated, arranged along the axis of blood flow. Venous ECs, however, may have polygonal shape and appear thicker (*Calò et Semplicini, 1998*).

By electron microscopy observation EC presents a luminal surface, an abluminal side and some specialized structures located on remaining parts. The luminal surface includes the areas located on surface facing the lumen, and is covered with a layer of mucous material, made of sulfate glycosaminoglycans, heparan sulfate, and glycoproteins. In the opposite side, the abluminal area takes the contact with the basement membrane, showing the course of "stress fibers" of cytoskeleton. On the side parts of EC membrane numerous intercellular junctions link adjacent cells into a continuous layer, including tight junctions and gap junctions. The tight junctions are areas of occlusion, responsible of the endothelial barrier function, while the gap junctions are areas of least resistance, that allow the ECs to communicate to each other. At the level of tight junctions the communication is prevented by the occlusion of the intercellular space by the plasma membranes of adjacent cells making them impervious to the transport of molecules. These junctions are dynamic structures that can be formed in different conditions, both *in vivo* and *in vitro*. Their structural complexity is related to their permeability that changes from one tissue to another (*Wolburg et al., 1994*). In the gap junctions, however, plasma membranes are closely juxtaposed till to block the intercellular space and permit the molecular exchange between cells only by intercellular channels. At microscopic level, gap junctions are composed of six associated subunits to form a cylindrical structure, which has a central channel. They probably participate in the development of metabolic cooperation and perhaps even to control the vascular endothelial growth (*Dejana, 1996*).

The cytoplasm of the EC contains a nucleus of oval shape, the Golgi apparatus, ribosomes, mitochondria and therefore it has all the facilities necessary to synthesis of

proteins and molecules, including glycosaminoglycans and substances involved in coagulation and fibrinolysis. The cytoskeleton is extremely important to maintain the cell shape. It consists of bundles of actin microfilaments, forming a peripheral system that assemble under the plasma membrane. The filaments of the cytoskeleton connect the basement membrane with the tight junction located on the sides of the cell. Weibel-Palade bodies are characteristic of the ECs. At the electron microscope they have the form of rods, covered by a membrane, containing arranged tubules in parallel to the major axis of the cell. Weibel-Palade bodies contain the antigen bound to factor VIII (von Willebrand protein) (*Craig et al., 1998*).

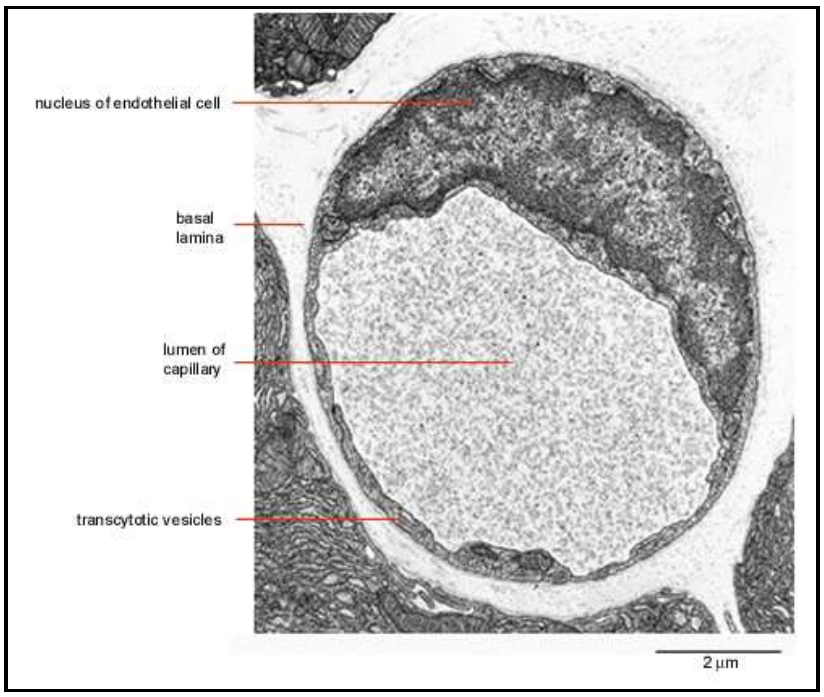

Fig. 4: Electron micrograph of a small capillary in cross-section. The wall is formed by a single endothelial cell surrounded by a basal lamina (*Bolender, 1974*).

Among the *in vivo* physiological functions of endothelium, the most important is the promotion of thromboresistance (*Vane et al., 1990*). A confluent monolayer of ECs on synthetic graft improves thromboresistance and prevents the development of pseudointimal hyperplasia by inhibition of bioactive substances responsible for SMC migration, proliferation and production of ECM (*Naito et al., 2011*).

1.2.5. The smooth muscle tissue and the smooth muscle cell (SMC)

The smooth muscle tissue, also known as involuntary, is formed by elongated elements: the SMCs, whose length varies from 25 to 80 µm. The fiber cells, characterized by oval or rod-shaped central nucleus and long and thin ends, are in close contact with each other, so the thin ends go between the thick parts of neighbouring cells, filling the intervals among the fiber cells. Gap junctions between adjacent fiber cells allow the contractile impulse propagation (*Motta, 1990*). The sarcoplasm contains myofibrils, short mitochondria, the Golgi apparatus, glycogen granules, lipid droplets and a poorly developed endoplasmic reticulum.

In blood vessels SMCs are gathered in small bundles within the connective tissue, and are associated to form sheets of different thickness. On the wall of the arteries SMCs are oriented circularly and innervated by the sympathetic nervous system: their contraction causes the constriction of the vessel lumen (*Chan-Park et al., 2009*).

1.2.6. The extracellular matrix (ECM)

The tissue generation is ensured by a dynamic interaction between the specific tissue cells and their microenvironment that appears to be largely made up of the ECM and other cell types (FBs, macrophages, mast cells and plasma cells) that the cell population interacts with. Until not so long ago it was suggested that the ECM was inert, only a scaffold for the physical stabilization of living tissues. Afterwards, it was shown that ECM is not only a mechanical support, but it has also an active role in regulating cell behaviour, influencing cell survival, development, migration, proliferation, shape and function (*Alberts et al. 1995*).

It’s main functions could be summarized as following listed:

1. determines the biomechanical properties of the tissue like strength and shape;
2. acts as a biological active support within cells can adhere and migrate;
3. regulates the cellular phenotype;
4. allows binding of many proteins such as growth factors and enzymes with protease activity and their inhibitors.

Biodegradable synthetic or organic scaffolds are used in Tissue Engineering (TE) as transient scaffolds that are replaced in time by ECM secreted by the colonizing cells. To be considered ideal TE substitutes, biomaterials should have biomechanical properties similar to native ECM as the cell growth and differentiation require a structured and

organized environment where cells can adhere to (*Naito et al., 2011*). The tissue mechanical properties depend on the formation of cross-linking bonds between molecules of collagen and elastic fibers, giving then passive resistance.

The ECM is composed of two essential molecules: the glycosaminoglycans (GAG) and fibrillary proteins. There are also small amounts of structural glycol-proteins with important roles in cellular adherence. The general structure appears like a network of scattered cells, which produce an abundant and organized network of fibrillary proteins arranged within a hydrated gel of GAGs (*Brooke et al., 2003*). Other tissue cells are anchored by means of cell-matrix junctions. The GAGs are unbranched polysaccharide chains composed of repeating disaccharide units of 70-200 residues. They can be divided into four groups, depending on the structure: hyaluronic acid, chondroitin and dermatan sulfate, heparan sulfate and heparin, keratin sulfate. They form the hydrated matrix of supporting tissues, whose properties are determined by the charge and the spatial arrangement of GAGs. There is great variability in their distribution in different tissues, which probably reflects the local needs for specific pore size and for the charge in the ECM (*Bowers et al., 2009*). The sulphite group (SO^{3-}) makes highly negatively charged these molecules and contributes to their ability to retain Na^{+} and water, because they do not fold into compact structures, but maintain a permanently open spiral structure, which gives them an intrinsic turgor. With the exception of hyaluronic acid, glycosaminoglycans bind covalently to proteins to form proteoglycans. Their spatial organization and charge facilitate the selective diffusion of molecules, probably allowing the opening of pores of various sizes in the gel matrix. Many proteins that form the backbone of proteoglycans have been isolated and characterized. The four proteins that form the fibrils in the ECM are collagen, elastin, fibrillin, fibronectin. Their role is to provide different elastic properties to support and anchor the cellular elements to tissues.

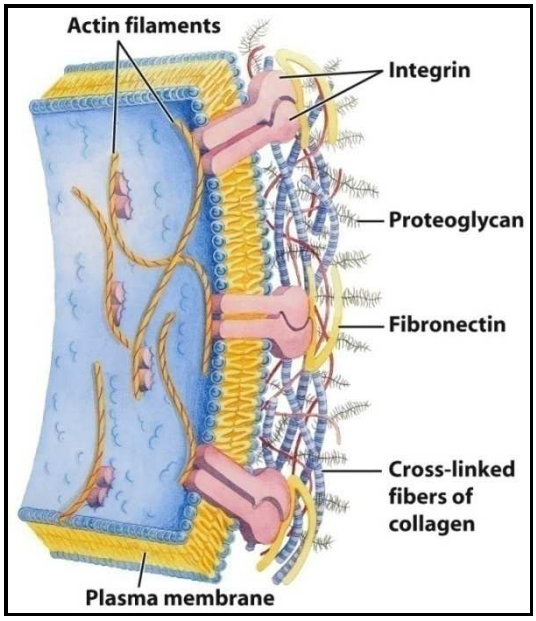

Fig. 5: The structure of the extracellular matrix (*Nelson et Cox, 2000*).

The ECM affects various cellular properties, for example the binding capacity of receptors, the growth regulation, the bonds of proteins, the inhibition of proteolytic enzymes. The effects of ECM on cell viability and metabolism are different and include: adhesion, angiogenesis, apoptosis, differentiation, embryogenesis, gene regulation, immune response, cell migration, mitosis, polarity, induction and signal transfer (*Bowers et al., 2009*). It is difficult to reproduce *in vitro* a natural ECM since each matrix is composed by several independent components. In cell culture systems, usually only few products play a dominant and important role: for example, collagen, laminin, fibronectin, and most recently, the pronectin, produced by genetic engineering. The surfaces of the plates or flasks for tissue culture can be treated with a single substance or a combination of these molecules. The attack to ECM facilitates cell growth and development of three-dimensional structures.

1.3. Scaffolds for vascular tissue engineering

1.3.1. Natural scaffolds for vascular tissue engineering

The most used natural materials for the development of a replacement vessel include collagen, elastin, fibrin, hyaluronic acid and materials based on polysaccharides. In particular, the collagen is an interesting material for its ability to "communicate" with cells. The use of collagen has led to a support with low burst strength, prone to failure when implanted as a simple tubular structure with a single component (*Pankajakshan et*

Agrawal, 2010). Despite the physical and chemical properties of these non-ideal materials, their interactions with cells are favourable. Implants based on polysaccharides have led to get *neo intima* in animal models without evidence of hyperplasia or formation of aneurysms. Excellent results were obtained by seeding ECs on fibrin of silk: cells adhere and elongate in the fiber direction showing a non-activated and adequate growth pattern (*Andrews et Hunt, 2009*).

A special case is the natural decellularized scaffold, similar in composition to natural scaffolds, they are obtained from vessels or other tissues/organs such as the ureter, skin, pericardium or small intestine, both animal and human. This approach has some advantages listed below:

- ✓ elastin components are maintained;
- ✓ the structure can be prepared in advance;
- ✓ have low immunogenicity.

The decellularized scaffolds may encourage cell growth, in particular of ECs, promoting the desired phenotype, morphology and confluence; on the other hand their ability to hold the cells after exposure to shear stress is too low and they suffer of the same thrombogenicity observed for the synthetic materials. The research is now moving towards pre-seeding plant cell and the cross-linking of the matrix to increase its mechanical properties and to retain the cells (*Andrews et Hunt, 2009*).

1.3.2. Effects of scaffold structure

Studies on the various and functionalized copolymers with molecules of adhesion, anti-thrombotic or antibiotics have shown that cells are sensitive to a large number of factors. A material used for a vascular prosthesis, as unique component or as a combination of layers, can theoretically be optimized in terms of physical properties and cellular interactions. The selected biomaterial for the bulk structure must be the best for what concerns the compliance and strength while the surface must be optimized by coating to influence interactions with cells (mainly ECs). Literature data show that cells are also sensitive to the material topography (the presence of fibers or pores, size of fibers or pores, the space between these elements, roughness, surface area, fiber orientation, scale micro or nano) (*Ju et al., 2010*). In particular it is known that FBs, grown on substrates characterized by wide range of pores and sweaters, show cooperative mechanisms of cell growth and spreading and use nearby cells such as bridges to overcome pores up to 50 µm in diameter; this possibility is foreclosed to ECs, which

prefer surface with pores smaller and with more defined structure (pores between 18 and 60 µm), SMCs are sensitive to surfaces with channels with a width of 40-160 µm where pass from a random alignment to that along the channel axis changing their morphology from FB-like to a slender type. These topographical features can be produced in a wide range of biomaterials through techniques such as electrospinning, photolithography, etching, by moulding or particulate leaching (*Andrews et Hunt, 2009*).

1.3.3. Effects of culture conditions *in vitro* and *in vivo*

In addition to the ability to alter the material, its surface and its topography, other variables can be considered to produce a replacement vessel. Among these variables note: cell types, different types of cultures, the seeding methods. When a vascular prosthesis is implanted it is immediately subjected to forces and stresses arising from the blood flow. Such stresses allow cells to aligned in the longitudinal direction but also stresses result in EC loss and thrombi formation that lead to the failure of the implant itself. In addition, the pulsatile pressure can cause a bad adaptation between the prosthesis and the native vessel resulting in changes in SMCs and intimal hyperplasia. Until now in most of the studies ECs were seeded in static conditions but recently the research has focused on the development of seeding technique under dynamic conditions. Combinations of static seeding and culture in perfusion, pre-coating of ECs with shear stress gradually increased, and ECs seeded on composite materials coated with biological molecules provide better retention levels of the endothelial monolayer. Cells used to repopulate vascular prothesis are ECs, FBs and SMCs even if many types of SC are being evaluated in, either alone or in combination, including SCs derived from fat tissue, muscle tissue, heart tissue and endothelial cell progenitors (*Andrews et Hunt, 2009*).

1.4. Polymers

A polymer is a macromolecule composed of a large number of small structural units called monomers, which can make two or more links. The bi-functional monomers give rise to linear polymers, monomers with more functions will form branched polymers or cross-linked polymers. When the macromolecule consists of a single repeated unit is called homo-polymers, while if there are two repeated units is called copolymers. The copolymers can be divided into statistical, alternating, block and "stapled" copolymers.

There is great diversity of structures and applications of polymeric compounds so they can be classified in different ways:

- by source: natural or synthetic polymers;
- by structure: homo-polymers or copolymers;
- by temperature behaviour: thermoplastic or thermosetting polymers;
- by polymerization mechanisms: addition or condensation polymers.

Another useful classification of polymers is based on the load/elongation diagram. A polymer that reaches the tensile strength without deformation is called cross-linked, a polymer with a moderate strain and breaking load also high is a fiber, a polymer with high deformation even for small loads is an elastomer, a polymer that has an intermediate behaviour between fiber and an elastomer is a plastic polymer. The inability to assign an exact molecular weight to a polymer is an aspect that most distinguishes a synthetic macromolecule from a simple organic molecule. This is because during the polymerization reaction polymer chains of different lengths formed (with a variable number of monomers). With a polymerization a number of macromolecules with different molecular weights are produced. At low temperatures, a polymer is always solid, increasing the temperature the attractive forces between the macromolecules and the system are broken, if it does not degrade, it becomes a more or less viscous liquid. In the field of polymer systems a strong product diversification can be achieved by changing the characteristics of base polymers by the addition of additives, reinforcing fillers or other polymers also of a different nature. Among these, the technology of mixing two or more polymers has gained great success about application, because it allows to obtain "new" materials having the characteristics of each polymer base, without incurring the substantial costs of implementation of new monomers and of new polymerization techniques.

Polymeric materials, both for their intrinsic properties both for the similarity with natural polymers, have a wide range of applications as biomaterials. They can be produced in the form of fibers, tissues, films, rods and viscous liquids. For applications in the field of medicine is important to emphasize the possibility of forming bonds between the synthetic polymers and the constituents of natural tissues.

Typically, nylons and polyamides are considered enough biocompatible materials. However, we must consider that they lose much of their strength when they are implanted *in vivo*, probably because of their hygroscopicity. In addition, nylons suffer of the attack of proteolytic enzymes.

1.4.1. The bioresorbable polymers

Both synthetic and natural polymers can be used to create scaffolds for TE. To select the appropriate polymer for TEVG, the cellular interaction with the polymer must first be understood. To date, however, a suitable polymer has not yet developed for vascular tissue engineering.

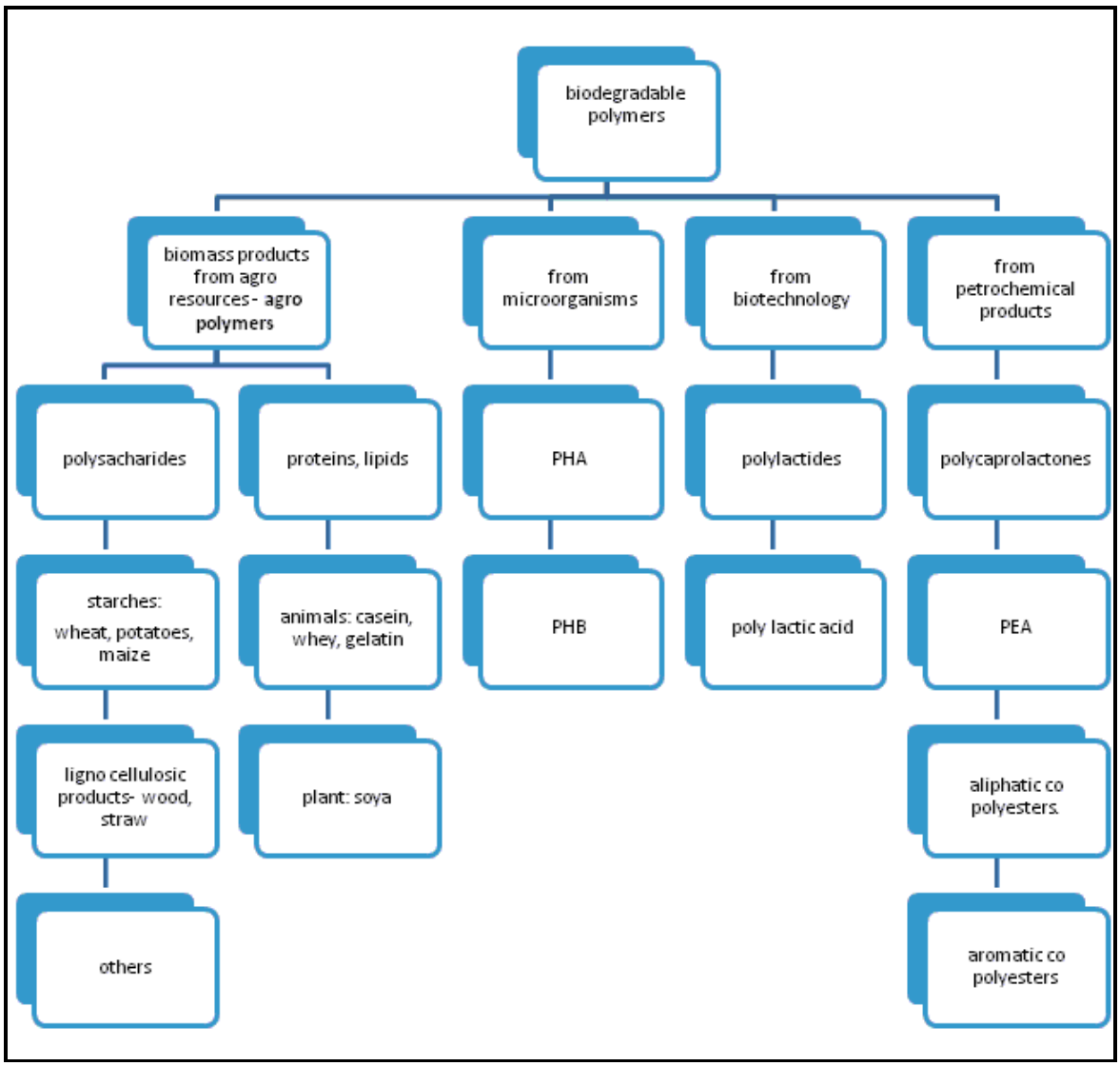

Fig. 6: Classification of biodegradable polymers (*Kambiz et al., 2007*).

Among the biodegradable scaffold poly(glycolic acid) (PGA) and poly(lactic acid) (PLA), synthetic polymers, are the most widely used in medicine. Their degradation rate varies depending on the initial molecular weight, the surface exposed area, the crystallization and *ratio* of monomers. The copolymer is degraded faster than the single polymers.

Poly-ε-caprolactone (PCL) is another very versatile biomaterial widely characterized and used in TE and in many other areas of medicine and biotechnology. Such a broad and diverse set of applications is justified by the chemical and physical properties of the polymer, by the qualities of biocompatibility, indispensable to the success of generic application in the biomedical field. It is a semi-crystalline aliphatic polyester synthetic polymer, non-toxic, biodegradable and hydrophobic, it is usually subject to bio-erosion surface (*Dong et al., 2009*).

In vivo it is degraded very slowly both by microorganisms either by not-enzymatic hydrolysis of the ester, followed by fragmentation and the release of oligomers, the only metabolite released is the acid-ε hydroxycaproic. The PCL has been extensively studied demonstrating that the degradation products are not toxic and they are eliminated through normal excretory routes (*Vert, 2009*). So the PCL was selected as a suitable material to make tubular structures. Looking to expand the range of potential biomaterials the hydroxyalcanoates (PHA) have been considered too. They form a broad class of polymers, isolated for the first time in 1925 by microbiologist Lemoigne in the *Megaterium Bacillus* (*Dong et al., 2009*), whose potential is currently being investigated in the cardiovascular field. The PHA, including poly-3hydroxybutirate-co-3-hydroxyvalerate (PHBV), are synthesized by various microorganisms in the form of granules which can be extracted by processes to eliminate any cellular component. About biocompatibility, *in vivo* studies have shown that the degradation of most of these polymers involves the release of hydroxyl-acids that are less acid and inflammatory then other bioresorbable polymers, such as PGA. Their biodegradation rate is long, however, this characteristic is not necessarily a limitation if we consider cases in which the regeneration of tissue should not be compromised by a rapid loss of implanted mechanical support (*Williams et Martin, 2002*). The PCL belongs to the class of thermoplastic polymers, and is characterized by a high workability that enables the rapid modelling in useful form. It also shows a high propensity to form compatible blends with a wide variety of polymers. In fact, blends of PCL and PHBV showed good cytocompatibility using mesenchymal stem cells (*Tang et Wu, 2005*).

1.5. The electrospinning technique

The electrospinning technique can produce nano and micro fibers starting from a wide range of polymers. Between 1934 and 1944 Formhals filed several patents in which he described an experimental set-up for the production of polymeric filaments by applying an electrostatic field (*Huang et al. 2003; Greiner et Wendorff, 2007*). Technically, the polymer is dissolved in selected solvents and the resulting polymer solution, collected in a syringe, is vented through a metal capillary connected to a high voltage generator, and also deposited on a metal target. In detail, the polymer solution remains initially adherent at the end of the capillary, in hemispherical shape due to surface tension. Increasing the tension, mutual repulsion between the charge carriers in the solution results in a force directly opposite to the surface tension with elongation of the hemispherical surface in a cone (Taylor cone). Above a critical voltage, the electrostatic forces exceed the surface tension, so an electrically charged polymeric stream is emitted from the apex of the Taylor cone. The jet of polymeric solution, into the air to the target, undergoes to instability because of electrostatic repulsive forces that lead to shrink with simultaneous evaporation of the solvent (*Frenot et Chronakis, 2003, Theron et al., 2004*). The process variables that affect the final result are numerous and can be summarized in the polymer selected parameters such as molecular weight and structure, properties of the polymeric solution (viscosity, conductivity and surface tension, depending on the solvent used) and process parameters such as flow value imposed on the polymeric solution through the capillary, the voltage applied to it and the distance from the target deposition, the environmental parameters can be considered too, such as temperature, humidity and air velocity in electrospinning room (*Doshi et Reneker, 1995; Frenot et Chronakis, 2003*). The high finesse electrospun fibers can produce materials with a high surface/volume ratio and high porosity. The possible fields of application are numerous: in technical textiles, biomedical (scaffolds for tissue growth and vascular grafts, transport systems and drug delivery), in industry (reinforced for composite materials, porous materials for laminates, supports for catalysts) or electronics. The typical result, applying this technique, consists of a matrix of polymeric fibers arranged into a completely random way, but it is also possible modulate the final morphology by introducing appropriate modifications in the experimental set-up. In fact, using a fixed collection target, a random arrangement of fibers is produced, but having, for example, a rotary collection target a polymeric-oriented fibers can be deposited,

whose degree of orientation can be changed depending on the speed of rotation imposed to the target. The latter option is particularly attractive for producing cylindrical tubular structures such as scaffolds proposed in this research project.

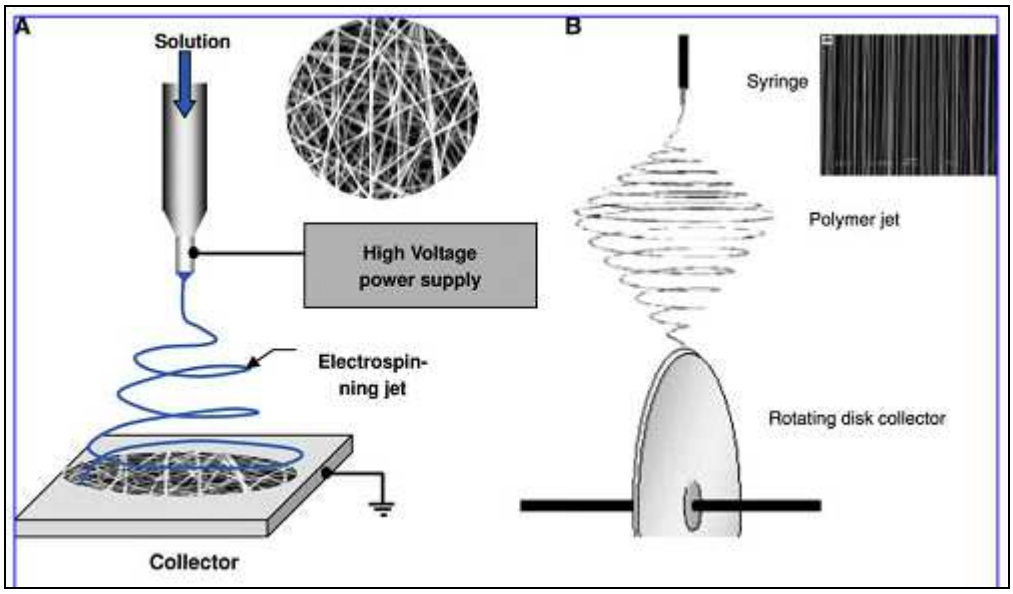

Fig. 7: Electrospinning technique on fixed collection target (A) and on rotating collection target (B), adapted from Dong et al., 2009.

1.5.1. Electrospun scaffolds for tissue engineering

TE has considered and is still considering the electrospinning as a method capable of providing good support employable for the regeneration of new biological tissue. Many experiences are constantly proposed to the attention of the world scientific community, and demonstrate the potential that the electrospinning can offer to achieve the objectives of this scientific approach (Fig 9).

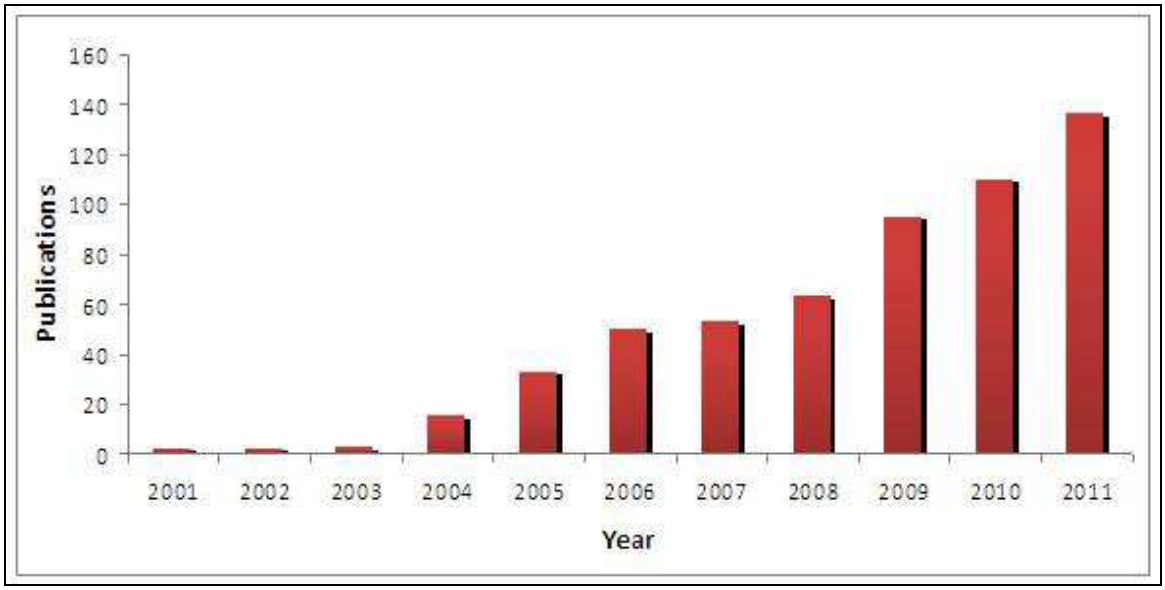

Fig. 8: Number of annual publications about the use of electrospinning in the field of tissue engineering. This graph was produced using the results obtained from a literature search in the PubMed database by typing the following key "electrospinning tissue engineering" (*http://www.ncbi.nlm.nih.gov/sites/entrez*) (*Del Gaudio, 2011*).

Several studies have investigated the potential of the electrospinning technique for cardiovascular applications, considering both the mechanical and the biological characteristics of the construct in terms of fitness synthetic environment offered to the cells. Considering the particular required application, the supports must have specific mechanical properties and consequently the selection of material with higher probability of success must be carefully evaluated. For this purpose, scaffolds of poly(glycolic acid) (PGA) coated with poly-hydroxyalcanoates (PHA) and poly(ε-caprolactone) (PCL) were compared under conditions of dynamic load simulating a physiological environment; a drastic reduction of mechanical properties in case of PGA/PHA scaffolds was observed (*Kloud et al., 2008*). The cellular response to structures of electrospun poly(lactic acid) (PLA) or poly(lactic-glycolic acid) (PLGA) was assessed by means of cardiomyocytes, that showed obvious contractile properties (*Zong et al., 2006*). About TEVG, many studies have been conducted *in vitro* by analyzing the properties of electrospun vascular grafts (*Inogouchi et al., 2006, Lee et al., 2007, Zhang et al., 2009*). The real potential of this therapeutic approach has been tested *in vivo* by evaluating the characteristics of degradation and promotion of autologous tissue of prothesis in PCL, implanted in rats, showing successful results at 6 months from implantation about the structure and endothelialization (*Pektok et al., 2008*). Similar results were reported about PCL/collagen

blend vascular grafts, used as aorta-iliac bypass in rabbits (*Tillman et al., 2009*). Still using mixtures of polymeric vascular grafts, collagen, elastin and poly(lacto-glycolic) copolymers were made by blending. These structures showed mechanical properties similar to those of native vessels and *in vivo* tests showed the absence of local or systemic toxic effects (*Stitzel et al., 2006*). Soffer et al. (*2008*) have proposed a different approach to realize electrospun tubular structures in fibrin, stabilizing the process with the addition of polyethylene oxide to the polymer solution, then removed. They showed interesting mechanical properties and citocompatibility for potential vascular applications.

2 MATERIALS AND METHODS

2.1. Electrospun mats and tubular scaffolds

The bioresorbable mats and tubular scaffolds used in this study will be designed, produced and characterized at the University of Rome "Tor Vergata", Department of Science and Chemical Technology, by Prof. Alessandra Bianco and Eng. Costantino Del Gaudio.

2.1.1. Fabrication of electrospun mats and tubular scaffolds

PCL (Mn=70000-90000) and PHBV (Mw=690000, 12% w PHV) were supplied by *Sigma-Aldrich*. Chloroform ($CHCl_3$, analytical grade) was supplied by *Carlo Erba Reagenti*. All materials and reagents were used as received. PCL, PHBV and PCL/PHBV (1:1) granules were dissolved in $CHCl_3$, the concentration was 14% w/v for the former and 20% w/v for the latter ones. Polymeric solutions were electrospun at room temperature through a blunt tip metallic needle (22G) at constant feed rate of 0.5 ml/h by means of a digital controlled infusion pump (*KD Scientific, USA*). A high voltage power supply (*Spellman, USA*) insured an applied voltage of 12 kV (PCL) or 15 kV (PHBV and PCL/PHBV). Electrospun mats and tubular scaffolds (inner diameter (ID)=5 mm) were collected, respectively, onto an a fixed grounded aluminum target and onto a rotating aluminum mandrel (about 25 g) located at 10 cm from the needle tip. All samples were vacuum dried for 48 h and stored in a desiccator.

2.1.2. Microstructural characterization of electrospun mats and tubular scaffolds

The microstructure was examined by means of scanning electronic microscopy (SEM) *(Leo-Supra 35)*. The average fiber diameter was determined from SEM micrographs by measuring about 50 fibers randomly selected *(ImageJ, NIH)*. Two-dimensional size estimation of voids comprised among polymeric fibers, computed as the diameter of circles having equivalent area, was evaluated processing SEM micrographs by means of a custom made image analysis software, as previously described (*Del Gaudio et al., 2009*). In the case of electrospun tubular scaffolds, fiber orientation was evaluated by means of a custom made software (*Matlab, The Mathworks, Natick, MA, USA*), similarly to the method reported by Geraets (*1998*). SEM image was firstly binarized and then rotated around its center in step of 2°. For each direction the fraction of bright pixels was computed and the resulting standard deviation calculated. Results were reported into a unitary polar plot, specific for the analyzed electrospun texture. As

measurement index, the eccentricity of the fitting ellipse of the polar plot, having the maximum radius as the major semiaxis and the 90° polar value as the minor semiaxis, was computed as follows:

$$E = \frac{A_M - A_m}{A_M + A_m}$$

where *AM* is the major axis and *Am* the minor axis. According to this formulation *E=1* indicates a straight line (unidirectional fiber alignment) and *E=0* indicates a perfect circle (randomly arranged fibers) (*Biela et al., 2009*).

2.1.3. Mechanical characterization of electrospun mats

Uniaxial tensile tests were carried out on dog-bone specimens (ASTM D1708) cut out from 2D mats. Mechanical tests were performed at 1.2 mm/min to rupture by means of an universal testing machine (UTM) equipped with a 100 N load cell (*Lloyd LRX*). At least four specimens were considered for each electrospun mats. The tensile modulus, evaluated within 0-5% strain, the ultimate tensile strength (UTS) and the elongation at break were calculated from the stress-strain curves. Mechanical parameters were calculated considering the nominal cross-sectional area of the tensile specimen.

2.1.4. Mechanical characterization of electrospun tubular scaffolds

Tests were performed following the standard ISO/DIN 7198 “Cardiovascular implants – Tubular vascular prostheses”. Circumferential tensile properties were evaluated stretching electrospun rings cut out from the collected tubular scaffolds, the average width being 10.8±1.8 mm. Rings were tested by means of an UTM equipped with a 100 N load cell (*Lloyd LRX*). Two stainless steel rods (1 mm diameter) were placed through the lumen of the ring and fixed to custom-made steel grips. Specimens were tested to rupture at 50 mm/min. Tensile modulus, ultimate tensile stress, referred to the nominal cross section area expressed as 2·width·thickness, elongation at break and circumferential strength (Tmax), as specified by the above mentioned standard, were calculated. The suture retention strength (SRS) was determined using the same testing standard considering both the “straight across” and “oblique” procedures. In the former, the tubular scaffold was cut normal to the long axis, a suture (*5-0, Assupro*) was inserted 2 mm from the cut end and fixed to a steel rod on the crosshead of 8the UTM. In the latter, the tests were similarly repeated cutting the electrospun scaffold at 45° to the long

axis and placing a suture alternatively at the base (heel), at ±90° from the base and at the top of the cut. At least five specimen were considered for each test.

2.2. Cell cultures

2.2.1. Isolation of Rat Cerebral Endothelial Cells (RCECs)

Microvascular RCECs were isolated following Abbott and co-workers method (*1992*) modified by Baiguera and collaborators (*2004*). Sprague-Dawley rats (*Charles-River, Como, Italy*) were used and the experiment protocol was approved by the local Ethics Committee of the University of Padua for Animal Testing (CEASA). The brains were removed and washed in saline solution (PBS) containing 10% of antibiotic-antimycotic solution (penicillin G 100UI/ml, streptomycin 100µg/ml and amphotericin B 0.25µg/ml) (*Sigma-Aldrich Corp., St. Louis, MO*). External connective share was removed and resting brain was minced. The suspension was washed in saline solution to reduce fat components and then it was incubated in 0.1% collagenase B-dispase (*Roche Applied Science, Penzberg, Germany*), HEPES (10mM) (*Sigma Aldrich Corp., St. Louis, MO*) and DNasi (20UI/ml) (*Sigma Aldrich Corp., St. Louis, MO*) saline solution at 37°C for 1 hour in Dubnoff shaking water bath (*GFL, Burgwedel, Germany*) to separate microvessels from extracellular matrix and other cellular components. After centrifugation the pellet was re-suspended into 25% Bovine Serum Albumin (BSA) (*Sigma-Aldrich Corp., St. Louis, MO*) density-dependent centrifugation solution in order to separate capillary fragment (heavier) to myelin, neurons, astrocytes and other cellular fragments (lighter). Capillary fragments were re-suspended in Endothelial Cell Growth Medium MV_2 (*PromoCell, Heildelberg, Germany*) and they were seeded into Petri dishes previously coated with human fibronectin (1µg/cm^2) (*Sigma-Aldrich Corp., St. Louis, MO*). The medium was changed with new MV_2 (*PromoCell*) every two days until confluence. After reaching the latter, RCECs were immunoseparated by magnetic beads and characterized for morphology, phenotype (expression of von Willebrand factor), and formation of capillary-like structures, as previously reported (*Conconi et al., 2004*).

2.2.2. Isolation of Rat Aortic Endothelial Cells (RAECs)

RAECs were isolated following the method of Albertin and colleagues (*2009*) with some modifications. The experimental protocol was approved by the Ethics Committee of the University of Padua for Animal Testing (CEASA). In this study RAECs from aorta of adult Sprague Dawley rat (*Charles River, Como, Italy*) were used. After harvesting, the aortas were immediately placed in saline solution (PBS) containing 1% of antibiotic-antimycotic solution and HEPES (10mM) (*Sigma-Aldrich Corp., St. Louis, MO*) and repeatedly rinsed. All impurities, such as blood cells, adherent connective tissue and fat were carefully removed. After washing, the isolated vessels were cut longitudinally and placed with the inner lumen in contact with the bottom of a culture plate with saline solution (PBS) containing 0.1% collagenase B (*Roche Applied Science*) 1% of antibiotic-antimycotic solution and HEPES (10mM) at 37°C. After 30 minutes the digested tissue was discarded and the cell suspension, obtained by flushing the vessels and the plate, was centrifuged at 250 g for 5 minutes. The pellet was then re-suspended in MV_2 (*Promocell*) with the addition of 20% Fetal Bovine Serum (FBS) (*PromoCell, Heidelberg, Germany*), and 1% UltroSer (*Ciphergen Biosystems, Cergy-Saint-Christophe, France*). Cells were seeded on plates previously coated with fibronectin (1 $\mu g/cm^2$) (*Sigma-Aldrich Corp., St. Louis, MO*) at 37°C and placed in a humidified incubator (5% CO2, 95% of air). The culture medium was changed with new MV_2 every two days until confluence. After reaching the latter, RAECs were immunoseparated by magnetic beads and characterized for morphology, phenotype (expression of von Willebrand factor), and formation of capillary-like structures, as previously reported (*Conconi et al., 2004*).

2.2.3. Purification and characterization of cell cultures

Purification

In order to separate endothelial cells from contaminant cells, immunoseparation was performed using a modification of the method described by Jackson and co-workers (*1990*) and Dynabeads M450 Tosylactivated magnetic beads (*Oxoid, Hampshire, UK*) coated with mouse anti-rat CD31 antibody (*AbD Serotec Ltd, Oxford, UK*) were used. Beads were prepared following the protocol utilized for Ulex europaenus agglutinin I (UEA)-coated beads. To obtain subcultures cell culture medium was removed and 0.02% EDTA and 0.25% Trypsin (1:1 v/v) (*Sigma Aldrich Corp., St. Louis, MO*) saline solution

was added to PBS washing cells. Detached cells were re-suspended in a determined volume of cell medium. 0.1ml of cells were added to 0.3ml of Trypan Blue (*Sigma Aldrich Corp., St. Louis, MO*) and counted in a Bürker chamber. Remaining cells were then seeded at desired concentration. In all the experiments II and III passage cells were used.

Characterization

The phenotype of RCECs was confirmed by means of expression of vWF. Immunocytochemistry was performed using antibody anti-vWf. Cells were seeded on fibronectin (1µg/cm2)-coated slides (Sigma-Aldrich Corp., St. Louis, MO) and grown until confluence. After three washing with PBS cells were fixed and with HCl and ethanol (1 part of 1% HCl and 99 parts of 70% ethanol). After washing with PBS cells were treated 20 minutes with 0.5% BSA (Sigma-Aldrich Corp., St. Louis, MO) saline solution to block non-specific binding sites and incubated with primary antibody (1:300) in 0.5% BSA (Sigma-Aldrich Corp.) saline solution for 1 hour at room temperature. After three washings with PBS cells were incubated with peroxidase conjugated anti-rabbit IgG antibody (diluted 1:150 in PBS) (Dako Corp., Carpinteria, CA) for 30 minutes at 37°C. The substrate, composed by 0.02% H2O2 with 3-amino-9-ethylcarbazole (AEC) dissolved in 20% dimethylformamide (DMF), a chromogenous soluble compound transformed into an insoluble reddish compound by peroxidase enzyme, was added (Vector Laboratories Ltd, Peterborough, UK). Slides were then washed with distilled water to remove the overplus of AEC. Negative control was performed omitting the primary antibody. Slides were mounted with Eukitt (Fluka, Buchs, Switzerland). Images were captured using a camera connected to optical Laborlux S microscope (Leitz, Wetzlar, Germany).

The phenotype of RAECs was confirmed by means of expression of vWF. Cells were seeded on fibronectin (1µg/cm^2)-coated slides (*Sigma-Aldrich Corp., St. Louis, MO*) and grown until confluence. After reaching the latter, the cells were fixed with 4% formalin in saline solution (PBS) for 15 minutes and then rinsed twice with wash buffer solution, 0.05% Tween-20 (*Sigma Aldrich Corp., St. Louis, MO*) in PBS. Then a permeabilization solution, 0.1% Triton X-100 in PBS, was added for 3 minutes. After 30 minutes in blocking solution, 1% Bovine Serum Albumin (BSA) (*Sigma Aldrich Corp., St. Louis, MO*) in PBS, cells were incubated with rabbit polyclonal anti-human von Willebrand factor (*Dako Corp., Carpinteria, CA*) (1:300) in blocking solution for 1 hour

at room temperature and then rinsed three times with wash buffer solution. Thereafter, the cells were incubated for 45 minutes at room temperature and protected from light with secondary antibody fluorescein anti-rabbit IgG (*Vector Laboratories, Burlingame, USA*) (1:200) (495 nm excitation wavelength, 517 nm emission wavelength) in PBS. After incubation, cells were rinsed three times and mounted with 4'-6-diamidino-2-phenylindole (DAPI) (*VECTASHIELD Mounting Medium with DAPI, Vector Laboratories, CA,USA*), as a fluorescence nucleic acid stain (350 nm excitation wavelength, 460 nm emission wavelength), on a slide and observed using a confocal laser scanning microscope (*Leica SP5, HCX PL APO 63x/0.50 oil objective*), the images were acquired using the LAS AF software. Negative control was performed omitting the primary antibody.

Angiogenic capability on *in vitro* Matrigel

To assess the functional characteristic of RCECs and RAECs, the capability to form capillary-like structures, cells were seeded on Matrigel, soluble basement membrane extract of the Engelbreth-Holm-Swarm tumor that gels at room temperature to form a genuine reconstituted basement membrane. The Matrigel used to perform experiments was Growth factor Reduced Matrigel™ Matrix (*Bencton-Dickinson Labware, Bedford, MA*). Matrigel was defrost overnight at 4°C and then 50µl/cm^2 of growth surface were added on ice-cold plates. Plates were incubated for 30 minutes at 37°C to allow Matrigel to became gel. Cells were seeded (2.5 x 10^4 cells/cm^2) on Matrigel in 500µl of MV_2 (*Promocell, Heildelberg, Germany*) added by 10% Fetal Bovine Serum (FBS) (*Promocell, Heildelberg, Germany*), 1% antibiotic-antimycotic (*Sigma-Aldrich Corp., St. Louis, MO*) solution and incubated for 24 hours at 37°C, 5% CO2. At the end of incubation cells were washed with PBS and fixed with 10% formaldehyde in PBS for 24 hours. Cells were observed by Laborlux S microscope (*Leitz, Wetzlar, Germany*) and images were captured using a camera connected to it.

2.2.4. Cell culture medium

The PromoCell Endothelial Cell Growth Medium MV2 (*PromoCell, Heidelberg, Germany*) was used for culturing endothelial cells, RCECs and RAECs. The medium kit contains the base medium and all supplements required for producing the complete medium. Before the first use the base medium was supplemented with PromoCell Supplement Pack and the complete growth medium was made up of:

Fetal Calf Serum 5%

Epidermal Growth Factor 5.0ng/ml

Hydrocortison 0.2µg/ml

Vascular Endothelial Growth Factor 0.5ng/ml

basic Fibroblast Factor 10ng/ml

R3 Insulin like Growth Factor (R3 IGF-1) 20ng/ml

Ascorbic Acid 1µg/ml

2.3. Cell cultures on electrospun mats and tubular scaffolds

PCL, PHBV and PCL/PHBV disks (12 mm diameter) cut out from electrospun mats or tubular scaffolds were previously sterilized by immersion in 70% v/v ethanol solution overnight and dried at room temperature in a sterile hood. Thereafter, in order to facilitate cell attachment, mats were treated with rat tail collagen solution (1µg/cm^2) (*Sigma-Aldrich, St Louis, MO*) dissolved in 0.05% acetic acid overnight and washed twice with PBS prior to cell seeding. RCECs or RAECs were seeded at a density 5x10^4 cells/well on polymeric disks in a 24-well microtiter plate, and cultured under standard conditions with the medium replaced every 2-3 days. RCECs and RAECs grown on tissue culture plate support, seeded at the same density of electrospun scaffolds, became confluent after 5 days. For this reason all the experiments were performed on electrospun constructs only.

To assess the cytocompatibility of the mats, the following experiments were performed on RCECs and RAECs. On the polymeric mats the adhesion assays were performed by means of DAPI nuclei staining and the Actin Cytoskeleton and Focal Adhesion Staining Kit; the viability assays were tested by means of MTS assay and the Promokine Apoptotic/Necrotic/Healthy Cells Detection kit; RCEC and RAEC proliferation was assayed by means of the Click-iT™ EdU Imaging Kit. To compare the possible differences of the RCEC and RAEC behaviour caused by the different electrospun fiber orientation and to coherently reproduce the seeding protocol used for the mats, circular samples of the same diameter (i.e., 12 mm) were cut out from the tubular scaffolds. RCEC and RAEC scanning electronic microscopy (SEM) was performed. Cell distribution and adhesion were assayed by means of DAPI nuclei staining and Actin Cytoskeleton and Focal Adhesion staining Kit; the viability assays were performed by

means of MTS assay and the Promokine Apoptotic/Necrotic/Healthy Cells Detection kit. The images obtained with the confocal laser scanning microscopy come out from the Z-stack projection of the same field of approximately 8 µm thickness (ImageJ, NIH).

2.4. *In vitro* citocompatibility assays

2.4.1. RCEC, RAEC distribution and RCEC focal adhesion assay

In order to investigate RCEC distribution after 4, 7, 9, 12 and 14 days from seeding and RAEC distribution after 7 and 14 days from seeding, polymeric constructs were washed once with PBS and fixed with 4% formaldehyde. Then, samples were incubated with DAPI (350 nm excitation wavelength, 460 nm emission wavelength) for 30 minutes at room temperature in darkness. The nuclei of the cells were observed by means of a confocal laser scanning microscopy (*Leica SP5, HCX PL Apo 63x/0.50 oil objective*) and imagines captured using LAS AF software. The evaluation of RCEC adhesion after 7 and 14 days from seeding was performed by means of Actin Cytoskeleton and Focal Adhesion Staining Kit (*Chemicon International, Temecula, California*). Briefly, constructs were fixed with 4% paraformaldehyde in PBS for 15 minutes at room temperature and washed twice with wash buffer (0.05% Tween-20 in PBS). Then, cells were treated with 0.1% Triton X-100 in PBS for 5 minutes at room temperature and washed twice with wash buffer. After 30 minutes in blocking solution (1% BSA in PBS), constructs were incubated 1 hour at room temperature in blocking solution containing anti-Vinculin (1:500), provided with the kit, and subsequently washed three times with wash buffer. Constructs were then incubated in a solution of TRITC-conjugated Phalloidin (1:200) (provided with the kit) (540nm excitation wavelength, 580nm emission wavelength) and DyLight™ 488-Labeled Antibody to mouse IgG (*KPL, Gaithersburg, USA*) (1:200) (488nm excitation wavelength, 525nm emission wavelength) for 60 minutes at room temperature protected from light. After incubation, constructs were washed three times and mounted with VECTASHIELD Mounting Medium for fluorescence with DAPI (*Vector Laboratories, Burlingame, CA*) (350nm excitation wavelength, 460nm emission wavelength) and observed by means of a confocal laser scanning microscopy (*in the experiments with the mats BioRadiance Confocal System 10X or 40X objective and the Lasersharp2000 software while the Leica SP5, HCX PL Apo 63x/0.50 oil objective and the LAS AF software for the vascular graft experiments*).

2.4.2. Viability assay

RCEC and RAEC viability was monitored after 7 and 14 days by the colorimetric MTS assay 3-(4,5-dimethylthiazol-2-yl)-5-(3-carboxymethoxyphenyl)-2-(4-sulfophenyl)-2H-tetrazolium, inner salt (*CellTiter 96 Aqueous Assay, Promega*). Metabolically active cells react with a tetrazolium salt in the MTS reagent to produce a soluble formazan dye that can be observed at 490nm. The cellular constructs were rinsed with PBS in order to wash out unattached cells, transferred into a new well in order to take in account only cells attached to the mat, and finally incubated with 20% MTS reagent in culture medium for 90 minutes. Thereafter, aliquots were pipetted into 96 well plates and the samples were read at 490nm in a microplate autoreader EL13 (*Bio-tek Instruments*). To discriminate apoptotic, necrotic and healthy cells, Promokine Apoptotic/Necrotic/Healthy Cells Detection kit (*PromoCell GmbH, Heidelberg, Germany*) was used. Cellular constructs were rinsed twice with Binding Buffer provided with the kit and 5µl FITC-Annexin V (492nm excitation wavelength, 514nm emission wavelength), 5 µl Ethidium Homodimer III (528nm excitation wavelength, 617nm emission wavelength) and 5µl of Hoechst 33342 (350nm excitation wavelength, 461nm emission wavelength) onto 100µl Binding Buffer was added to every construct. After 15 minutes of incubation the samples were washed twice with Binding Buffer, mounted with coverslip and observed by means of a confocal laser scanning microscopy (*Leica SP5, HCX PL Apo 63x/0.50 oil objective*) and imagines were captured using LAS AF software. Healthy cells are stained blue, apoptotic cells are stained both green and blue, necrotic cells are stained both red and blue and triple colours blue, red and green are dead cells processing from apoptotic cell population.

2.4.3. Proliferation assay

To assay RCEC proliferation after 4, 7, 9, 12 and 14 days from the seeding and RAEC proliferation after 7 and 14 days from seeding, Click-iT™ EdU Imaging Kit (*Invitrogen, Molecular Probes Inc*) was used. Briefly, 24 hours before the end of the incubation period 10µM of EdU solution was added to the cells. At the end of incubation cellular constructs were fixed in 4% formaldehyde in PBS for 15 minutes, washed twice with 3% BSA in PBS and treated with 0.5% Triton X-100 in PBS for 20 minutes at room temperature. Constructs were then washed twice with 3% BSA in PBS and Click-iT™ reaction cocktail (containing Alexa Fluor® 488 azide, 495nm excitation wavelength and 519nm emission wavelength) was added for 30 minutes, protected from light, following

manufacture instructions. At the end of incubation constructs were washed once with 3% BSA in PBS and once with PBS. Then, 5µg/ml of Hoechst 33342 (350nm excitation wavelength, 460nm emission wavelength) provided with the kit was added to cells and incubated for 30 minutes at room temperature, protected from light. After two washing with PBS, constructs were mounted with coverslip, observed by a confocal laser scanning microscopy (*Leica SP5, HCX PL Apo 63x/0.50 oil objective*) and imagines were captured using LAS AF software.

2.5. *In vivo* experiments

The experimental protocol was approved by the Ethics Committee of the University of Padua for Animal Testing (CEASA).

In the *in vivo* experiments adult Sprague-Dawley rats (*Charles-River, Como, Italy*) were used and polymeric mats (diameter of 1 cm and thickness about 0,5 mm) were implanted in their dorsal subcutaneous tissue.

In particular, Sprague-Dawley rats were divided into 2 groups:

- Group 1 included the rats in which a PCL mat was implanted on the left side of the spine and a PHBV mat on the right side;
- Group 2 included rats in which a PCL mat was implanted on the left side of the spine and a PCL/PHBV mat on the right side.

PCL, PHBV and PCL/PHBV mats were previously sterilized by immersion in 70% v/v ethanol solution overnight and dried at room temperature in a sterile hood, and exposed to UV light (30 minutes/side). The disks were stored in sterile PBS until use, after some washing in PBS to remove ethanol.

2.5.1. Implant of polymeric mats and animal sacrifice

A Fluovac pump (*Harvard Apparatus Ltd, Kent, England*) for Isofluorane, was connected to the animal during the surgical procedure. The Isofluorane (*Forane ®, Abbott SpA*) at a concentration of 3% with oxygen flow at 1 liter/minute was distributed in a transparent Plexiglas box, suitable for the induction of anesthesia. Then Isofluorane 1.5% with oxygen flow at 1 liter/minute was administered to maintain the anesthesia state.

Once checked the state of animal anesthesia, the skin was shaved and disinfected with Betadine (*Meda Pharma S.p.a., Milano*). In each rat, control PCL polymer and the polymer to test, PHBV or PCL/PHBV were implanted. For this reason, two incisions

were made (1,3 cm) at the sides of the spine. At the incision level, two pockets were created to insert the polymer (PCL in the left pocket and the polymer to be evaluated in the right pocket). Then the skin was closed with absorbable sutures type 2-0 (*Ethicon Vicryl, Johnson & Johnson Medical S.p.a., New Jersey*), the suture was again disinfected with Betadine (*Meda Pharma S.p.a., Milano*).

The animals in the post-surgical operation period were kept one par cage in standard laboratory conditions. After surgery, antibiotic treatment with Terramycin ® (60 mg/kg intramuscular) was given. Post-surgical analgesia was provided by treatment with Contramal ® (5 mg/kg intramuscular) repeated every 12 hours for the first 24 hours.

The animals of each group were sacrificed by euthanasia at 1, 2 and 4 weeks after implantation. All animals were euthanized by means of anesthetic drug overdose. The mats were taken for morphological and histological studies.

2.6. Explanted polymer analysis

2.6.1. Histological analysis

At each endpoint the rats were sacrificed and mats were recovered, frozen by nitrogen vapour and stored at -80° C to prevent decomposition. Mats were then cryosectioned at 5µm thickness using the *Leica CM 1850 UV Cryostat*. The samples were fixed in 4% PBS-buffered paraformaldehyde for 10 minutes, washed once with PBS and twice with distilled water for 5 minutes. The sections were treated with hematoxylin for 3 minutes (*Mayer's Emallume solution, Bio-Optica, Milan*), purple nuclear staining solution, previously filtered with a filter paper. The excess dye was removed with a double and quick rinse in distilled water, and the slides were immersed in tap water for 6 minutes. The samples were then treated for 2 minutes with 0.5% eosin G aqueous solution (*Merck, Germany*), a cytoplasmatic dye that contrasts hematoxylin. Then the sections were quickly rinsed in distilled water. The slides, dried at room temperature, were mounted with Bio Mount, synthetic based mounting media for histology and cytology (*Bio-Optica, Milan*), covered with a coverslip and observed under an optical microscope (*Leica DM 2000, Germany*), images were captured using a camera connected to it.

2.7. Statistical analysis

Data are expressed as mean ± standard deviation. Statistical analysis was performed by means of non parametric tests (*Matlab, The Mathworks, Natick, MA, USA*). Differences were checked in two steps: data were compared by using the Kruskal-Wallis nonparametric test; if significant differences were found, groups were compared by means of the Mann-Whitney U test. Significant level was set at $p<0.05$.

3 RESULTS

3.1. Electrospun mats and tubular scaffolds

The bioresorbable mats and tubular scaffolds used in this study were designed, produced and characterized at the University of Rome "Tor Vergata", Department of Science and Chemical Technology, by Prof. Alessandra Bianco and Eng. Costantino Del Gaudio.

3.1.1. Microstructure of electrospun mats and tubular scaffolds

SEM observation showed that all collected non-woven mats were comprised of polymeric fibers free of beads (Fig. 9), the average diameter was 3.2±0.6 µm, 3.2±0.4 µm and 2.9±0.5 µm for PCL, PHBV and PCL/PHBV mats, respectively ($p>0.05$). The two dimensional average void size was 8±3 µm, 7±3 µm and 8±3 µm for PCL, PHBV and PCL/PHBV mats, respectively ($p>0.05$).

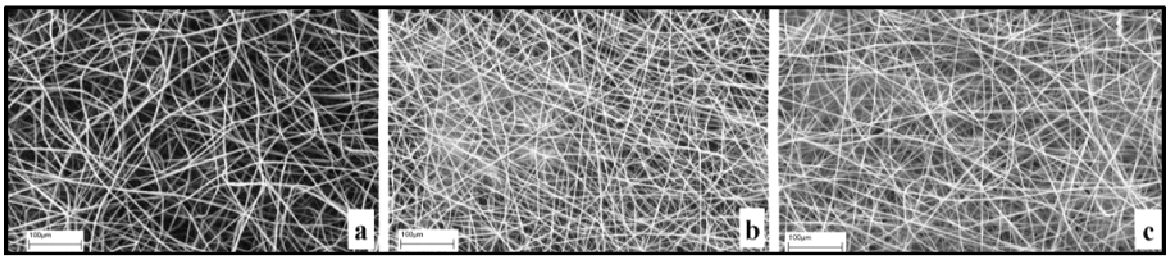

Fig. 9: SEM micrographs of PCL (A), PHBV (B) and PCL/PHBV (C) mats.

PCL and PCL/PHBV tubular scaffolds were comprised of defect-free electrospun fibers, in the case of PCL/PHBV a higher packing density has been observed (Fig. 10A). Conversely, the PHBV tubular sample showed several microstructural defects. PCL tubular scaffold was characterized by a bimodal fiber distribution, the average diameters being 3.5±0.8 µm and 0.7±0.2 µm, while a value of 1.5±0.5 µm was computed for PCL/PHBV ($p<0.05$). The average fiber diameter of PHBV tubes was 2.1±0.5 µm, along the fiber several beads of 9.5±2.0 µm were detected. Both PCL and PCL/PHBV electrospun grafts showed an overall and comparable aligned fiber pattern, the eccentricity of the fitting ellipse resulting from the orientation analysis was 0.29±0.12 and 0.33±0.06, respectively ($p>0.05$). PBHV did not reveal a preferential fiber alignment, being the eccentricity equal to 0.12±0.03 and significantly different from the two previous cases. Finally, graft thickness was 0.6±0.2 mm, 0.4±0.1 and 0.4±0.1 for PCL, PHBV and PCL/PHBV, respectively ($p>0.05$). Regarding the electrospun grafts collected at low

speed rotation, a random fiber arrangement was observed for the three cases, the PBHV showing the most non-homogeneous fiber deposition due to bead formation (Fig. 10B). The average fiber diameter was 3.7±0.3 µm and 3.5±0.4 µm for PCL and PCL/PHBV graft, respectively. PHBV graft was characterized by an average fiber diameter of 1.6±0.3 µm and an average bead size of 7.4±1.7 µm. The eccentricity of the fitting ellipse, as resulted from the orientation analysis, was 0.04±0.02, 0.02±0.01 and 0.05±0.02 for PCL, PHBV and PCL/PHBV grafts, respectively ($p>0.05$). As expected, the statistical analysis revealed a significant difference between low/high speed rotation tubular scaffolds made of the same material.

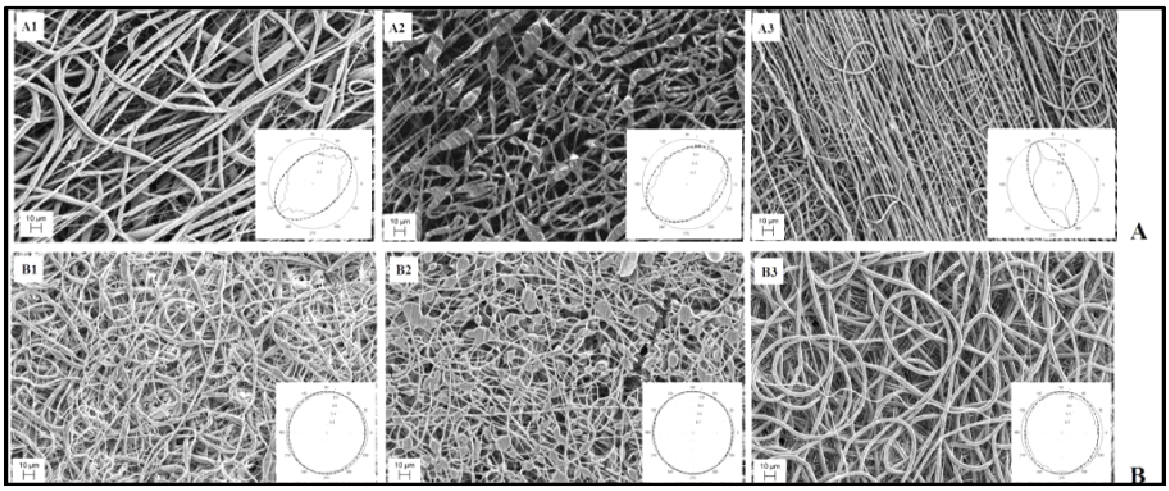

Fig. 10: A - SEM micrographs of PCL (A1), PHBV (A2) and PCL/PHBV (A3) tubular grafts collected at high rotational speed. **B** - SEM micrographs of PCL (B1), PHBV (B2) and PCL/PHBV (B3) tubular grafts collected at low rotational speed. Insert in each picture reported the computed fiber alignment pattern.

3.1.2. Mechanical characterization of electrospun mats

Mechanical properties of electrospun mats as resulted from the uniaxial tensile tests are summarized in Fig. 11. As expected, PCL showed the lowest tensile modulus and TS and the largest deformation at break. The acquired results showed an increasing for the tensile modulus and the tensile strength directly related to the PHBV content. The opposite trend was observed for the elongation at break.

Sample	E (MPa)	TS (MPa)	εmax (%)
PCL	6.4 ± 0.2	0.8 ± 0.1	350 ± 50
PHBV	77 ± 15°	1.8 ± 0.2°	30 ± 20°
PCL/PHBV	22 ± 7°, #	1.4 ± 0.3°	270 ± 80#

° p<0.05 with respect to PCL
# p<0.05 with respect to PHBV

Fig. 41: Mechanical properties of electrospun mats: tensile modulus (E), tensile strength (TS) and elongation at break (εmax).

3.1.3. Mechanical characterization of electrospun tubular scaffolds

Circumferential mechanical characteristics computed from the tested rings are summarized in Fig. 12, both for high speed and low speed fabrication. The SRS "straight across" values were 2.7±0.3 N, 1.3±0.3 N and 1.9±0.2 N (p<0.05), while the "oblique" values were 3.1±0.6 N, 0.7±0.2 N and 2.6±0.8 N for PCL, PHBV and PCL/PHBV, respectively (p<0.05 with respect to PHBV).

	Sample	E (MPa)	TS (MPa)	εmax (%)
High speed	PCL	4.2 ± 0.4	2.1 ± 0.5	950 ± 250
	PHBV	7.4 ± 1.5°	1.4 ± 0.5	73 ± 10°
	PCL/PHBV	7.0 ± 0.4°	1.7 ± 0.5	290 ± 90°, #
Low speed	PCL	2.2 ± 0.1§	1.6 ± 0.1	723 ± 47
	PHBV	3.1 ± 1.0§	0.7 ± 0.3°	39 ± 4°, §
	PCL/PHBV	4.5 ± 2.0§	1.5 ± 0.5	183 ± 33°, #

° p<0.05 with respect to PCL within each set of tubular scaffolds collected at a selected speed
# p<0.05 with respect to PHBV within each set of tubular scaffolds collected at a selected speed
§ p<0.05 comparing tubular scaffolds made of the same material for the two fabrication conditions

Fig. 12: Circumferential mechanical properties of electrospun tubular scaffolds collected at high and low rotational speed: tensile modulus (E), tensile strength (TS) and elongation at break (εmax).

3.2. Characterization of cell cultures

3.2.1. Characterization of rat cerebral endothelial cells (RCECs)

To verify that the immunoseparated rat cerebral endothelial cells (RCECs) were indeed endothelial cells and free from contaminating non endothelial cells, expression of endothelial-specific marker von Willebrandt factor (vWf) was investigated by immunocytochemistry. RCECs exhibited positive cytoplasmatic staining with anti-vWf (Fig. 13A). No background staining was observed omitting the primary antibody. Indeed RCECs are able to form capillary-like structures on Matrigel, maintaining the functional capability in *in vitro* cultures (Fig. 13B).

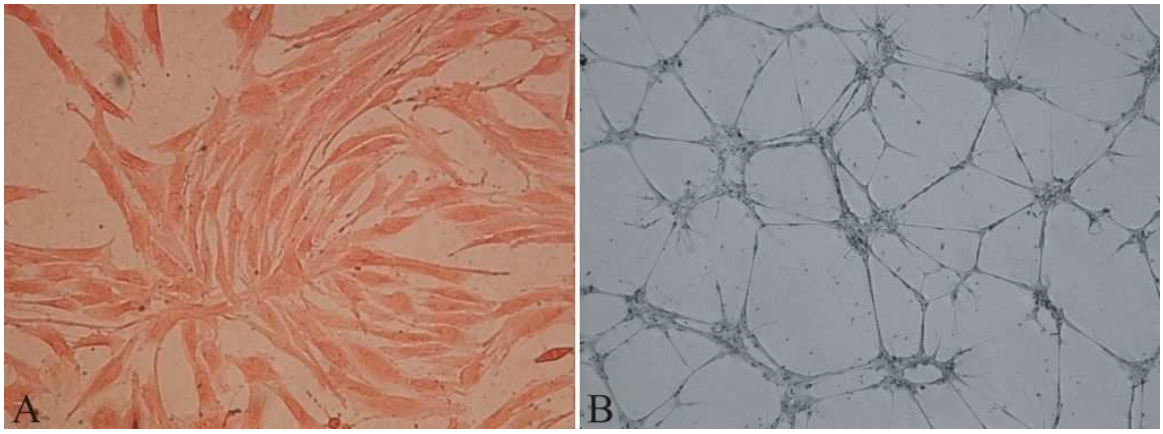

Fig. 13: Immunocytochemistry of RCECs showing the expression of endothelial-specific marker con Willebrandt factor (vWf). RCECs were highlight using 3-amino-9-etil-carbazol (AEC). Magnification 50X (A). No primary antibody was used in negative controls. RCECs seeded in Matrigel after 24 hours (B). RCECs maintain the ability to form capillary-like structures *in vitro*.

3.2.2. Characterization of rat aortic endothelial cells (RAECs)

To verify that the immunoseparated rat aortic endothelial cells (RAECs) were indeed endothelial cells and free from contaminating non ECs, expression of endothelial-specific marker von Willebrandt factor (vWf) was investigated by immunocytochemistry. RAECs exhibited positive cytoplasmatic staining with anti-vWf (Fig. 14A, 14C, 14E, 14G). No background staining was observed omitting the primary antibody. Indeed RAECs are able to form capillary-like structures on Matrigel, maintaining the functional capability in *in vitro* cultures (Fig. 14B, 14D, 14F, 14H).

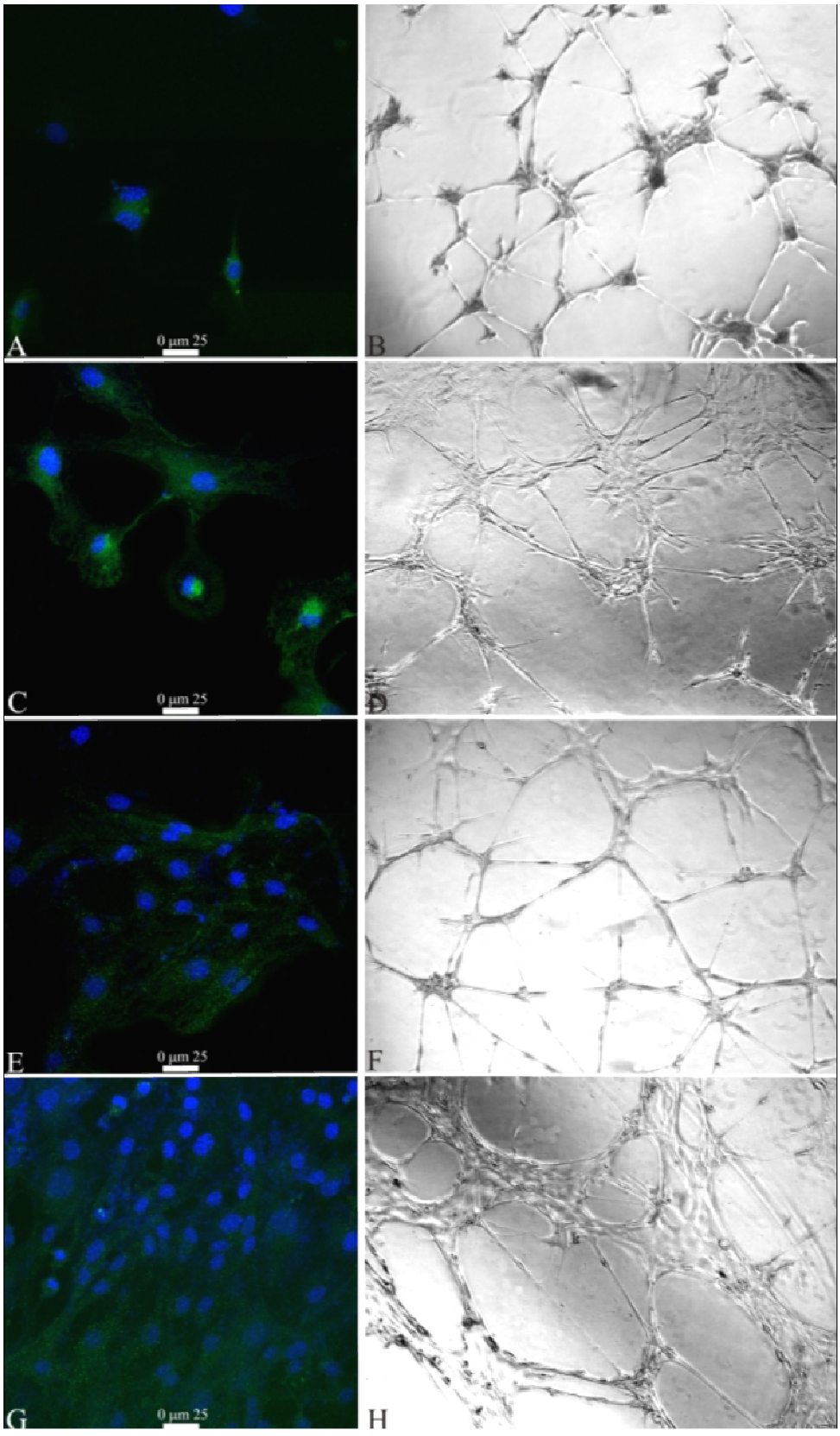

Fig. 14: Confocal laser scanning microscopy of RAECs at II, IV, VI and VIII passage (respectively A, C, E ,G), showing the expression of endothelial-specific marker von Willebrandt factor (vWf). RAECs at II, IV, VI and VIII passage (respectively B, D, F, H) seeded in Matrigel after 24 hours. RAECs maintain the ability to form capillary-like structures *in vitro*.

3.3. *In vitro* experiments on electrospun mats

3.3.1. RCEC, RAEC distribution and RCEC focal adhesion assay

RCEC response on the electrospun mats was observed by means of DAPI (labelling nuclei) and the adhesion kit composed by actin (labelling cytoskeleton filaments and their orientation) and vinculin (labelling focal contacts) staining. RCECs spread on the surface of PCL, PHBV and PCL/PHBV mats at 4, 7, 9, 12 and 14 days from seeding, the most representative time points are shown in Fig. 15. In particular, cells grew uniformly onto the surface of PCL mats, while a cluster distribution was observed on PHBV. A different cell behavior was highlighted for the PCL/PHBV mats, being initially characterized by the presence of cell clusters until day 9 (data not shown) followed by an uniform surface starting from day 12.

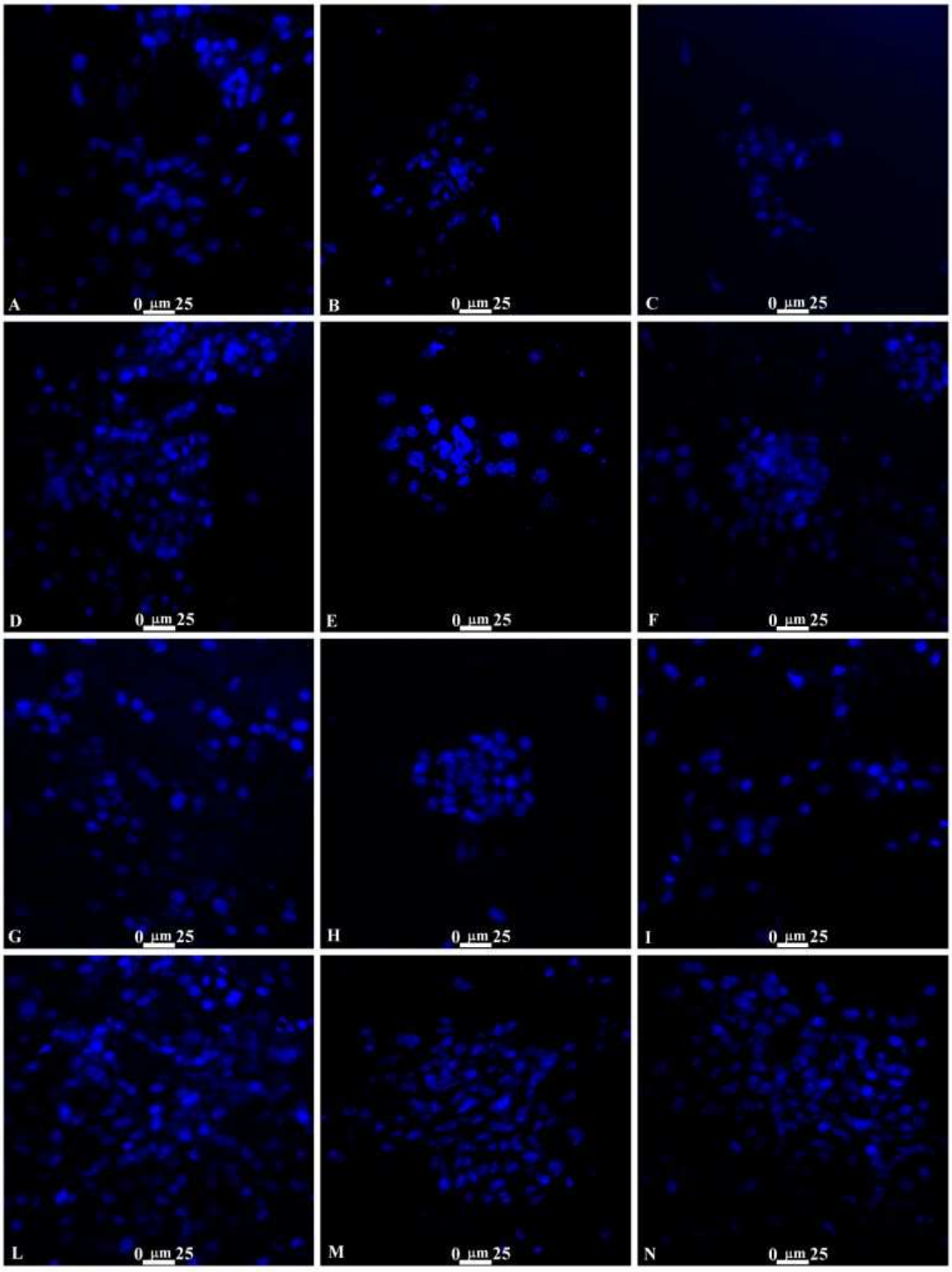

Fig. 15: Confocal laser scanning microscopy of RCEC nuclei stained with DAPI performed on PCL (A, D, G, L), PHBV (B, E, H, M) and PCL/PHBV (C, F, I, N) mats at 4 days (A, B, C), 7 days (D, E, F), 12 days (G, H, I) and 14 days (L, M, N) after seeding.

Adhesion assay performed with immunocytochemical kit at 7 and 14 days from seeding (Fig. 16) demonstrated that RCECs expressed both actin and vinculin onto PCL mats. Differently, on PHBV and PCL/PHBV substrates, RCECs expressed vinculin as well as on PCL mats but the expression of actin protein was lower, demonstrating less adhesion to the substrate but a very good focal adhesion among cells.

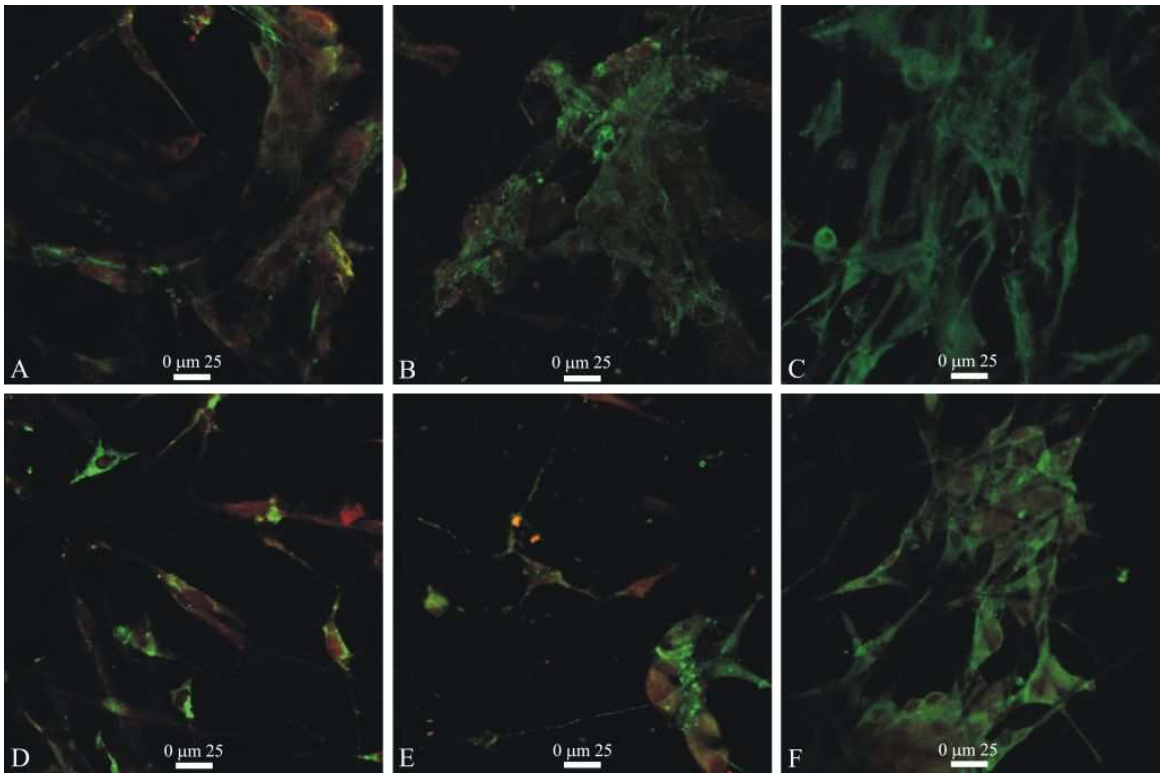

Fig. 16: Confocal laser scanning microscopy of focal adhesion and actin cytoskeleton in RCEC seeded on PCL (A, D), PHBV (B, E) and PCL/PHBV (C, F) mats at 7 days (A, B, C) and 14 days (D, E, F) after seeding. F-actin was detected using TRITC-conjugated Phalloidin, focal contacts were revealed using anti-Vinculin monoclonal antibody and DyLightTM 488-labeled antibody.

RAEC response on the electrospun mats was observed by means of DAPI (labelling nuclei). At 7 days from seeding RAECs spread on all mats, cells grew uniformly and were more numerous and well distributed onto the mat surface within 14 days (Fig. 17).
When testing the RAEC adhesion on polymeric mats, the Actin Cytoskeleton and Focal Adhesion Staining Kit (*Chemicon International, Temecula, California*) was no longer commercially available and no similar kit by other company was available, thus the adhesion assay was not performed.

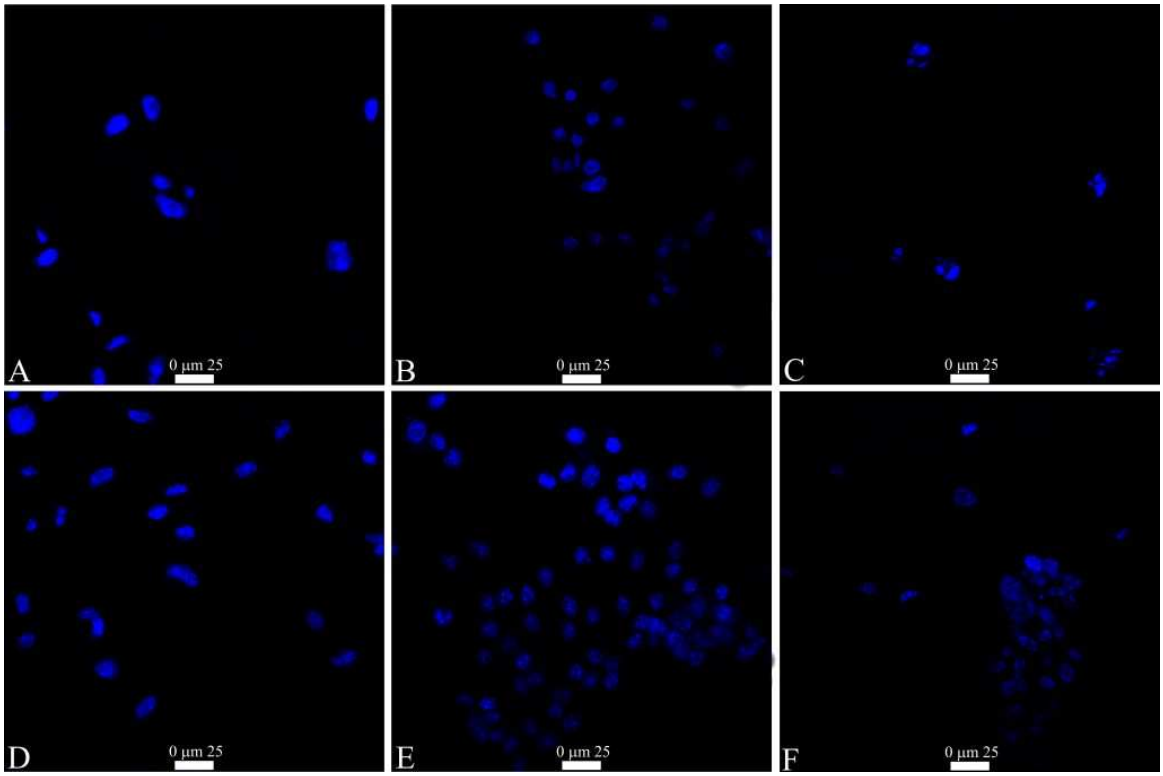

Fig. 17: Confocal laser scanning microscopy of RAEC nuclei stained with DAPI performed on PCL (A, D), PHBV (B, E) and PCL/PHBV (C, F) mats at 7 days (A, B, C) and 14 days (D, E, F) after seeding.

3.3.2. RCEC and RAEC viability assay

The RCEC viability on PCL, PHBV and PCL/PHBV mats was evaluated by means of the MTS assay at 7 and 14 days from seeding (Fig. 18). The data demonstrated that RCECs grew and were metabolically active when cultured on PCL and PHBV mats at both time-points. Conversely, RCEC MTS reduction on PCL/PHBV mats significantly ($p<0.05$) decreased after 14 days with respect to 7 days.

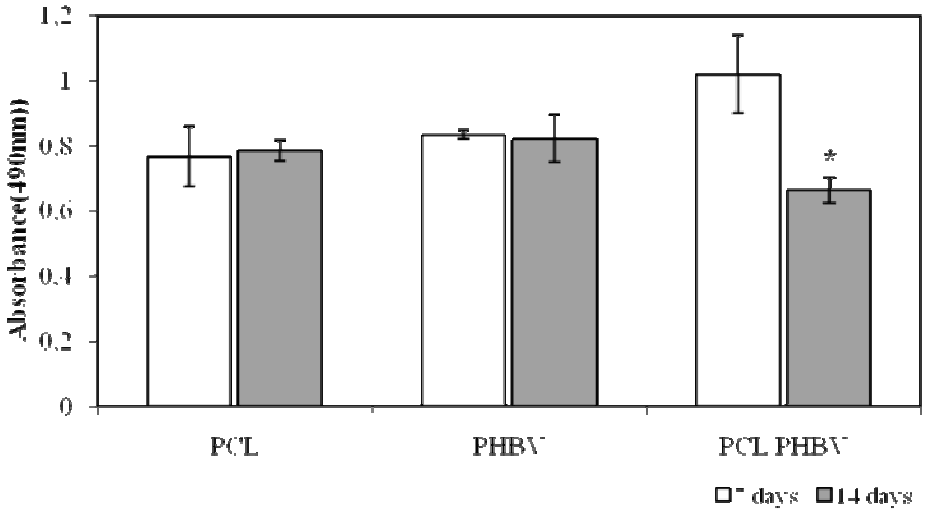

Fig. 18: RCEC MTS assay on PCL, PHBV and PCL/PHBV mats at 7 and 14 days after seeding.

* $p<0.05$ to 7 days.

Apoptotic, necrotic and healthy cells were stained by means of three different fluorophores, as reported in Fig. 19. At 7 and 14 days from seeding, most of the RCECs were healthy (blue stained) while only few necrotic cells (red stained) were detected on PCL and PHBV mats, suggesting that the main cell death way is the necrotic one. On PCL/PHBV mats death cells were more abundant at 14 days than at 7 days. These results showed a comparable trend with the MTS assay.

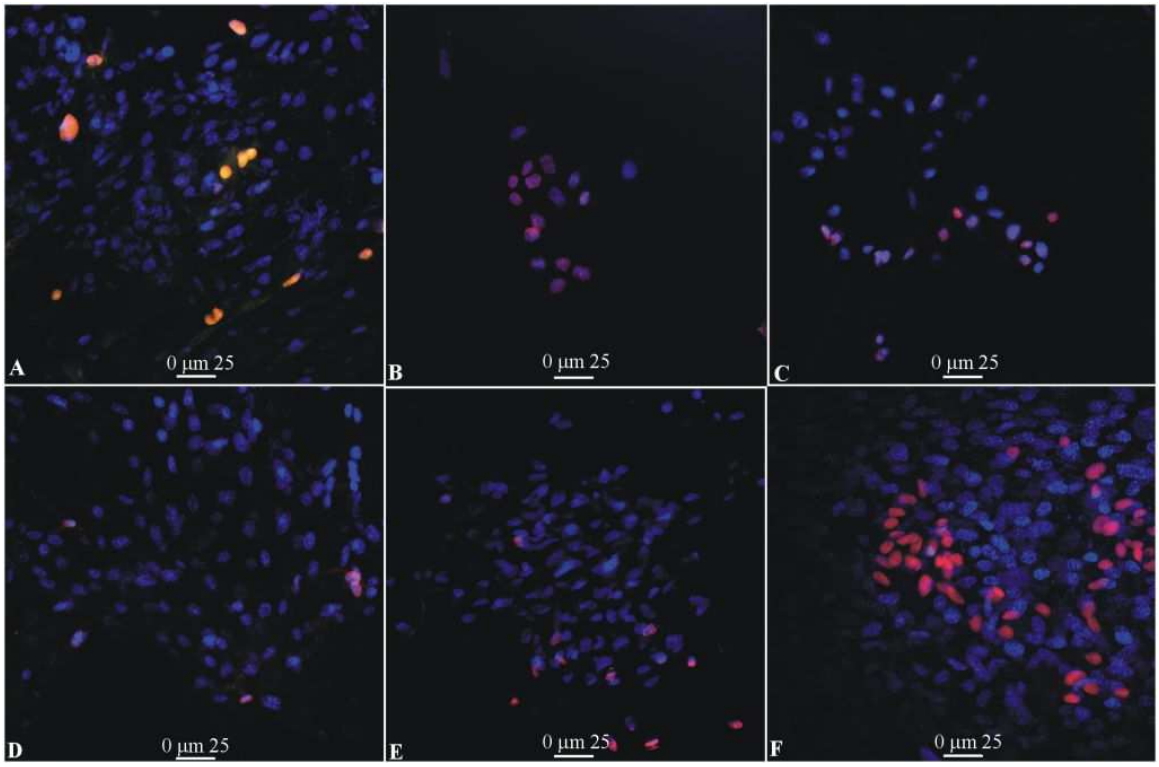

Fig. 19: Confocal laser scanning microscopy of viability assay of RCECs seeded on PCL (A, D), PHBV (B, E) and PCL/PHBV (C, F) mats at 7 days (A, B, C) and 14 days (D, E, F). Healthy cells are stained blue, necrotic cells are stained both red and blue and triple colors blue, red and green are dead cells processing from apoptotic cell population.

The RAEC viability on PCL, PHBV and PCL/PHBV mats was evaluated by means of the MTS assay at 7 and 14 days from seeding (Fig. 20). The data demonstrated that RAECs grew and were metabolically active on PCL, PHBV and PCL/PHBV mats at 7 days similarly. RAEC MTS reduction on PHBV and PCL/PHBV mats increased in highly significant ($p<0.01$) way after 14 days with respect to 7 days.

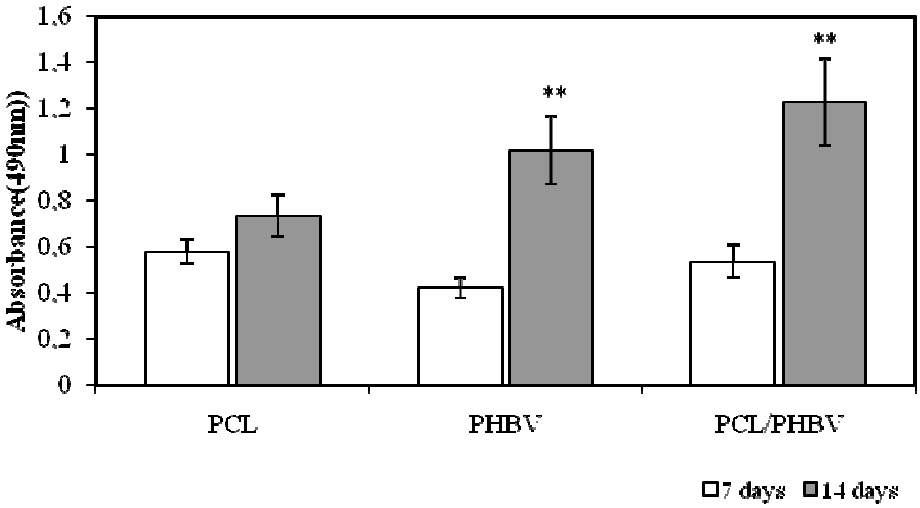

Fig. 20: RAEC MTS assay on PCL, PHBV and PCL/PHBV mats at 7 and 14 days after seeding.

** $p<0.01$ to 7 days.

Apoptotic, necrotic and healthy cells were stained by means of three different fluorophores, as reported in Fig. 21. At 7 days from seeding, few RAECs were necrotic (red stained) on PCL, PHBV and PCL/PHBV mats. At 14 days most of RAECs on PCL and PCL/PHBV were healthy (blue stained) while only few necrotic cells (red stained) were detected. These results showed a comparable trend with the MTS assay.

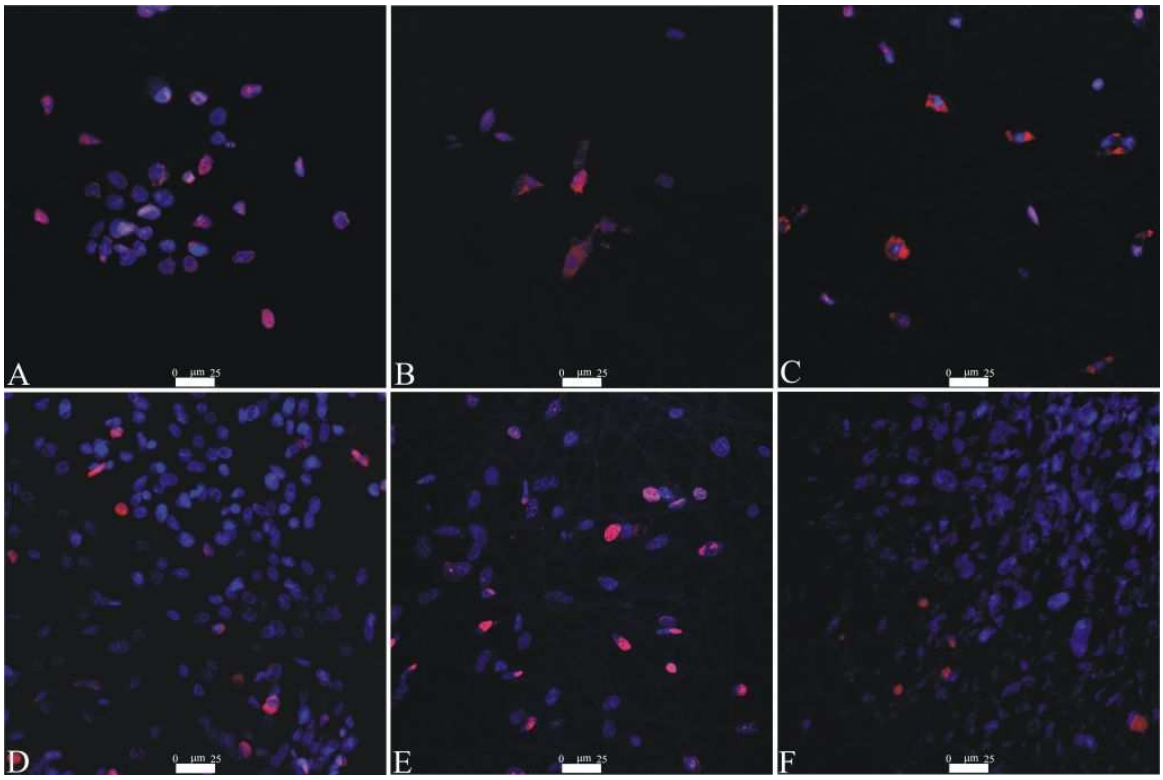

Fig. 51: Confocal laser scanning microscopy of viability assay of RAECs seeded on PCL (A, D), PHBV (B, E) and PCL/PHBV (C, F) mats at 7 days (A, B, C) and 14 days (D, E, F). Healthy cells are stained blue, necrotic cells are stained both red and blue and triple colors blue, red and green are dead cells processing from apoptotic cell population.

3.3.3. RCEC and RAEC proliferation assay

In order to assess the potential influence of electrospun mats on RCEC and RAEC proliferation, an immunocytochemical kit based on the discrimination between the total (DAPI staining, blue) and the proliferative cells (stained with the Alexa Fluor 488 azide staining, green) was used. RCECs proliferated on all the investigated mats as resulted from the observational time-points, 7, 12 and 14 days from seeding, the most significant ones are reported in Fig. 22. In particular, PCL (Fig. 22A, 22D and 22G) supported cell proliferation, while PHBV (Fig. 22B, 22E) and PCL/PHBV (Fig. 22C and 22F) mats were characterized by a similar response up to day 14 when a lower proliferation was detected with respect to PCL (Fig. 22H and 22I). Moreover, at 12 days the proliferative RCECs increased on all the investigated mats in comparison to 7 and 14 days.

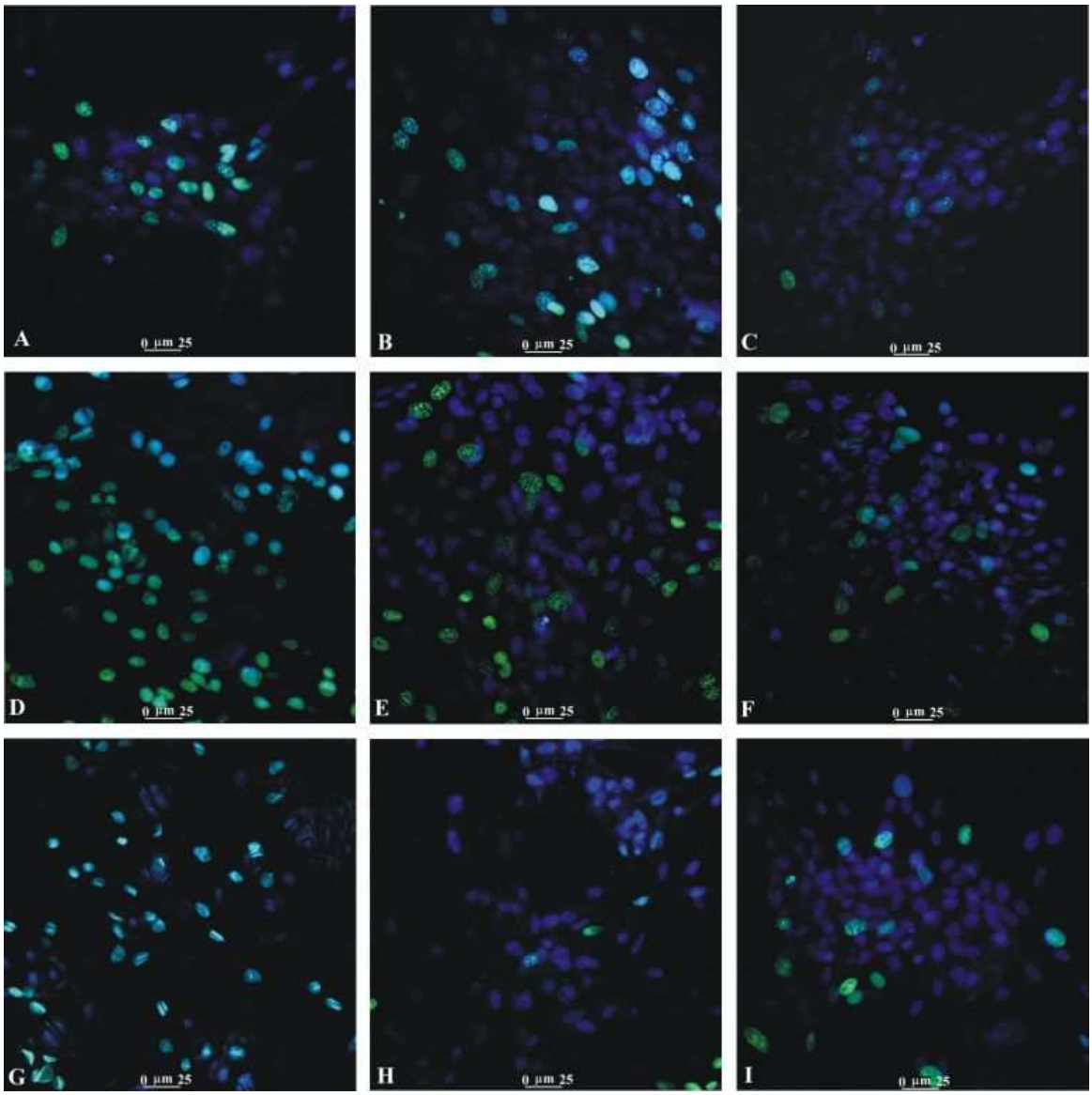

Fig. 22: Confocal laser scanning microscopy of proliferation assay of RCECs on PCL (A, D, G), PHBV (B, E, H), PCL/PHBV (C, F, I) mats at 7 days (A, B, C), 12 days (D, E, F) and 14 days (G, H, I). Nuclei are stained blue, proliferative nuclei are stained both green and blue.

At 7 days from seeding RAECs proliferated on all investigated mats similarly (Fig. 23). At 14 days the proliferative RAECs increased on all the investigated mats in comparison to 7 days.

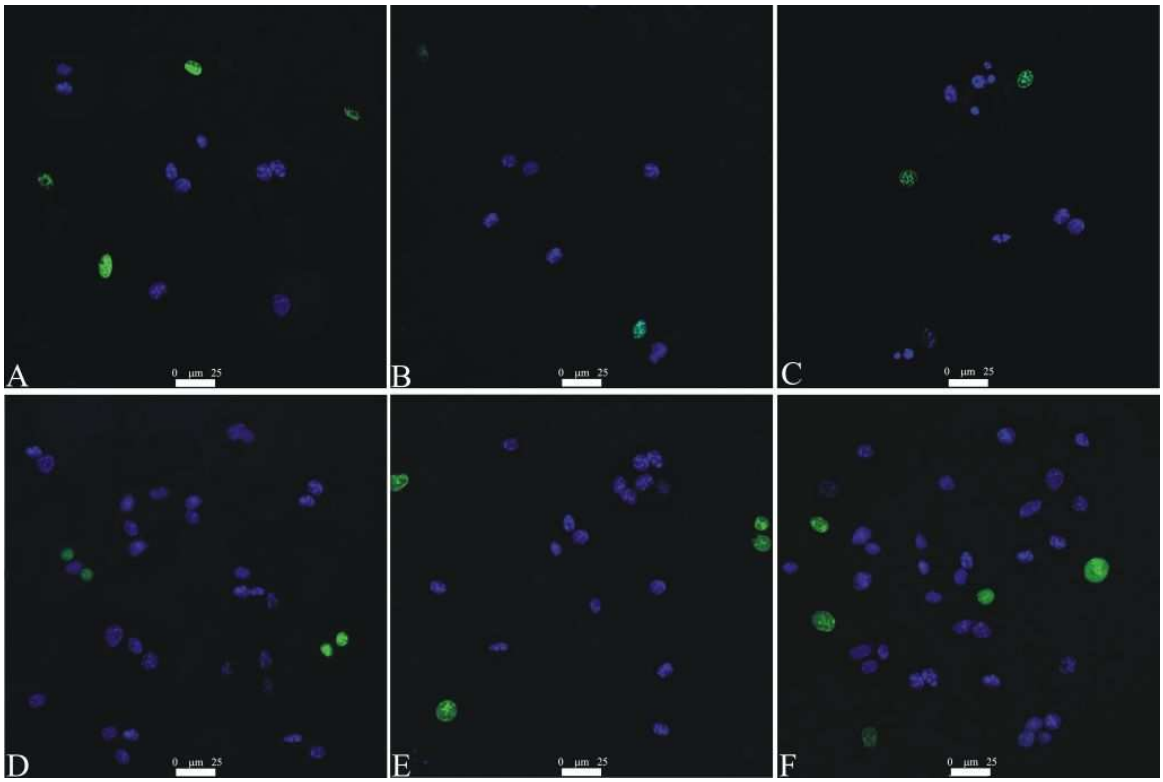

Fig. 23: Confocal laser scanning microscopy of proliferation assay of RAECs on PCL (A, D), PHBV (B, E), PCL/PHBV (C, F) mats at 7 days (A, B, C) and 14 days (D, E, F). Nuclei are stained blue, proliferative nuclei are stained both green and blue.

3.4. *In vitro* experiments on circular samples cut out from the tubular scaffolds

3.4.1. RCEC, RAEC distribution and RCEC focal adhesion assay

RCEC response on circular samples cut out from the tubular scaffolds was observed by means of DAPI (labelling nuclei) and the adhesion kit composed by actin (labelling cytoskeleton filaments and their orientation) and vinculin (labelling focal contacts) staining. RCECs spread on the surface of PCL and PCL/PHBV mats at 7 and 10 days from seeding while at 12 and 14 days from seeding they decreased (Fig. 24). Cells grew uniformly onto the surface of both mats. On PHBV no cells were observed at any time point (data not shown). No other experiments with RCECs were performed on PHBV.

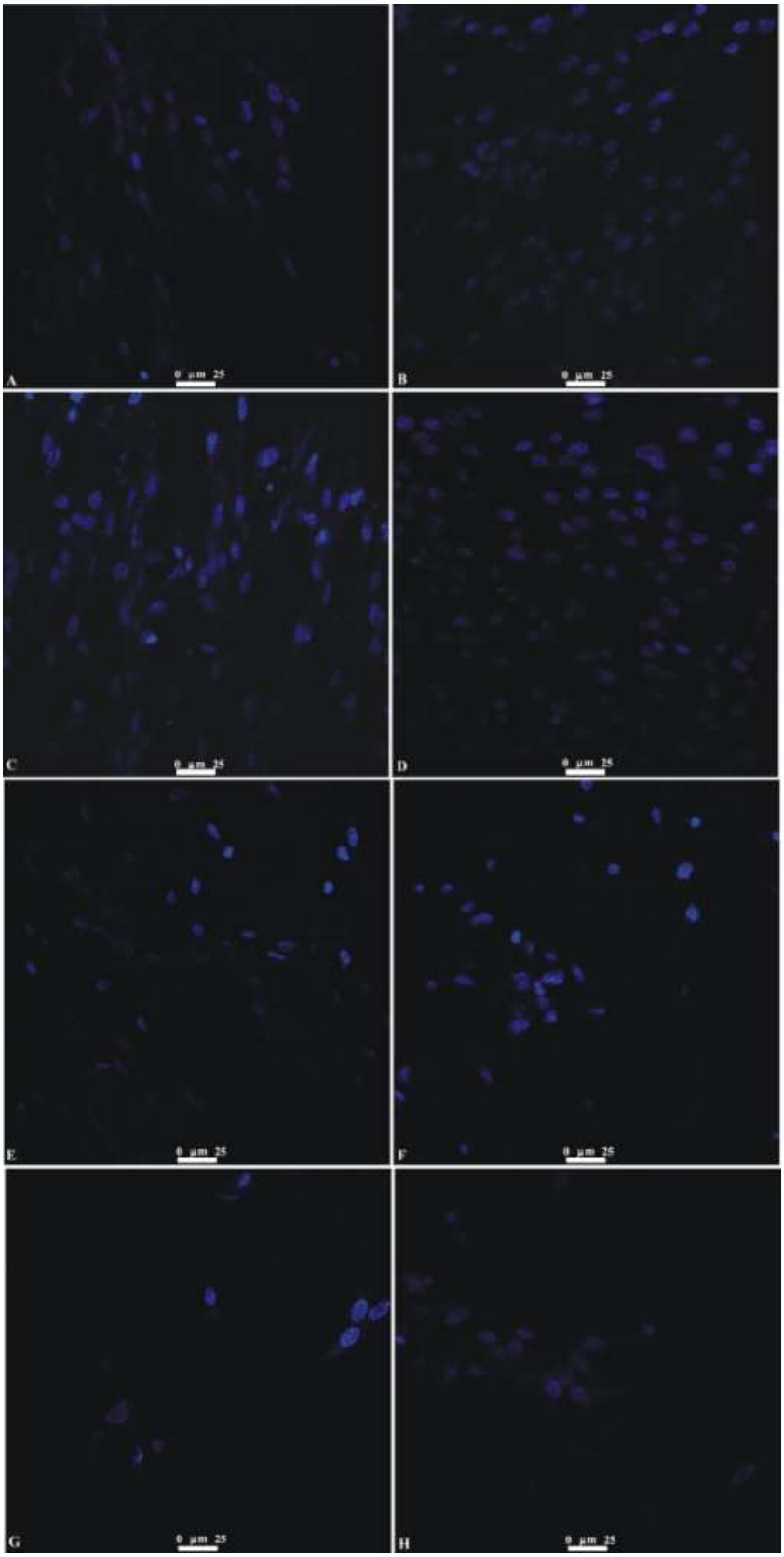

Fig. 24: Confocal laser scanning microscopy of RCEC nuclei stained with DAPI performed on PCL (A, C, E, G) and PCL/PHBV (B, D, F, H) circular samples cut out from the tubular scaffolds at 7 days (A, B), 10 days (C, D), 12 days (E, F) and 14 days (G, H) after seeding.

The adhesion assay on circular samples cut out from the tubular scaffolds was performed using the same immunocytochemical kit used for the electrospun mats. A confocal laser scanning microscopy having the UV laser allows the observation of the cell nuclei stained with DAPI. RCECs on PCL expressed both actin and vinculin at 7 days from seeding, also showing a preferential orientation with the electrospun fibers, suggesting a direct influence of the substrate morphology on cell spreading (Fig. 25A). This response appeared more evident on PCL/PHBV (Fig 25B). After 14 days the number of cells on PCL (Fig. 25C) and PCL/PHBV (Fig. 25D) decreased in comparison to 7 days.

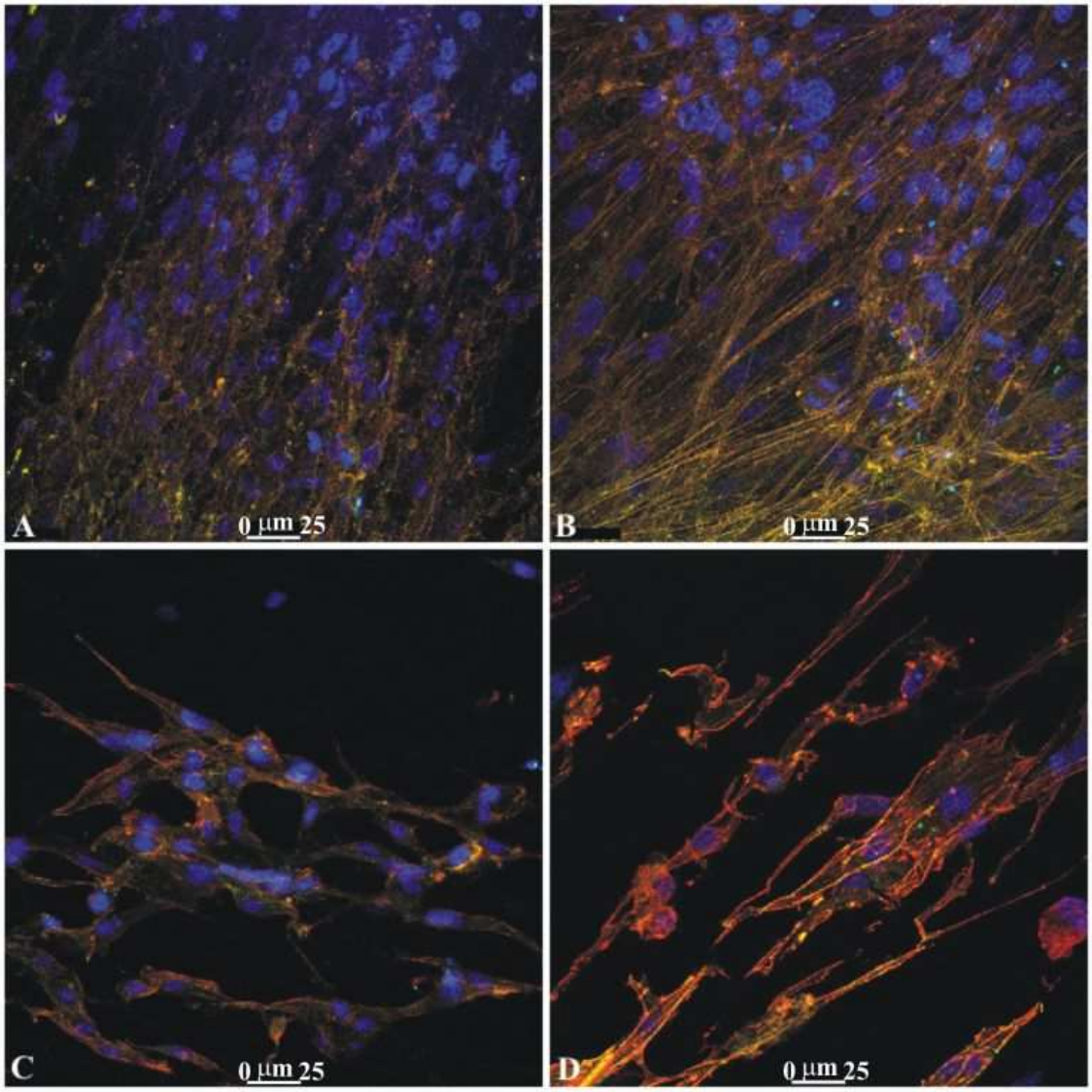

Fig. 25: Confocal laser scanning microscopy of focal adhesion and actin cytoskeleton in RCEC seeded on PCL (A, C) and PCL/PHBV (B, D) circular samples cut out from the tubular scaffolds at 7 days (A, B) and 14 days (C, D) of culturing. F-actin was detected using TRITC-conjugated Phalloidin, focal contacts were revealed using anti-Vinculin monoclonal antibody and DyLightTM 488-labeled antibody and nuclei are stained with DAPI.

RAEC response on circular samples cut out from the tubular scaffolds was observed by means of DAPI (labelling nuclei). At 7 days from seeding lots of RAECs were detected on PCL and PCL/PHBV, only few cells on PHBV. At 14 days RAECs increased on all samples and grew uniformly on PCL and PCL/PHBV surface(Fig. 26).

When testing the RAEC adhesion on circular samples cut out from the tubular scaffolds, the Actin Cytoskeleton and Focal Adhesion Staining Kit (*Chemicon International, Temecula, California*) was no longer commercially available and no similar kit by other company was available, thus the adhesion assay was not performed.

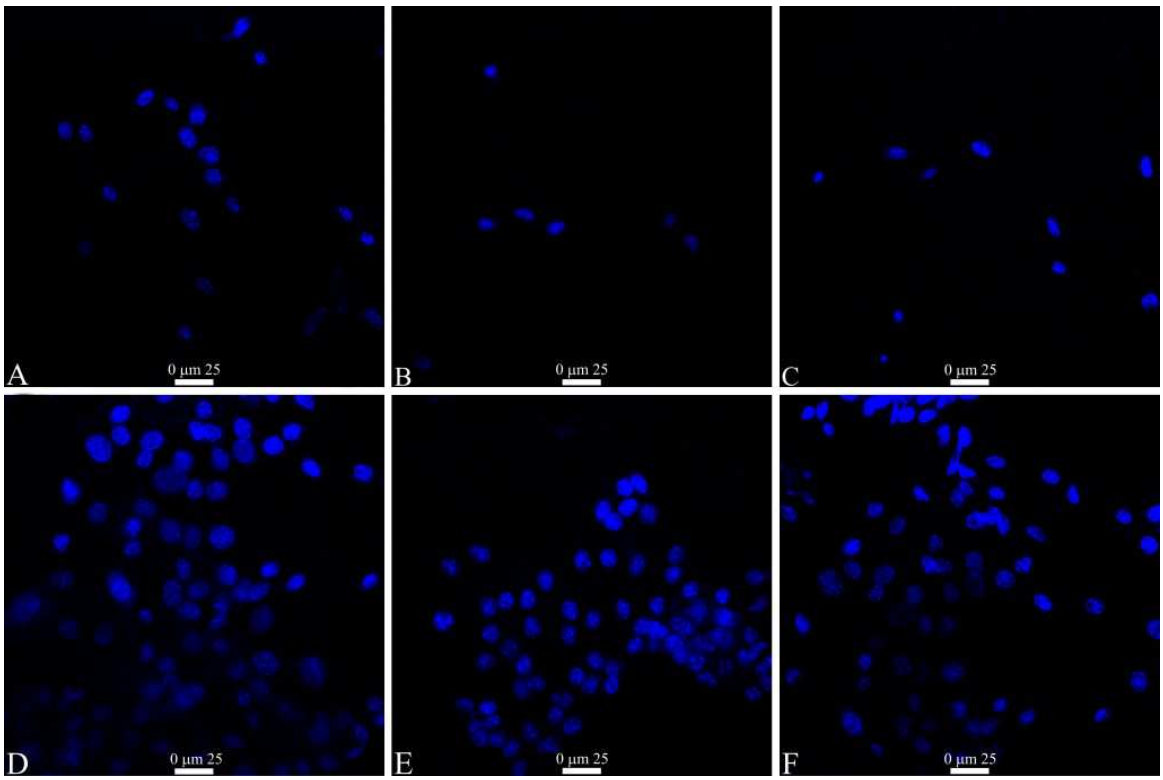

Fig. 26: Confocal laser scanning microscopy of RAEC nuclei stained with DAPI performed on PCL (A, D), PHBV (B, E) and PCL/PHBV (C, F) circular samples cut out from the tubular scaffolds at 7 days (A, B, C) and 14 days (D, E, F) after seeding.

3.4.2. RCEC and RAEC viability assay

The RCEC viability on PCL and PCL/PHBV circular samples cut out from the tubular scaffolds was evaluated by means of the MTS assays at 7 and 14 days from seeding (Fig. 27). Since at 14 days a significant decrease of the cell redox activity was observed, the MTS assay was also performed at intermediate times, particularly at 10 and 12 days from seeding. RCEC MTS reduction on PCL sample significantly ($p<0.05$)

increased after 10 days with respect to 7 days. On the contrary, RCEC MTS reduction on PCL sample decreased in highly significant ($p<0.01$) and in significant ($p<0.05$) way after 12 and 14 days respectively in comparison to 7 days and in significant ($p<0.05$) way both after 12 and 14 days in comparison to 10 days. Moreover RCEC MTS reduction on PCL/PHBV sample decreased in highly significant ($p<0.01$) way after 12 and 14 days with respect to 7 and 10 days.

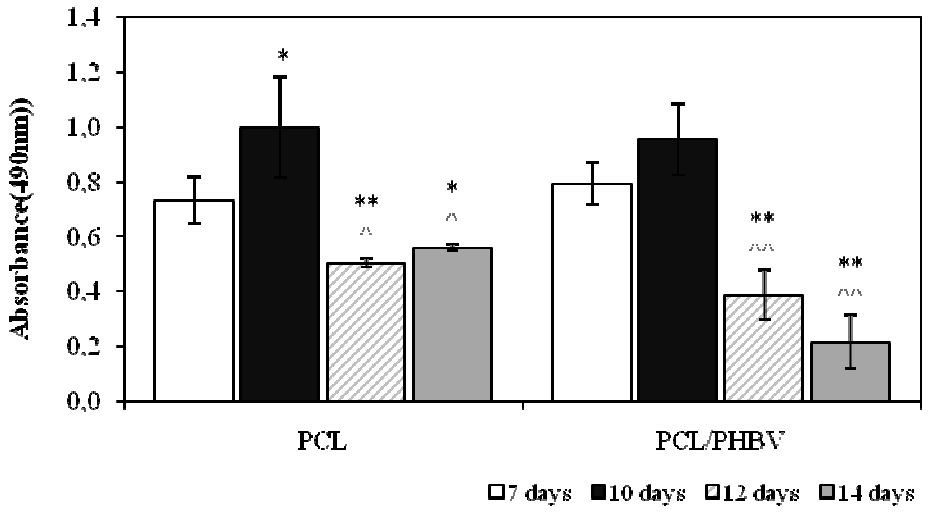

Fig. 27: RCEC MTS assay on PCL and PCL/PHBV circular samples cut out from the tubular scaffolds at 7, 10, 12 and 14 days after seeding. * $p<0.05$ and ** $p<0.01$ to 7 days; ^ $p<0.05$ and ^^ $p<0.01$ to 10 days.

Apoptotic, necrotic and healthy cells were stained by means of the same immunocytochemical kit used for the electrospun mats (Fig. 28). At 7 days from seeding, most of RCECs were healthy (blue stained) while only few necrotic cells (red stained) were detected on PCL and PCL/PHBV mats, suggesting that the main cell death way is the necrotic one. At 10 days from seeding most of RCECs were red stained on PCL and green stained on PCL/PHBV suggesting a different death way, the necrotic one for PCL and the apoptotic one for PCL/PHBV. Starting from 12 days after seeding on PCL/PHBV constructs, cells were less abundant compared to the other time points and cell death was more marked. These results showed a comparable trend with the MTS assay.

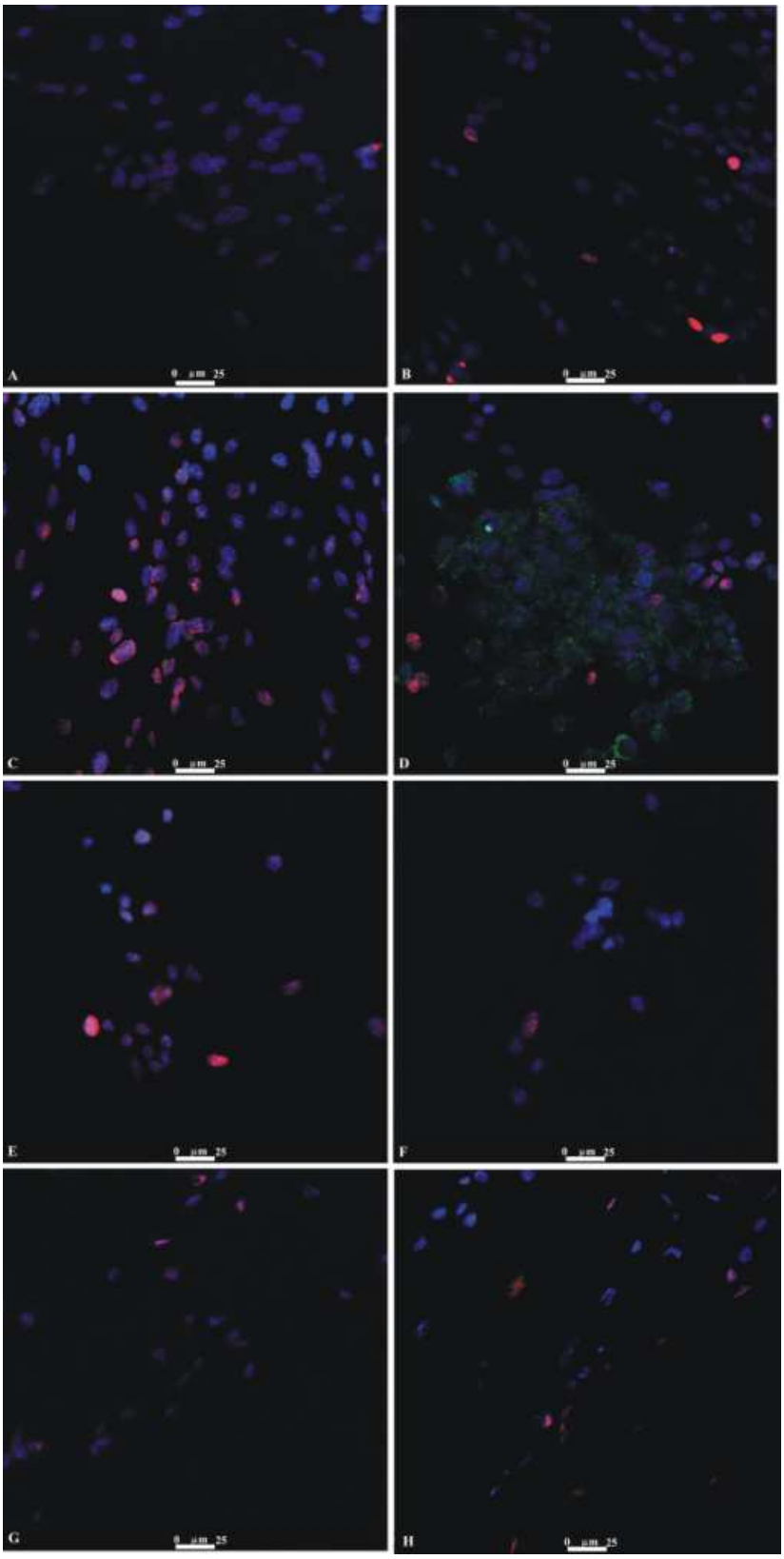

Fig. 28: Confocal laser scanning microscopy of viability assay of RCECs seeded on PCL (A, C, E, G) and PCL/PHBV (B, D, F, H) circular samples cut out from the tubular scaffolds at 7 days (A, B), 10 days (C, D), 12 days (E, F) and 14 days (G, H). Healthy cells are stained blue, necrotic cells are stained both red and blue and triple colors blue, red and green are dead cells processing from apoptotic cell population.

All samples cut out from tubular scaffolds supported RAEC viability. At 7 days from seeding the RAEC MTS reduction is higher on PCL in comparison to PHBV and PCL/PHBV. The RAEC metabolic activity on all samples was highly significant ($p<0.01$) at 14 days in respect to 7 days (Fig. 29).

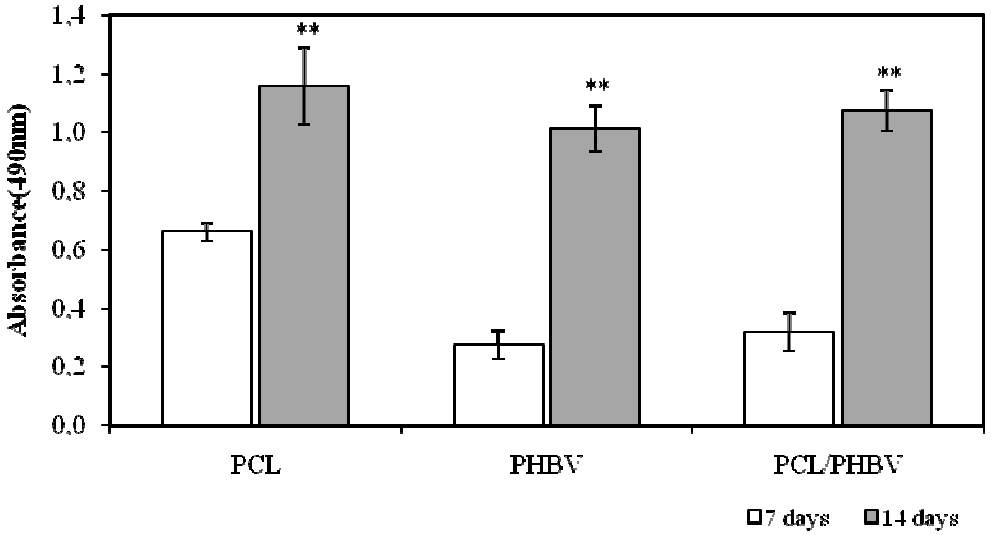

Fig. 29: RAEC MTS assay on PCL, PHBV and PCL/PHBV mats at 7 and 14 days after seeding.

** $p<0.01$ to 7 days.

Apoptotic, necrotic and healthy cells were stained by means of the same immunocytochemical kit used for the electrospun mats (Fig. 30).At 7 days from seeding most of RAECs were healthy (blue stained) while only few necrotic cells (red stained) were detected, suggesting that the main cell death way is the necrotic one. At 14 days RAECs were healthy on all samples. These results showed a comparable trend with the MTS assay.

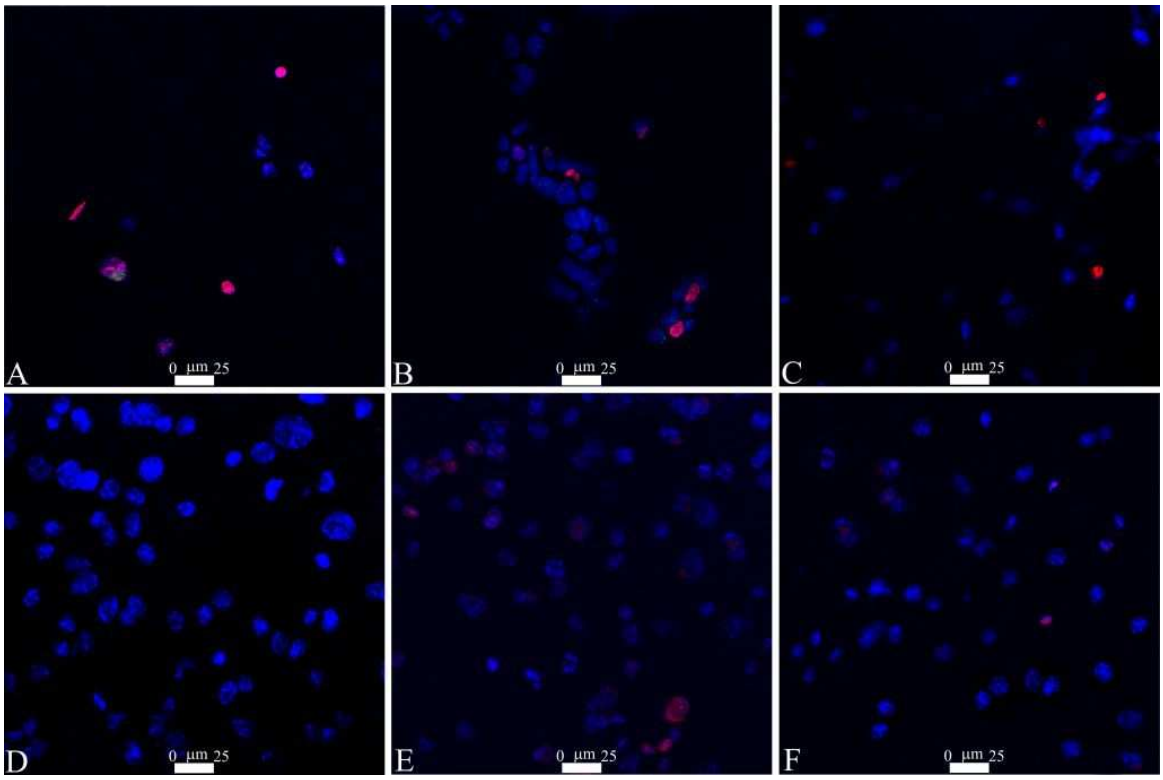

Fig. 30: Confocal laser scanning microscopy of viability assay of RAECs seeded on PCL (A, D), PHBV (B, E) and PCL/PHBV (C,FH) circular samples cut out from the tubular scaffolds at 7 days (A, B,C) and 14 days (D, E, F). Healthy cells are stained blue, necrotic cells are stained both red and blue and triple colors blue, red and green are dead cells processing from apoptotic cell population.

3.4.3. RCEC and RAEC proliferation assay

The potential influence of samples cut out from tubular scaffolds on RCEC and RAEC proliferation, was evaluated by means of the same immunocytochemical kit used for the electrospun mats. RCECs proliferated on PCL and PCL/PHBV samples. In particular, at 10 days from seeding the proliferative RCECs highly increased on PCL/PHBV in comparison to 7 days. At 12 days no cells were observed (Fig. 31).

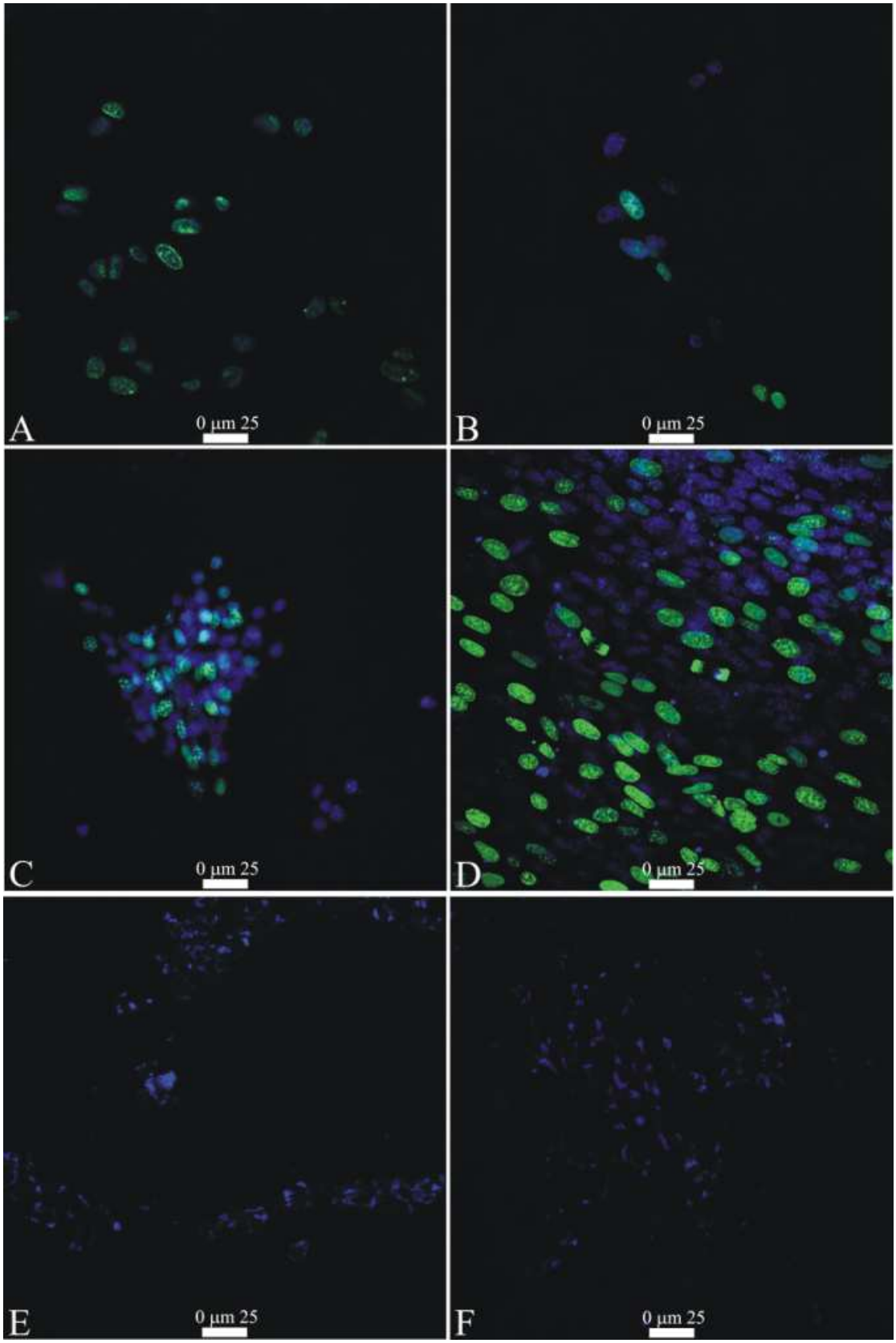

Fig. 31: Confocal laser scanning microscopy of proliferation assay of RCECs on PCL (A, C, E) and PCL/PHBV (B, D, F) circular samples cut out from the tubular scaffolds at 7 days (A, B), 10 days (C,D,) and 12 days (E, F). Nuclei are stained blue, proliferative nuclei are stained both green and blue.

At 7 days from seeding RAECs proliferated on all investigated samples similarly. At 14 days RAECs increased on PHBV and PCL/PHBV samples cut out from the tubular scaffolds, numerous proliferative cells were detected in respect to PCL samples (Fig. 32).

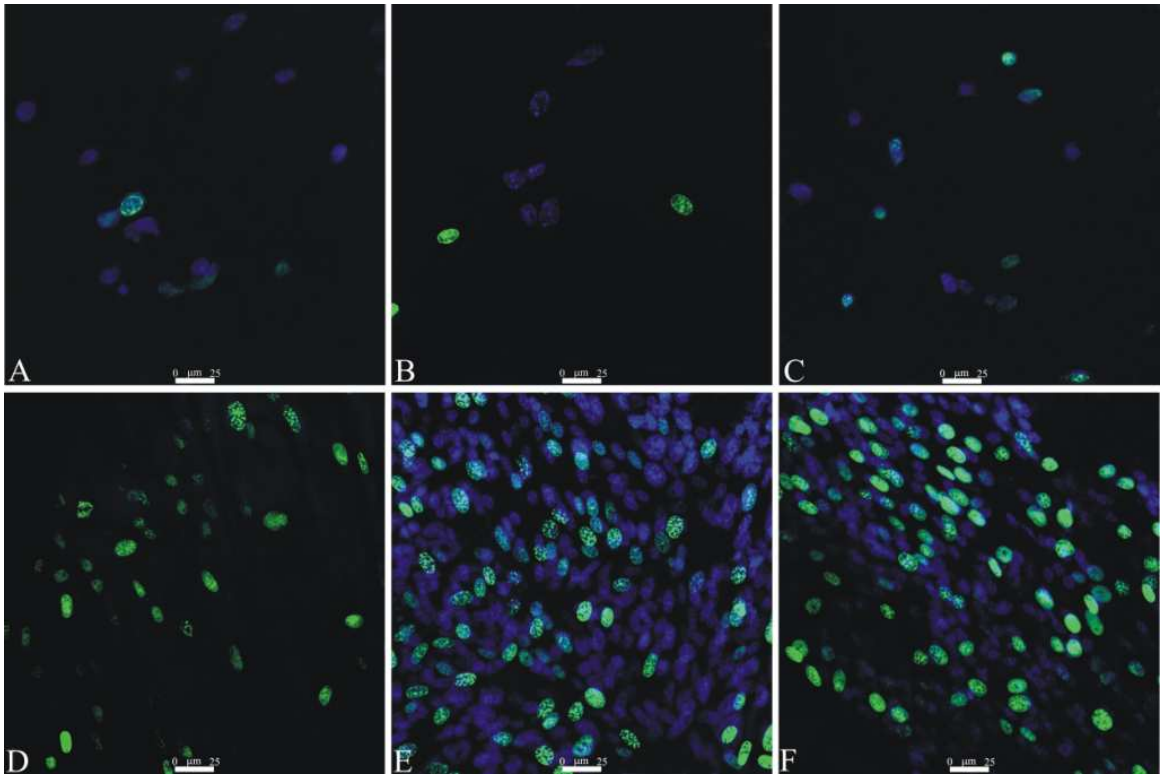

Fig. 32: Confocal laser scanning microscopy of proliferation assay of RAECs on PCL (A, D), PHBV (B, E) and PCL/PHBV (C, F) circular samples cut out from the tubular scaffolds at 7 days (A, B, C) and 14 days (D, E, F). Nuclei are stained blue, proliferative nuclei are stained both green and blue.

3.5. *In vivo* experiments

The PCL, PHBV and PCL/PHBV mats were implanted in the dorsal subcutaneous tissue of Sprague-Dawley rats to evaluate their biocompatibility. All animals survived, did not contract infections, have not experienced rejection and were sacrificed at the following time-points after surgery: 7 days, 14 days or 28 days.

3.5.1. Explanted polymeric mat macroscopic analysis

At the explant time-points, all mats kept the original size(Fig. 33), were integrated into the host tissue and were partially vascularized. The PHBV mat explants folded during the time lapse but their form was conserved.

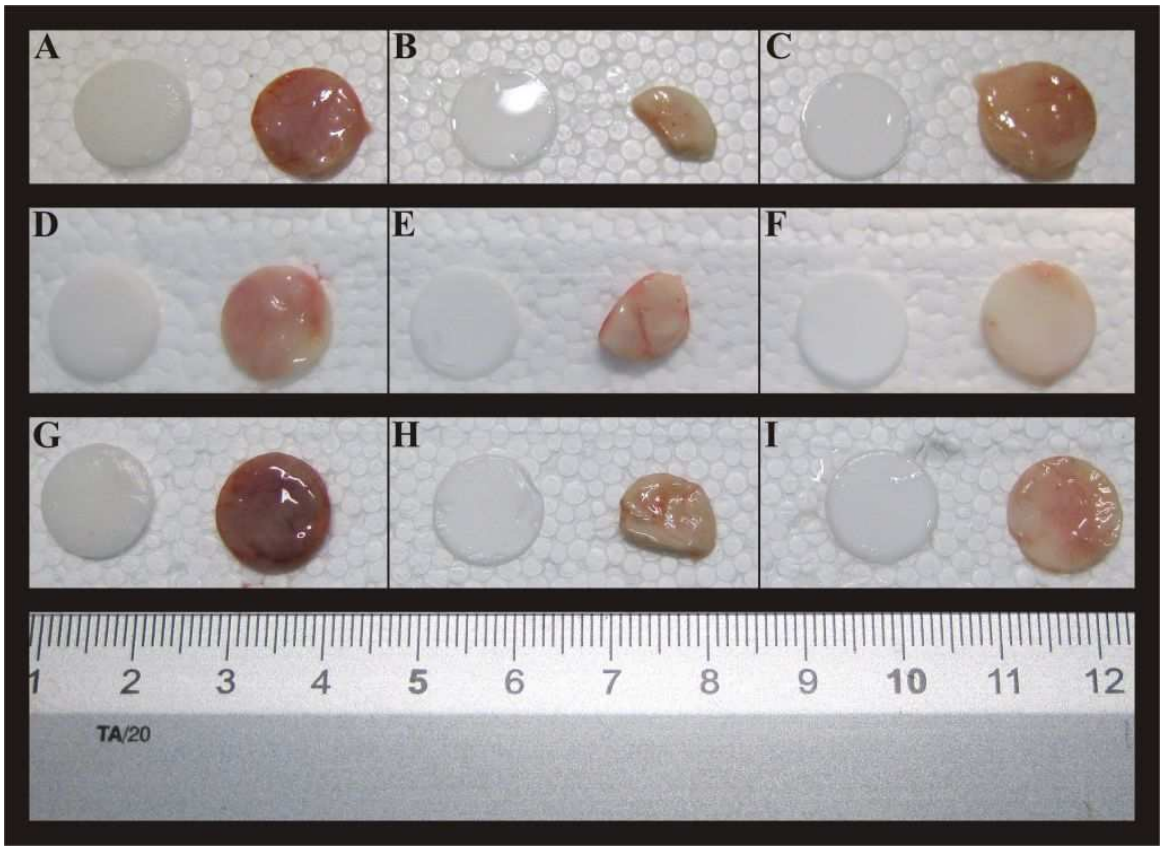

Fig. 33: PCL (A, D, G), PHBV (B, E, H) and PCL/PHBV (C, F, I) mats at 7 days (A, B, C), 14 days (D, E, F) and 28 days (G, H, I) from the subcutaneous implantation. On the left of each box the mats before the implant and on the right the mats explanted.

3.5.2. Explanted polymeric mats histochemical analysis

The explanted polymeric mats, cryosectioned at 5µm thickness, were stained with hematoxylin and eosin and observed at 100x magnification (Fig. 34), 200x magnification (Fig. 35) and 400x magnification (Fig. 36). At 7 days after surgery, the PCL mats showed high inflammatory response and infiltration (probably granulocytes and macrophages, localized at the edges but absent in the central part of the mat) and numerous vessels were observed. At 14 days after surgery, the inflammatory infiltrate was still high and localized at the fibrous capsule borderland, which was decreased in thickness, and vessels were observed into the mats. On borderline some cells began to migrate inward. At 28 days, the inflammatory infiltrate was still high and the fibrous capsule was not completely reabsorbed. The polymers were fully invaded by cells.

At 7 days after implantation, the PHBV mats were covered by a fibrous capsule thinner than PCL mats and the inflammatory response was lower compared to the PCL mats.

After 14 days the cellular infiltration was higher in respect to 7 days. In different borderline cells migrated into the inner part of the mats. In fact at 28 days some areas were completely colonized by cells.

At all time-points, the PCL/PHBV mats were less inflamed and less infiltrated in comparison to PCL mats. At 28 days, the fibrous capsule was still present, although at 7 and 14 days was thinner than on the PCL. The cellular infiltration decreased and disappeared at 28 days. On the borderland few migratory cells, probably myoblasts, were observed.

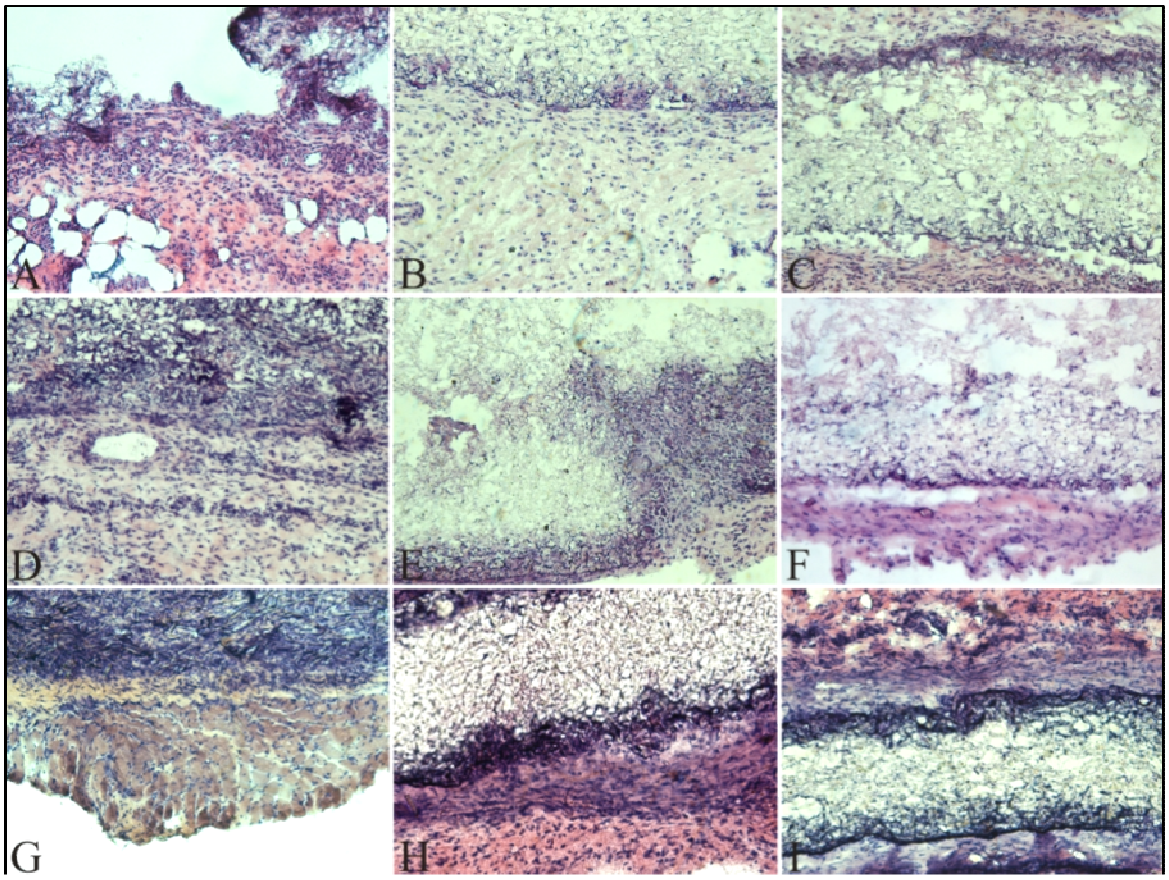

Fig. 34: Cross sections (5 μm) of polymeric mats: PCL (A, D, G), PHBV (B, E, H) and PCL/PHBV (C, F, I) mats at 7 days (A, B, C), 14 days (D, E, F) and 28 days (G, H, I) from the subcutaneous implantation (100x magnification).

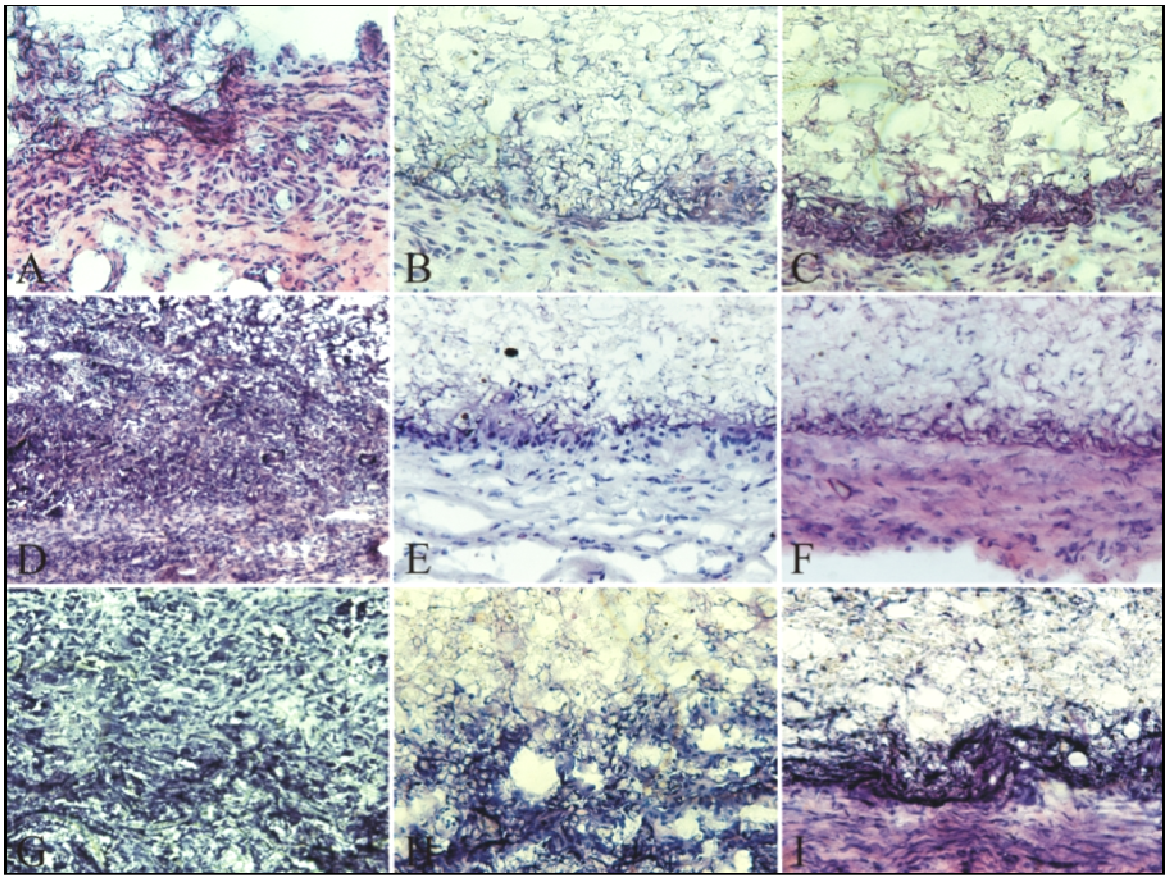

Fig. 35: Cross sections (5 µm) of polymeric mats: PCL (A, D, G), PHBV (B, E, H) and PCL/PHBV (C, F, I) mats at 7 days (A, B, C), 14 days (D, E, F) and 28 days (G, H, I) from the subcutaneous implantation (200x magnification).

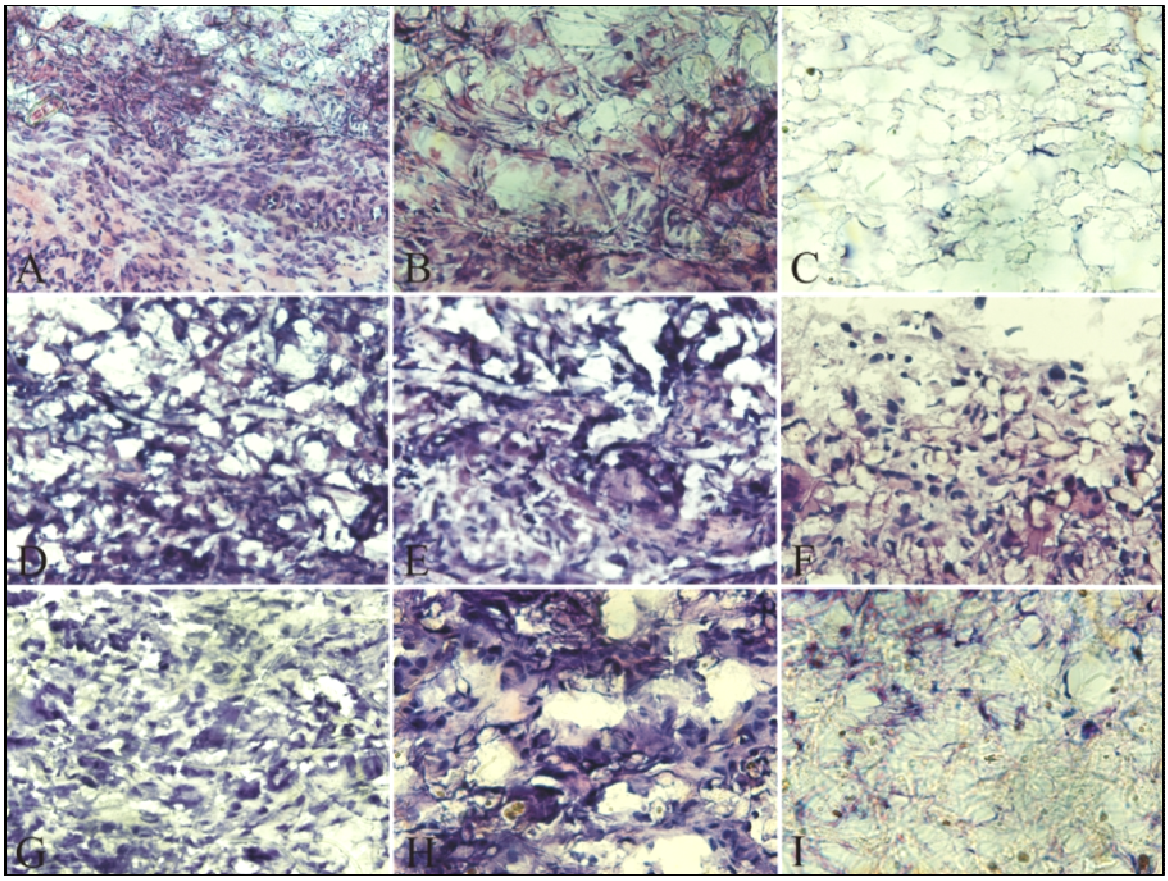

Fig. 36: Cross sections (5 μm) of polymeric mats: PCL (A, D, G), PHBV (B, E, H) and PCL/PHBV (C, F, I) mats at 7 days (A, B, C), 14 days (D, E, F) and 28 days (G, H, I) from the subcutaneous implantation (400x magnification).

4 DISCUSSION

Atherosclerosis and cardiovascular diseases are the most common causes of morbidity and mortality in patients all over the world (*Unal et al., 2003*), most of which need surgical intervention. The limited availability of healthy autologous vessels for bypassing grafting procedures has led to the fabrication of prosthetic vascular conduits. Synthetic polymeric materials, while providing the appropriate mechanical strength, lack the compliance and biocompatibility that bioresorbable and naturally occurring protein polymers offer (*Ravi et al., 2009*). The development of suitable vessel grafts is a relevant issue to be addressed, especially referring to small-diameter ones since *Dacron* and *Teflon* prostheses showed rates of thrombosis greater than 40% after 6 months when used to bypass arteries (*Hoerstrup et al., 2001*). Cardiovascular tissue engineering has the prospect of biological, living and autologous blood vessel to meet the need for a functional conduits (*Zhang et al., 2007*). In this respect, the selection of an appropriate biomaterial formed in a functional fashion, able to support cell adhesion, proliferation and migration and to promote ECM formation, is of paramount importance. Several approaches have been adopted to modify vascular graft surfaces, such as EC seeding, relevant proteins (e.g., collagen, albumin and laminin) coating, or addition of anti-coagulants and growth factor (*Zhang et al., 2007*). Although tissue engineering vascular graft (TEVGs) based on biodegradable scaffolds have yielded promising results, limitations remain. Challenges of cell sourcing are compounded by long culture periods that range between 2 and 6 months, and the proliferative capacity of cells isolated from elderly patients is limited (*Ravi et al., 2009; L'Heureux et al., 2006*).

The poly(ε-caprolactone) (PCL) is a synthetic aliphatic polyester, intensively investigated biomaterial; its advantages are ease of fabrication, pliability, and tunable mechanical strength. It can be produced to conduits with the required dimensions, optimum porosity and viscoelasticity (*Pankajakshan et Agrawal, 2010*). However, its generally poor cell affinity due to hydrophobicity, lack of cell-binding signals and its slow degradation rate *in vivo* (*Nottelet et al., 2009*) have become the major obstacle to be an ideal tissue engineering material (*Xiang et al., 2011*). Consequently PCL blended with natural polymers could be a promising approach in vascular tissue engineering (*Pankajakshan et Agrawal, 2010*). Moreover, blend of synthetic with natural polymers have shown good cytocompatibility with mesenchymal stem cells (*Tang et Wu, 2005*). The poly(3-hydroxybutyrate-co-3-hydroxyvalerate) (PHBV) is a natural material produced by

numerous bacteria. Its *in vivo* degradation involves the release of hydroxy acids, less acid and less inflammatory than other bioresorbable polymers (*Williams et Martin, 2002*). Its various properties such as natural origin, biodegradability, biocompatibility, non-toxicity (*Ke at al., 2010*) make it a good candidate for blending with PCL.

Starting from these assumptions, in this work, the potential advantage of intimate blending soft PCL, already approved by the Food and Drug Administration, with hard PHBV has been evaluated. The bioresorbable polymeric mats and tubular scaffolds were designed, produced and characterized at the University of Rome "Tor Vergata", Department of Science and Chemical Technology, by Prof. Alessandra Bianco and Eng. Costantino Del Gaudio. In particular, non-woven mats and small-diameter tubular scaffolds of PCL, PHBV and the blend 50% PCL/50% PHBV (PCL/PHBV) were fabricated by means of electrospinning technique. The aim of the present study was to evaluate the characteristics of the materials and of their construct to obtain EC growth in a short time, firstly studying the most suitable material among PCL, PHBV and PCL/PHBV by means of *in vitro* cytocompatibility and *in vivo* biocompatibility assays, then the influence of fiber organization on cell growth and colonization. By means of the material and its construct it has been possible to discriminate the actual influence of the polymeric substrates, giving insights on the role of the mechanical characteristics of morphologically similar 2D mats and the micro-pattern topology of tubular scaffolds. These two topics are strictly correlated since a relevant number of previous studies dealt with electrospun vascular grafts characterized by either randomly arranged (*Inoguchi et al., 2006; Stitzel et al., 2006; Soffer et al., 2008; Nottelet et al., 2009*) or circumferentially aligned fibers (*Xu et al., 2004; McClure et al., 2009*). Moreover, electrospun sheets can be considered as a potential alternative for the production of arterial grafts through a rolling procedure (*McClure et al., 2009*). Therefore, a specific luminal texture that can effectively support EC growth, also depending on the mechanical properties of the selected biomaterial, needed to be further investigated. In fact lack of lining ECs on graft lumen is a significant factor contributing to graft poor patency (*Mitchell et Niklason, 2003*). In this study, ECs from diverse compartments, rat cerebral endothelial cells (RCECs) and rat aortic endothelial cells (RAECs) were used, in *in vitro* well-established model. The response is linked to the concept that the unique ultra-structural characteristics of microvascular and macrovascular ECs are intrinsic to the cells themselves and are not determined by differential culture conditions (*Craig et al., 1998*).

Moreover the aortic endothelial cells grow rapidly and are larger, more polygonal, and do not grow as tightly apposed as the microvascular endothelial cells (*Craig et al., 1998*).

The biological results, obtained by the *in vitro* studies, showed that PCL mats supported RCEC viability, proliferation and adhesion during the observation period (14 days). Necrosis and apoptosis were observed on PCL mats, without the affection of redox activity in the MTS assay. The result is in agreement with previous studies, since apoptotic signals have been reported to be implicated in a variety of cellular functions, including cell proliferation, survival, differentiation and inflammatory response (*Izumi et al., 2005*). RCECs grown on PCL mats expressed adhesion proteins, actin and vinculin, and formed a three-dimensional network according to the architecture of the fibrous structure. Cells cultured on PCL were able to homogenously grow on the mat. Cell adhesion to the substrate and the formation of cell-cell contacts are two required processes for scaffold colonization, cell survivor and proliferation, since the characteristics of the substrate itself regulate cell morphology, rates of movement and cell activation (*Curtis et Wilkinson, 1997*). Similar observations were previously reported investigating the fibroblast response to the nanotopography of poly(L-lactic acid) scaffolds. Improvements in cell response were found to correlate with focal contact and actin microfilament development (*Milner et Siedlecki, 2007*).

PCL mats supported RAEC viability, proliferation and adhesion during the observation period (14 days). Some necrotic cells were observed at both time-points, differently the RAEC apoptosis was never observed. At 14 days the MTS reduction is not significantly higher in respect to 7 days but RAECs were able to homogenously grow on the mat and to colonize the surface. Regarding PHBV, RCECs grew non-homogeneously forming clusters. More precisely, at the beginning (*i.e.* up to day 12) RCECs colonized the overall surface, later and until day 14 a scattered cell growth was observed. The adhesion assay demonstrated the weak expression of actin protein and the marked expression of vinculin. Very recently, Ke et al. (*2010*) seeded sheep bone mesenchymal stem cells on salt-leached scaffolds and reported that cellular adhesion increased until 6 hours and by day 3 no cells were observed on the polymeric substrate. It can be assumed that, due to the poor cell-material interaction, the establishment of reciprocal cellular contacts enabled them to survive. Observing SEM micrographs large interconnected voids were present within fibers and the fiber surface is probably less rough with respect to PCL and PCL/PHBV. In fact it is well known that the porosity, pore sizes and interconnection between the pores affect nutrient diffusion to cells and guide cell organization and tissue ingrowth. This

parameters are some of the most important in the design of a scaffold to provide a substitute initially for wound contraction forces and later for the remodelling of the tissue (*Ke et al., 2010*). Differently to PCL, where RCECs were characterized by both apoptosis and necrosis, cells on PHBV mats were mainly affected by necrosis. The RAECs seeded on PHBV showed a significantly higher MTS reduction at 14 days in comparison to 7 days. These data were confirmed by the viability assay, in fact at 14 days more healthy cells were observed. Also the RAEC proliferative activity is higher at 14 days. On PCL/PHBV, RCECs were characterized by an intermediate behaviour between that of PCL and PHBV. Up to day 12, RCECs grew on scattered way, expressed lower adhesion proteins, proliferated and dead similarly to PHBV. Afterwards the cellular response was similar to that observed for PCL. The lower cellular adhesion observed during the incubation period probably affected cell survivor. RCEC redox activity decreased at 7 day incubation and cells dead by necrosis. Probably during the last 7 day of incubation, the RCECs seeded on PCL/PHBV mats reach the confluence and then at 14 days dead by necrosis, confirming their growth in a short time on this material. RAECs seeded on PCL/PHBV showed the highest metabolic activity in the MTS assay at 14 days. The viability assay confirmed the MTS result, in fact the surface is completely colonized by cells, most of them healthy. The RAEC behaviour is similar on PCL and PCL/PHBV. The results obtained from RCEC and RAEC cytocompatibility assays demonstrated that both PCL and PCL/PHBV seem to have appropriate characteristics for vascular tissue regeneration. These electrospun mats were characterized by comparable microstructural features both in terms of average fiber diameter and void size. Reasonably, the observed different behaviour of RCECs and RAECs could be related to the mechanical characteristics of the three investigated electrospun mats, being well known that stiffness plays a specific role in cell-scaffold interaction. Brown et al. (*2005*) reported that vascular smooth muscle cell proliferation rate was inversely related to the stiffness scaffolds made of polydimethylsiloxane, cell number increasing 20-fold on the softest substrate. A similar behaviour was verified for ECs plated on collagen or fibrin gels of differing flexibility, showing a decrease in network-like structures on stiffer gels (*Georges et Janmey, 2005*). Differently, human dermal fibroblasts showed an increasing proliferation rate directly with the matrix stiffness (*Hadjipanayi et al., 2009*). On this basis, the cell model here considered seems to have positively interacted with PCL and PCL/PHBV fibrous substrates characterized by a stiffness value below 30 MPa.

To evaluate the influence of fiber alignment on cell response, circular samples of the same diameter of the previously used mats were cut out from tubular scaffolds and the same experimental conditions were applied. RCECs seeded on PCL and PCL/PHBV circular samples cut out from the tubular scaffolds clearly colonized the surface and express both actin and vinculin at day 7 following the fiber layout. Morphological investigation of electrospun tubular scaffolds showed that PCL and PCL/PHBV samples were characterized by a comparable fiber alignment, more marked in the case of the blend and when collected at high rotational speed. Viability assays confirmed that cells are viable at 7 days, being mainly healthy and only few were necrotic. At day 14 less RCEC nuclei were visualized, they less adhered than at day 7 and most of them were dead. Experiments were then performed at 10 and 12 days trying to understand when and the reason for cell death. The viability assays demonstrated that RCECs grew until 10 days from seeding and then they dead by necrosis on PCL and by apoptosis on PCL/PHBV. Therefore, it can be assumed that, differently from *in vivo*, in this *in vitro* system cells might die due to contact inhibition (*Johnson et Fass, 1983*). This is a well known limitation of *in vitro* experiments while *in vivo* different physiological mechanisms are activated to prevent the death cell by contact inhibition. PCL tubular scaffold showed the lowest tensile modulus, the highest tensile strength and deformation at break, confirming the extreme deformability of this polyester able to support a constant increasing stress level up to break. This feature can be related to the fiber architecture. Generally, electrospun scaffolds firstly experience a re-arrangement of the fibers in the loading direction, leading then to the final response that depends on the specific material (*Del Gaudio et al., 2011*). In this case, the grafts were minimally subjected to morphological modifications during the tensile tests, since the fibers were preferentially oriented in the loading direction, and therefore the highest strength measured for the PCL tubular scaffolds can be ascribed to the fiber dimension. SEM micrographs revealed a bimodal diameter distribution and it is reasonable to assume that sub-micrometric fibers contributed to this effect, being well stated that thinner fibers improve the mechanical characteristics of fibrous material (*Amornsakchai et al., 1993; Li et al., 2002*). PCL vascular grafts were characterized by comparable tensile strength with respect to tissue engineered blood vessels and native ones (*Konig et al., 2009*). The SRS characterization showed similar values to those measured for decellularized human saphenous vein and human mammary artery (*Schaner et al., 2004; L'Heureux et al., 2006*) and *in vitro* cell conditioned polymeric vascular grafts (*Hoerstrup et al., 2001*). These results proved that

the investigated scaffolds are mechanically consistent with previous (*Del Gaudio et al., 2009; Del Gaudio et al., 2011*) proposed biological or synthetic substitutes, suggesting for the fibrous structure a potential role in vascular applications. No RCECs were observed on PHBV circular samples cut out from the tubular scaffolds at 7 and 14 days confirming that PHBV scaffolds are not suitable for RCEC growth. Probably that is due to their intrinsic characteristics and to the non-homogenous fiber deposition with several microdefects of the material structure, suggesting that the processing conditions should be optimized in order to improve its microstructural, mechanical and subsequent biological features. The poor cell adhesion observed on these experiments may result in an easy detachment of cells during the protocol washings (DAPI nuclei staining and adhesion kit). No other experiments with RCECs were performed on PHBV. Differently, the RAEC response seeded on PCL, PHBV and PCL/PHBV samples cut out from the tubular scaffolds is similar, in fact at 14 days from seeding the MTS reduction is significantly higher in respect to 7 days. The viability assay confirmed that RAECs grew on all samples and were able to colonize the sample surface within 14 days. At this time-point only few necrotic cells were observed on samples cut out from the PHBV tubular scaffolds. Probably the similar RAEC response to different materials is due to some intrinsic RAEC characteristics. They are larger and do not grow as tightly apposed as the microvascular endothelial cells (*Craig et al., 1998*). Thus the microstructure and the fiber alignment of the scaffolds do not affect in a high significant way the RAEC behaviour. The proliferation assay showed that RAECs maintained their duplication capability within 14 days, more expressed on samples cut out from the PCL/PHBV tubular scaffolds. These results are particularly relevant as PCL and PCL/PHBV samples supported RCEC growth on the inner surface in a short time (within 7 days) and the RAEC growth in 14 days. Moreover in the case of PCL and PCL/PHBV electrospun tubular scaffolds, RCECs colonized the luminal surface arranging toward a monolayer as for the inner structure of a blood vessel. In fact ECs align parallel to the direction of unidirectional flow, through the reorganization of cytoskeletal filaments and focal adhesion complexes (*Butcher at al., 2004*). A stable EC monolayer is essential to line the luminal surface of grafts to provide physiological vasoactive , anti-thrombotic properties (*Stephan et al., 2006*), transport of nutrients and transduction of mechanical and biochemical signals (*Davies et al., 1997*). It has to be highlighted that our results are particularly encouraging since it is well known that the long-term failure of the small-diameter vascular grafts is mainly associated to the incomplete lining of ECs leading to myointimal hyperplasia (*Ma et al., 2005*) and

thrombus formation. Intimal hyperplasia leads to vessel reclosure and compliance mismatch between prothesis and adjacent artery (*Musey et al., 2002*).

In order to investigate the biocompatibility of PHBV and PCL/PHBV, compared to PCL, the polymeric mats were implanted in the dorsal subcutaneous tissue of anesthetized Sprague-Dawley rats, following an experimental protocol approved by the local Ethics Committee of the University of Padua for Animal Testing (CEASA). At 7 days after implantation, the PHBV mats were covered by a fibrous capsule thinner than PCL mats and the inflammatory response was lower compared to PCL. Some cells migrated into the inner part of the mats, at the last time-point (28 days) some areas were completely colonized by cells. The PHBV mat explants folded during the time lapse but their form was conserved, this is probably due to its increased hydrophobicity, stiffness and reduced thickness. The *in vivo* degradation of poly-hydroxyalcanoates, including the PHBV, involves the release of hydroxy acids, less acidic and less inflammatory products in respect to bioresorbable synthetic polymers (*Williams et Martin, 2002*). In addition, tubular structures were tested *in vivo* in lambs as a substitute for abdominal aorta giving an insignificant inflammatory response (*Shum-Tim et al., 1999*). At all time-points, the PCL/PHBV mats were less inflamed and less infiltrated in comparison to PCL mats. In fact at 28 days after surgery the PCL constructs still showed high inflammatory infiltrate, the fibrous capsule was not completely reabsorbed and numerous vessels were observed. Transmural cellular infiltration and formation of neocapillaries in graft body are the major graft healing characteristics (*Pektok et al., 2008*). The preserved scaffold structure suggests that this material possesses a very slow degradation rate *in vivo* and the degradation products are not toxic and eliminated through normal excretory routes (*Vert, 2009*). PCL small diameter vascular grafts for the replacement of abdominal aorta of the rat have shown good reliability at 24 weeks compared to implants of polytetrafluoroethylene (PTFE) normally used when there are no vessels derived autologous (*Pektok et al., 2008*). Further experiments of immunohistochemistry must be performed on explanted polymeric mats in order to evaluate the cell infiltrated phenotype and to understand the inflammatory response.

In conclusion, the results, obtained in the *in vitro* cytocompatibility assays and in the *in vivo* experiments, suggest that the blend PCL/PHBV as a possible alternative material to the PCL in the field of vascular tissue engineering because it combines the good mechanical and physical characteristics of the synthetic material with the degradation properties and biocompatibility of natural material respectively. The blending

option can be valuably considered for tailoring specific features of selected biomaterials for the improvement of the overall scaffold performance.

REFERENCES

Abbott NJ, Hughes CC, Revest PA, Greenwood J. *Development and characterisation of a rat brain capillary endothelial culture: towards an in vitro blood-brain barrier*. J Cell Sci. 1992 Sep;103 (Pt 1):23-37

Aebischer P, Valentini RF, Winn SR, Galletti PM. *The use of a semi-permeable tube as a guidance channel for a transected rabbit optic nerve.* Prog Brain Res. 1988;78:599-603

Albertin G, Guidolin D, Sorato E, Spinazzi R, Mascarin A, Oselladore B, Montopoli M, Antonello M, Ribatti D. *Pro-angiogenic activity of Urotensin-II on different human vascular endothelial cell populations*. Regul Pept. 2009 Oct 9;157(1-3):64-71. Epub 2009 Apr 10

Alberts B, Bray D, Lewis J, Raff M, Watson JD. *Biologia molecolare della cellula.* Terza Edizione Zanichelli, 1995

Amornsakchai T, Cansfield DLM, Jaward SA, Pollard G, Ward IM. *The relation between filament diameter and fracture strength for ultra-high-modulus polyethylene fibres.* J Mater Sci 1993;28:1689–1698

Andrews KD, Hunt JA. *Developing smaller-diameter biocompatible vascular grafts*. 2009. Woodhead Publishing Limited, CRC Press, Chapter 9

Baguneid MS, Seifalian AM, Salacinski HJ, Murray D, Hamilton G, Walker MG. *Tissue engineering of blood vessels*. Br J Surg. 2006 Mar;93(3):282-90

Baiguera S, Conconi MT, Guidolin D, Mazzocchi G, Malendowicz LK, Parnigotto PP, Spinazzi R, Nussdorfer GG. *Ghrelin inhibits in vitro angiogenic activity of rat brain microvascular endothelial cells*. Int J Mol Med. 2004 Nov;14(5):849-54

Baiguera S, Del Gaudio C, Fioravanzo L, Bianco A, Grigioni M, Folin M. *In vitro astrocyte and cerebral endothelial cell response to electrospun poly(epsilon-caprolactone) mats of different architecture*. J Mater Sci Mater Med. 2010 Apr;21(4):1353-62

Barbarisi A, Rosso F. *Ingegneria tissutale ed organi artificiali: la medicina ricostruttiva.* 104° Congresso Nazionale. Società Italiana di Chirurgia, 2002,Vol. I pp. 3-16

Barbarisi M, Pace MC, Passavanti MB, Maisto M, Mazzariello L, Pota V, Aurilio C. *Pregabalin and transcutaneous electrical nerve stimulation for postherpetic neuralgia treatment.* Clin J Pain. 2010 Sep;26(7):567-72

Bell E. *Tissue engineering in perspective*. in: Lanza RT, Langer R., Vacanti J.P., Principle of tissue engineering, Academic Press, San Diego, CA, 2000, p. xxxv

Biela SA, Su Y, Spatz JP, Kemkemer R. *Different sensitivity of human endothelial cells, smooth musclecells and fibroblasts to topography in the nano-micro range*. Acta Biomater 2009;5:2460-6

References

Bolender RP. *Stereological analysis of the guinea pig pancreas. I. Analytical model and quantitative description of non stimulated pancreatic exocrine cells*. J Cell Biol. 1974 May;61(2):269-87

Bouïs D, Kusumanto Y, Meijer C, Mulder NH, Hospers GA. *A review on pro- and anti-angiogenic factors as targets of clinical intervention*. Pharmacol Res. 2006 Feb;53(2):89-103, Review

Bowers SL, Banerjee I, Baudino TA. *The extracellular matrix: at the center of it all*. J Mol Cell Cardiol. 2010 Mar;48(3):474-82. Epub 2009 Aug 31

Brooke BS, Karnik SK, Li DY. *Extracellular matrix in vascular morphogenesis and disease: structure versus signal*. Trends Cell Biol. 2003 Jan;13(1):51-6

Brown XQ, Ookawa K, Wong JY. *Evaluation of polydimethylsiloxane scaffolds with physiologically-relevant elastic moduli: interplay of substrate mechanics and surface chemistry effects on vascular smooth muscle cell response*. Biomaterials. 2005 Jun;26(16):3123-9

Butcher JT, Penrod AM, García AJ, Nerem RM. *Unique morphology and focal adhesion development of valvular endothelial cells in static and fluid flow environments*. Arterioscler Thromb Vasc Biol. 2004 Aug;24(8):1429-34

Calò L. et Semplicini A. *L'endotelio vascolare. Aspetti morfofunzionali, fisiopatologici e terapeutici*. 1998.Piccin, Padova, 14-22

Chan-Park MB, Shen JY, Cao Y, Xiong Y, Liu Y, Rayatpisheh S, Kang GC, Greisler HP. *Biomimetic control of vascular smooth muscle cell morphology and phenotype for functional tissue-engineered small-diameter blood vessels*. J Biomed Mater Res A. 2009 Mar 15;88(4):1104-21

Chlupác J, Filová E, Bacáková L. *Blood vessel replacement: 50 years of development and tissue engineering paradigms in vascular surgery*. Physiol Res. 2009;58 Suppl 2:S119-39

Clark ER, Clark EL. *Growth and behavior of epidermis as observed microscopically in observation chambers inserted in the ears of rabbits*. Am J Anat. 1953 Sep;93(2):171-219

Clowes AW, Kirkman TR, Reidy MA. *Mechanisms of arterial graft healing. Rapid transmural capillary ingrowth provides a source of intimal endothelium and smooth muscle in porous PTFE prostheses.* Am J Pathol. 1986 May;123(2):220-30

Conconi MT, Lora S, Baiguera S, Boscolo E, Folin M, Scienza R, Rebuffat P, Parnigotto PP, Nussdorfer GG. *In vitro culture of rat neuromicrovascular endothelial cells on polymeric scaffolds*. J Biomed Mater Res A 2004;71:669-74

Cortesini R. *Stem cells, tissue engineering and organogenesis in transplantation.* Transpl Immunol. 2005 Dec;15(2):81-9 Review

References

Craig LE, Spelman JP, Strandberg JD, Zink MC. *Endothelial cells from diverse tissues exhibit differences in growth and morphology*. Microvasc Res. 1998 Jan;55(1):65-76

Curtis A, Wilkinson C. *Topographical control of cells*. Biomaterials. 1997 Dec;18(24):1573-83

Davies PF, Barbee KA, Volin MV, Robotewskyj A, Chen J, Joseph L, Griem ML, Wernick MN, Jacobs E, Polacek DC, dePaola N, Barakat AI. *Spatial relationships in early signaling events of flow-mediated endothelial mechanotransduction*. Annu Rev Physiol. 1997;59:527-49

Dejana E. *Endothelial adherens junctions: implications in the control of vascular permeability and angiogenesis*. J Clin Invest. 1996 November 1; 98(9): 1949–1953

Del Gaudio C, Bianco A, Folin M, Baiguera S, Grigioni M. *Structural characterization and cell response evaluation of electrospun PCL membranes: micrometric versus submicrometric fibers*. J Biomed Mater Res A. 2009 Jun 15;89(4):1028-39

Del Gaudio C, Ercolani E, Nanni F, Bianco A. *Assessment of poly(ε-caprolactone)/poly(3-hydroxybutyrate-co-3-hydroxyvalerate) blends processed by solvent casting and electrospinning*. Mater Sci Eng A 2011;528:176451772

Dong Y, Liao S, Ngiam M, Chan CK, Ramakrishna S. *Degradation behaviors of electrospun resorbable polyester nanofibers*. Tissue Eng Part B Rev. 2009 Sep;15(3):333-51

Doshi J, Reneker DH. *Electrospinning process and applications of electrospun fibers*. Journal of Electrostatics 1995;35:151-60

Folkman J, Haudenschild C. *Angiogenesis in vitro*. Nature. 1980 Dec 11;288(5791):551-6

Frenot A, Chronakis IS. *Polymer nanofibers assembled by electrospinning*. Curr Opinion Coll Interface Sci 2003;8:64-75

Gafni Y, Zilberman Y, Ophir Z, Abramovitch R, Jaffe M, Gazit Z, Domb A, Gazit D. *Design of a filamentous polymeric scaffold for in vivo guided angiogenesis*. Tissue Eng. 2006 Nov;12(11):3021-34

Gauvin R, Ahsan T, Larouche D, Lévesque P, Dubé J, Auger FA, Nerem RM, Germain L. *A novel single-step self-assembly approach for the fabrication of tissue-engineered vascular constructs*. Tissue Eng Part A. 2010 May;16(5):1737-47

Georges PC, Janmey PA. *Cell type-specific response to growth on soft materials*. J Appl Physiol. 2005 Apr;98(4):1547-53. Review

Geraets WG. *Comparison of two methods for measuring orientation*. Bone. 1998 Oct;23(4):383-8

Gimbrone MA Jr, Nagel T, Topper JN. *Biomechanical activation: an emerging paradigm in endothelial adhesion biology*. J Clin Invest. 1997 Dec 1;100(11 Suppl):S61-5. Review

References

Gould MN, Biel WF, Clifton KH. *Morphological and quantitative studies of gland formation from inocula of monodispersed rat mammary cells.* Exp Cell Res. 1977 Jul;107(2):405-16

Greiner A, Wendorff JH. *Electrospinning: a fascinating method for the preparation of ultrathin fibers*. Angew Chem Int 2007;46:2-36

Gupta S, Johnstone R, Darby H, Selden C, Price Y, Hodgson HJ. *Transplanted isolated hepatocytes: effect of partial hepatectomy on proliferation of long-term syngeneic implants in rat spleen.* Pathology. 1987 Jan;19(1):28-30

Hadjipanayi E, Mudera V, Brown RA. *Close dependence of fibroblast proliferation on collagen scaffold matrix stiffness*. J Tissue Eng Regen Med. 2009 Feb;3(2):77-84

Harrington DA, Sharma AK, Erickson BA, Cheng EY. *Bladder tissue engineering through nanotechnology*. World J Urol, 2008; 26:315-322

He W, Ma Z, Teo WE, Dong YX, Robless PA, Lim TC, Ramakrishna S. *Tubular nanofiber scaffolds for tissue engineered small-diameter vascular grafts*. J Biomed Mater Res A. 2009 Jul;90(1):205-16

Hench LL, Polak JM. *Third-generation biomedical material.* Science. 2002;295: 1014-1017

Hirschi KK, D'Amore PA. *Pericytes in the microvasculature*. Cardiovasc Res. 1996 Oct;32(4):687-98. Review

Hoerstrup SP, Zünd G, Sodian R, Schnell AM, Grünenfelder J, Turina MI. *Tissue engineering of small caliber vascular grafts*. Eur J Cardiothorac Surg. 2001 Jul;20(1):164-9

Holtz J, Giesler M, Bassenge E. *Two dilatory mechanisms of anti-anginal drugs on epicardial coronary arteries in vivo: indirect, flow-dependent, endothelium-mediated dilation and direct smooth muscle relaxation.*Z Kardiol. 1983;72 Suppl 3:98-106

Huang ZM, Zhang YZ, Kotaki M, Ramakrishna S. *A review on polymer nanofibers by electrospinning and their applications in nanocomposites*. Composites Science and Technology 2003;63:2223-53

Inoguchi H, Kwon IK, Inoue E, Takamizawa K, Maehara Y, Matsuda T. *Mechanical responses of a compliant electrospun poly(L-lactide-co-epsilon-caprolactone) small-diameter vascular graft*. Biomaterials. 2006;27(8):1470-8

Isenberg BC, Williams C, Tranquillo RT. *Endothelialization and flow conditioning of fibrin-based media-equivalents.* Ann Biomed Eng. 2006 Jun;34(6):971-85

Izumi Y, Kim-Mitsuyama S, Yoshiyama M, Omura T, Shiota M, Matsuzawa A, Yukimura T, Murohara T, Takeya M, Ichijo H, Yoshikawa J, Iwao H. *Important role of apoptosis signal-regulating kinase 1 in ischemia-induced angiogenesis*. Arterioscler Thromb Vasc Biol. 2005 Sep;25(9):1877-83

References

Jackson CJ, Garbett PK, Nissen B, Schrieber L. *Binding of human endothelium to Ulex europaeus I-coated Dynabeads: application to the isolation of microvascular endothelium*. J Cell Sci. 1990 Jun;96 (Pt 2):257-62

James M, Anderson MD. *Mechanisms of inflammation and infection with implanted devices*. Cardiovascular Pathology, Volume 2, Issue 3, Supplement, July-September 1993, Pages 33-41

Johnson CM, Fass DN. *Porcine cardiac valvular endothelial cells in culture. A relative deficiency of fibronectin synthesis in vitro*. Lab Invest. 1983 Nov;49(5):589-98

Ju YM, Choi JS, Atala A, Yoo JJ, Lee SJ. *Bilayered scaffold for engineering cellularized blood vessels*. Biomaterials. 2010 May;31(15):4313-21

Kambiz AN, Hossein SZ, Sung CY. *The production of a cold-induced extracellular biopolymer by Pseudomonas fluorescens BM07 under various growth conditions and its role in heavy metals absorption*. Process biochemistry. 2007; 42 (847-855)

Karamysheva AF. *Mechanisms of angiogenesis*. Biochemistry (Mosc). 2008 Jul;73(7):751-62, Review

Ke Y, Wang YJ, Ren L, Zhao QC, Huang W. *Modified PHBV scaffolds by in situ UV polymerization: structural characteristic, mechanical properties and bone mesenchymal stem cell compatibility*. Acta Biomater. 2010 Apr;6(4):1329-36

Khait L, Birla RK. *Bypassing the patient: Comparison of biocompatible models for the future of vascular tissue engineering.* Cell Transplant. 2011 Mar 9

Kloud L, Vaz CM, Mol A, Baaijens FP, Bouten CV. *Effect of biomimetic conditions on mechanical and structural integrity of PGA/P4HB and electrospun PCL scaffolds*. J Mater Sci Mater Med. 2008;19(3):1137-44

Konig G, McAllister TN, Dusserre N, Garrido SA, Iyican C, Marini A, Fiorillo A, Avila H, Wystrychowski W, Zagalski K, Maruszewski M, Jones AL, Cierpka L, de la Fuente LM, L'Heureux N. *Mechanical properties of completely autologous human tissue engineered blood vessels compared to human saphenous vein and mammary artery*. Biomaterials. 2009 Mar;30(8):1542-50

Kovacs EJ, Di Pietro LA. *Fibrogenic cytokines and connective tissue production.* FASEB J. 1994 Aug; 8(11):854-61

Kurz H. *Physiology of angiogenesis*. J Neurooncol. 2000 Oct-Nov;50(1-2):17-35, Review

Lamszus K, Schmidt NO, Ergün S, Westphal M. *Isolation and culture of human neuromicrovascular endothelial cells for the study of angiogenesis in vitro*. J Neurosci Res. 1999 Feb 1;55(3):370-8

Langer R, Vacanti JP. *Tissue engineering*. Science. 1993 May 14;260(5110):920-6

References

Lee SJ, Yoo JJ, Lim GJ, Atala A, Stitzel J. *In vitro evaluation of electrospun nanofiber scaffolds for vascular graft application*. J Biomed Mater Res A. 2007;83(4):999-1008

Leon L, Greisler HP. *Vascular grafts*. Expert Rev Cardiovasc Ther. 2003 Nov;1(4):581-94

L'Heureux N, Dusserre N, Konig G, Victor B, Keire P, Wight TN, Chronos NA, Kyles AE, Gregory CR, Hoyt G, Robbins RC, McAllister TN. *Human tissue-engineered blood vessels for adult arterial revascularization*. Nat Med. 2006 Mar;12(3):361-5

Li WJ, Laurencin CT, Caterson EJ, Tuan RS, Ko FK. *Electrospun nanofibrous structure: a novel scaffold for tissue engineering*. J Biomed Mater Res. 2002 Jun 15;60(4):613-21

Lysaght MJ, Jaklenec A, Deweerd E. *Great expectations: private sector activity in tissue engineering, regenerative medicine, and stem cell therapeutics*. Tissue Eng Part A 2008;14:305-15

Ma Z, Kotaki M, Yong T, He W, Ramakrishna S. *Surface engineering of electrospun polyethyleneterephthalate (PET) nanofibers towards development of a new material for blood vessel engineering*. Biomaterials. 2005 May;26(15):2527-36

Marieb EN, Mallatt J, Wilhelm PB. *Human Anatomy*. 2007. Pearson Education (US), chapter 20

Mauck RL, Baker BM, Nerurkar NL, Burdick JA, Li WJ, Tuan RS, Elliott DM. *Engineering on the straight and narrow: the mechanics of nanofibrous assemblies for fiber-reinforced tissue regeneration*. Tissue Eng Part B Rev. 2009 Jun;15(2):171-93. Review.

Mayhew TA, Williams GR, Senica MA, Kuniholm G, Du Moulin GC. *Validation of a quality assurance program for autologous cultured chondrocyte implantation.* Tissue Eng. 1998 Fall;4(3):325-34

McClure MJ, Sell SA, Ayres CE, Simpson DG, Bowlin GL. *Electrospinning-aligned and random polydioxanone-polycaprolactone-silk fibroin-blended scaffolds: geometry for a vascular matrix*. Biomed Mater. 2009 Oct;4(5):055010

Milner KR, Siedlecki CA. *Fibroblast response is enhanced by poly(L-lactic acid) nanotopography edge density and proximity*. Int J Nanomedicine. 2007;2(2):201-11

Mironov V, Kasyanov V and Markwald RR. *Nanotechnology in vascular tissue engineering: from nanoscaffolding towards rapid vessel biofabrication*. Cell Press, 2008, 338-334

Mitchell SL, Niklason LE. *Requirements for growing tissue-engineered vascular grafts*. Cardiovasc Pathol. 2003 Mar-Apr;12(2):59-64. Review

Molnar TF, Pongracz JE. *Tissue engineering and biotechnology in general thoracic surgery*. Eur J Cardiothorac Surg. 2010 Jun;37(6):1402-10

Motta P. *Color atlas of microscopic anatomy*. Piccin, Padova 1990

References

Musey PI, Ibim SM, Talukder NK. *Development of artificial blood vessels: seeding and proliferation characteristics of endothelial and smooth muscle cells on biodegradable membranes*. Ann N Y Acad Sci. 2002 Jun;961:279-83. Review

Naito Y, Shinoka T, Duncan D, Hibino N, Solomon D, Cleary M, Rathore A, Fein C, Church S, Breuer C. *Vascular tissue engineering: Towards the next generation vascular grafts*. Adv Drug Deliv Rev. 2011 Mar 21. PMID: 21421015

Nelson DL, Cox MM. *Lehninger Principles of Biochemistry*. 3rd ed. 2000.Worth Publisher, New York

Nerem RM, Seliktar D. *Vascular tissue engineering*. Annu Rev Biomed Eng. 2001;3:225-43. Review. PMID: 11447063

Niklason LE, Gao J, Abbott WM, Hirschi KK, Houser S, Marini R, Langer R. *Functional arteries grown in vitro.* Science. 1999 Apr 16;284(5413):489-93

Noishiki Y, Yamane Y, Okoshi T, Tomizawa Y, Satoh S. *Choice, isolation, and preparation of cells for bioartificial vascular grafts.* Artif Organs. 1998 Jan;22(1):50-62

Nottelet B, Pektok E, Mandracchia D, Tille JC, Walpoth B, Gurny R, Möller M. *Factorial design optimization and in vivo feasibility of poly(epsilon-caprolactone)-micro- and nanofiber-based small diameter vascular grafts*. J Biomed Mater Res A. 2009 Jun 15;89(4):865-75. PMID: 18465817

Nuti S. *Tissue Engineered Vascular Grafts: The Bright Future of Heart Health.* Yale Scientific Magazine (2010)

Pankajakshan D, Agrawal DK. *Scaffolds in tissue engineering of blood vessels*. Can J Physiol Pharmacol. 2010 Sep;88(9):855-73

Pasqualino A. et Nesci E. *Anatomia umana fondamentale*. 1980. Utet, Torino, 289-293

Pektok E, Nottelet B, Tille JC, Gurny R, Kalangos A, Moeller M, Walpoth BH. *Degradation and healing characteristics of small-diameter poly(epsilon-caprolactone) vascular grafts in the rat systemic arterial circulation*. Circulation. 2008;118(24):2563-70

Persson AB, Buschmann IR. *Vascular growth in health and disease*. Front Mol Neurosci. 2011;4:14. Epub 2011 Aug 24

Rainer A, Centola M, Spadaccio C, De Porcellinis S, Abbruzzese F, Genovese JA, Trombetta M. *A biomimetic three-layered compartmented scaffold for vascular tissue engineering*. Conf Proc IEEE Eng Med Biol Soc. 2010;2010:839-42

Ratner BD and Bryant SJ. *Biomaterials: where we have been and where we are going.* Annu.Rev.Biomed.Eng. 2004. 6:41-75

Ravi S, Qu Z, Chaikof EL. *Polymeric materials for tissue engineering of arterial substitutes*. Vascular. 2009 May-Jun;17 Suppl 1:S45-54. Review

References

Rodgers U.R., Weiss A.S. *Cellular interactions with elastin*. Pathol. Bio. 2005, 53 (7): 390-398

Rosenman JE, Kempczinski RF, Pearce WH, Silberstein EB. *Kinetics of endothelial cell seeding.* J Vasc Surg. 1985 Nov;2(6):778-84

Schaner PJ, Martin ND, Tulenko TN, Shapiro IM, Tarola NA, Leichter RF, Carabasi RA, Dimuzio PJ. *Decellularized vein as a potential scaffold for vascular tissue engineering*. J Vasc Surg. 2004 Jul;40(1):146-53

Seunarine K, Meredith DO, Riehle MO, Wilkinson CDW, Gadegaard N. *Biodegradable polymer tubes with lithographically controlled 3D micro- and nanotopography*. Microelectronic EngineeringVolume 85, Issues 5-6, May-June 2008, Pages 1350-1354

Shieh SJ and Vacanti JP. *State-of-the-art tissue engineering: From tissue engineering to organ building*. Surgery 2005;137(1) 1-7

Shin'oka T, Breuer C. *Tissue-engineered blood vessels in pediatric cardiac surgery*. Yale J Biol Med. 2008, 81(4): 161-6

Shin'oka T, Imai Y, Ikada Y. *Transplantation of a tissue-engineered pulmonary artery*. N Engl J Med. 2001 Feb 15;344(7):532-3. No abstract available. PMID: 11221621

Shum-Tim D, Stock U, Hrkach J, Shinoka T, Lien J, Moses MA, Stamp A, Taylor G, Moran AM, Landis W, Langer R, Vacanti JP, Mayer JE Jr. *Tissue engineering of autologous aorta using a new biodegradable polymer*. Ann Thorac Surg. 1999 Dec;68(6):2298-304; discussion 2305

Soffer L, Wang X, Zhang X, Kluge J, Dorfmann L, Kaplan DL, Leisk G. *Silk-based electrospun tubular scaffolds for tissue-engineered vascular grafts*. J Biomater Sci Polym Ed. 2008;19(5):653-64

Stephan S, Ball SG, Williamson M, Bax DV, Lomas A, Shuttleworth CA, Kielty CM. *Cell-matrix biology in vascular tissue engineering*. J Anat. 2006 Oct;209(4):495-502. Review

Stitzel J, Liu J, Lee SJ, Komura M, Berry J, Soker S, Lim G, Van Dyke M, Czerw R, Yoo JJ, Atala A. *Controlled fabrication of a biological vascular substitute*. Biomaterials. 2006;27(7):1088-94

Tang XJ, Wu QY. *Mesenchymal stem cellular adhesion and cytotoxicity study of random biopolyester scaffolds for tissue engineering*. J Mater Sci Mater Med. 2006;17(7):627-32

Theron SA, Zussman E, Yarin AL. *Experimental investigation of the governing parameters in the electrospinning of polymer solutions*. Polymer 2004;45:2017-30

Tillman BW, Yazdani SK, Lee SJ, Geary RL, Atala A, Yoo JJ. *The in vivo stability of electrospun polycaprolactone-collagen scaffolds in vascular reconstruction*. Biomaterials. 2009;30(4):583-8

References

Unal B, Critchley JA, Capewell S. *Missing, mediocre, or merely obsolete? An evaluation of UK data sources for coronary heart disease*. J Epidemiol Community Health. 2003 Jul;57(7):530-5

Vacanti J. *Tissue engineering and regenerative medicine: form first principles to state of the art*. Journal of Pediatric Surgery, (2010); 45:291-294

Vane JR, Anggård EE, Botting RM. *Regulatory functions of the vascular endothelium*. N Engl J Med. 1990 Jul 5;323(1):27-36

Vert M. *Degradable and bioresorbable polymers in surgery and in pharmacology: beliefs and facts*. J Mater Sci Mater Med. 2009;20:437-46

Williams SF, Martin DP. *Applications of PHAs in medicine and pharmacy*. In Biopolymers Vol. 4, edited by Y. Doi and A. Steinbüchel. Wiley-VCH, 2002

Williamson MR, Black R, Kielty C. *PCL-PU composite vascular scaffold production for vascular tissue engineering: attachment, proliferation and bioactivity of human vascular endothelial cells*. Biomaterials. 2006 Jul;27(19):3608-16

Wolburg H, Neuhaus J, Kniesel U, Krauss B, Schmid EM, Ocalan M, Farrell C, Risau W. *Modulation of tight junction structure in blood-brain barrier endothelial cells. Effects of tissue culture, second messengers and cocultured astrocytes*. J Cell Sci. 1994 May;107 (Pt 5):1347-57

Xiang P, Li M, Zhang CY, Chen DL, Zhou ZH. *Cytocompatibility of electrospun nanofiber tubular scaffolds for small diameter tissue engineering blood vessels*. Int J Biol Macromol. 2011 Oct 1;49(3):281-8

Xu CY, Inai R, Kotaki M, Ramakrishna S. *Aligned biodegradable nanofibrous structure: a potential scaffold for blood vessel engineering*. Biomaterials. 2004 Feb;25(5):877-86

Yazdani SK, Tillman BW, Berry JL, Soker S, Geary RL. *The fate of an endothelium layer after preconditioning*. J Vasc Surg. 2010 Jan;51(1):174-83

Zhang L, Zhou J, Lu Q, Wei Y, Hu S.*A novel small-diameter vascular graft: in vivo behavior of biodegradable three-layered tubular scaffolds***.** Biotechnol Bioeng. 2008 Mar 1;99(4):1007-15

Zhang X, Wang X, Keshav V, Wang X, Johanas JT, Leisk GG, Kaplan DL. *Dynamic culture conditions to generate silk-based tissue-engineered vascular grafts*. Biomaterials. 2009;30(19):3213-23

Zong X, Bien H, Chung CY, Yin L, Fang D, Hsiao BS, Chu B, Entcheva E. *Electrospun fine-textured scaffolds for heart tissue constructs*. Biomaterials. 2005;26(26):5330-8

ACKNOWLEDGEMENTS

First of all, I would like to thank Prof. Marcella Folin for her help and supervision of my research work.

I would like to thank my Correlator Prof. Alessandra Bianco and Eng. Costantino Del Gaudio, who designed, produced and characterized the polymeric mats and tubular scaffolds used in this research work.

I would like to thank Dr. Lara Fioravanzo, who helped me in the experiments and supported me during my PhD years.

A special thank to Prof. Maria Teresa Conconi (Department of Pharmaceutical Sciences, University of Padua) for the collaboration to realize the *in vivo* experiments and the disponibility of instruments.